Cranfield University

JONG-KYU PARK

MODELLING AND CONTROL OF A LIGHT-DUTY HYBRID ELECTRIC TRUCK

School of Engineering

MSc by research Thesis

Cranfield University

SCHOOL OF ENGINEERING

MSc by Research THESIS

Academic Year 2005-2006

JONG-KYU PARK

MODELLING AND CONTROL OF A LIGHT-DUTY HYBRID ELECTRIC TRUCK

Supervisor: Professor N.D. Vaughan

September 2006

This thesis is submitted in partial fulfilment of the requirements for the degree of MSc by Research

ABSTRACT

This study is concentrated on modelling and developing the controller for the light-duty hybrid electric truck. The hybrid electric vehicle has advantages in fuel economy. However, there have been relatively few studies on commercial HEVs, whilst a considerable number of studies on the hybrid electric system have been conducted in the field of passenger cars. So the current status and the methodologies to develop the LD hybrid electric truck model have been studied through the literature review.

The modelling process used in this study is divided into three major stages. The first stage is to determine the structure of the hybrid electric truck and define the hardware. The second is the component modelling using the AMESim simulation tool to develop a forward facing model. In order to complete the component modelling, the information and data were collected from various sources including references and ADVISOR. The third stage is concerned with the controller which was written in Simulink. This was run in a co-simulation with the AMESim vehicle model. Through the initial simulation, the charge-sustaining performance of this controller was verified and improved.

Finally, the simulations for the complete model were carried out over a number of drive cycles, such as CBDTRUCK, JE05, and TRL LGV drive cycle, to evaluate and analyse the effect on the fuel economy and the vehicle performance by the engine operating zone and the EM power capacity. The report presents a comparison of the fuel efficiency of the conventional vehicle and the LD hybrid electric truck. The results obtained by the simulation show the feasibility to build the complete vehicle with the designed controller.

Keywords: Modelling, hybrid vehicles, fuel economy, truck, controller

ACKNOWLEDGEMENT

First of all, I would like to express my sincere gratitude and appreciation to my supervisor, Professor N.D. Vaughan, for his constructive advices and constant encouragement during this academic course. His thorough understanding and knowledge of the subject have been a great help to me.

I would like to thank the Hyundai Motor Company and Kia Motor Corporation and many colleagues in the commercial vehicle product planning team for giving a opportunity to study overseas for a year.

I would also like to express my gratitude to my family, especially to my wife and my son, who have encouraged me to complete this work with kind support and happy smiles.

TABLE OF CONTENTS

TABLE OF FIGURES

TABLE OF TABLES

ABBREVIATIONS

AMESim	Advanced Modelling Environment for performing Simulation of Engineering System, which is a simulation software developed by Imangine Co.
AMT	Automated Manual Transmission
AT	Automatic Transmission
CV	Commercial vehicles, such as trucks and buses
CVT	Continuously Variable Transmission
DP	Dynamic Programming
DS	Driveline Synthesis, which is a method for choosing powertrain configuration
ECMS	Equivalent Consumption Minimization Strategy, which is a kind of control strategy
ELPH	Electrically Peaking Hybrid Electric Vehicle, which is a hybrid electric system suggested by Texas A&M University
EM	Electric Motor
EV	Electric Vehicle
FCV	Fuel Cell Vehicle
GVW	Gross Vehicle Weight
HDV	Heavy Duty Vehicles with over GVW 8ton
HEV	Hybrid Electric Vehicle
ICE	Internal Combustion Engine
LDV	Light Duty Vehicles with GVW 4-8ton
OOL	Optimum Operation Line
PPS	Peaking Power Source, such as battery
SoC	State of Charge of the battery
VRLA	Valve Regulated Lead Acid Battery
ZEV	Zero Emission Vehicle

NOTATION

A	Front area of the vehicle (m^2)
a	Vehicle linear acceleration (m/s^2)
acc_com	Acceleration command from the driver model (0-1)
B_f	Front axle braking force
B_r	Rear axle braking force
brk_com	Brake command
C_d	Coefficient of air drag
DOD_o	Initial depth of discharge (%)
F	Rolling friction coefficient
F_{aer}	Aerodynamic resistance (N)
F_{cl}	Climbing resistance (N)
F_{dyn}	Coulomb friction force in clutch (N)
F_{ext}	Input optional force (N)
F_{fric}	Friction force(N)
F_{roll}	Rolling resistance
G	Acceleration of gravity (m/s^2)
I	Current (A)
i_{fd}	Final drive ratio
i_g	Transmission ratio of the engaged gear
J	Inertia of the 4 wheels ($kg.m^2$)
K	Velocity coefficient
M_{equ}	Mass of the vehicle (kg)
M_v	Vehicle weight (kg)
N	Engine speed (rev/min)
N_{cell}	Number of cells in series per bank
P_{el}	Electric power (W)
P_m	Motor power (kW)
P_{max}	Vehicle maximum power (kW)
P_{mech}	Mechanical power (W)

Q	Charge used by the load (As)
Q_{nom}	Rated capacity (As)
R	Equivalent internal resistance (ohm)
R_{whl}	Rolling radius of the drive wheels (m)
S_{bank}	Number of battery banks in series arrangement
S_i	Startability (%)
t_a	Acceleration time (s)
T_{acc}	Total torque demand calculated by using acc_com (Nm)
T_{brk}	Braking torque (Nm)
T_{brk_frt}	Braking torque on the front wheel
T_{brk_rear}	Braking torque on the front wheel
T_{e_lwr}	Lower threshold torque to determine the engine operation zone
T_{e_max}	Maximum torque of the engine
T_{e_opt}	Torque at the OOL of the engine (Nm)
T_{e_upr}	Upper threshold torque to determine the engine operation zone
T_{fric}	Friction torque developed between the two plates (Nm)
T_{lim}	Limited torque (Nm)
T_m	Torque on the shaft of the motor at port 1 (Nm)
$T_{m\_brk\_rear}$	Regenerative braking torque in the generator
T_{m_max}	Maximum torque of the motor
T_{mbrk}	Braking torque produced by the mechanical brake
T_p	Primary shaft torque (Nm)
T_{reg}	Regenerative braking torque at rear wheels
T_s	Torque transmitted by the gearbox
T_{slip}	Maximum Coulomb friction torque (Nm)
T_{tmax}	Total maximum torque which can be produced from all the power sources at current speed
V	Voltage (V)
V_0	Open circuit voltage (V)
v_b	Velocity speed corresponding to the base speed of motor (m/s)

V_{bank}	Bank output voltage (V)
v_{c_rel}	Relative velocity between the shafts
v_{c_thr}	Velocity threshold
V_{cell}	Cell output voltage (V)
v_f	Final high speed to which the vehicle is accelerated from 0 speed (m/s)
v_{set}	Preset vehicle speed below for the motor only mode (km/h)
v_{veh}	Vehicle linear velocity (m/s)
v_{wind}	Wind speed (m/s)
W_f	Static weight on the front axle
W_f'	Dynamic load on the front axle
W_r	Static weight on the rear axle
Wr'	Dynamic load on the rear axle
z	Dynamic load transfer contribution, or moment of inertia by the total brake force
δ	Correction coefficient of rotating mass
η_{fd}	Efficiency of the final drive axle
η_g	Efficiency of the engaged gear
η_t	Transmission efficiency
$\eta_{t,e}$	Transmission efficiency from motor to the drive wheels
$\eta_{t,m}$	Transmission efficiency from motor to drive wheels
θ	Uphill grade
ρ	Air density (kg/m^3)
τ	Time constant (s)
ω	Rotary velocity at port 1 (rad/s)
ω_{rel}	Relative rotary velocity (rad/s)
ω_{thr}	Rotary velocity threshold (rad/s)

1 Introduction

1.1 Background

There have been serious concerns about the depletion of the earth's petroleum resources for a few decades, which have caused rapid increases of oil prices. For example, on the basis of Brent crude oil, the oil price has now risen to more than twice the value from the 1990's [1] so that some people have called it 'the third oil crisis.' This emphasises the importance of fuel economy in vehicles.

In addition, the environmental problems, such as air pollution and global warming, are another concern and becoming more important. The increasing large number of automobiles around the world has caused and continues to cause serious problems for human life as well as the environment. All countries are trying to reduce the emissions by enforcing the stricter regulations or agreements, such as the Euro 4/5 standards and the Kyoto protocol. In the case of heavy duty diesel engines, Euro Ⅳ regulations took effect after October 2005 and Euro Ⅴ standards are supposed to be effective in 2008 [2]. Table 1-1 shows EU emission standards.

Table 1-1 EU Emission Standards for HD Diesel Engines, g/kWh (source: [2])

Tier	Date & Category	Test Cycle	CO	HC	NOx	PM	Smoke (g/m)
Euro I	1992, <85 kW	ECE R-49	4.5	1.1	8	0.612	-
	1992, >85 kW		4.5	1.1	8	0.36	-
Euro II	1996.1		4	1.1	7	0.25	-
	1998.1		4	1.1	7	0.15	-
Euro III	*1999.10, EEVs only*	*ESC & ELR*	*1.5*	*0.25*	*2*	*0.02*	*0.15*
	2000.1	ESC & ELR	2.1	0.66	5	0.1 0.13*	0.8
Euro IV	2005.1		1.5	0.46	3.5	0.02	0.5
Euro V	2008.1		1.5	0.46	2	0.02	0.5

* - for engines of less than 0.75 dm3 swept volume per cylinder and a rated power speed of more than 3000 rev/min

Automotive manufacturers have concentrated on the development of new powertrain technologies to cope with the demands of fuel economy and the environment. They have spent large amounts of money in the research and development of electric vehicles (EV), hybrid electric vehicles (HEVs), fuel-cell vehicles (FCVs), and alternative fuel engines. However, EVs, regarded as Zero Emission Vehicles (ZEVs), are very hard to produce and commercialise because the development progress of the battery system is not as fast as had been expected. FCVs are referred to as the long-term solution for automotive energy sources, and are expected to achieve the economic feasibility in a few decades. The HEVs are the most promising alternative powertrain at present [3].

HEVs have a variety of advantages over conventional vehicles: improvement of fuel efficiency by energy recovery and using regenerative brake reuse, downsizing of the primary engine, and optimised operation with a proper control strategy. In addition, it is possible for them to be produced easily, considering the change of package layout of conventional vehicles. Actually the annual sales volume of hybrid electric vehicles has increased rapidly to around 300 thousand units in 2004, after Toyota produced the first HEV, the Prius, in 1998. The Nomura Research Institute in Japan expects that the volume will reach about 1,500 thousand units per year in 2010, as Figure 1-1 [4].

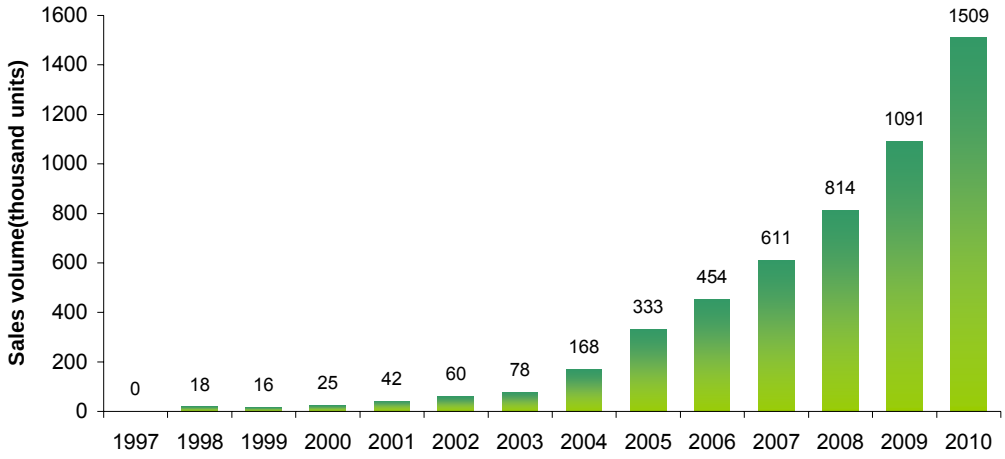

Figure 1-1 Estimated sales volume of hybrid electric vehicles in 2010

In the field of commercial vehicles (CVs) such as trucks and buses, interest in HEVs has been growing, too. As these commercial vehicles usually use much more fuel

compared with passenger cars, better fuel savings and emission reductions could be achieved. However, no more than a few CVs have been launched in the market due to the difficulty to apply hybrid systems to the heavier vehicles. There have been relatively few studies on commercial HEVs, most of which concentrate on the city bus to improve the fuel economy under conditions of urban driving.

As a result of transport analysis in London, the number of freight vehicles, including lorries and vans, is much higher than that of buses and coaches [5]. This means that the hybrid truck is appropriate for urban driving, too. Especially, the light-duty (LD) truck with a GVW below 7.5t is a promising vehicle type. It is predominantly operated in urban conditions with frequent stop/start, whilst heavy-duty trucks are run on the highways. If the hybrid system is applied to an LD truck with an appropriate control strategy, a good effect on energy reduction and emission improvement are expected.

This type of vehicle is preferred to other heavier commercial vehicles for hybridisation, taking the feasibility to be commercialised into consideration. However, the vehicle performance must be maintained and cannot be jeopardised by hybridisation, because it has a priority and is regarded as a necessity in the field and LD truck is usually used for delivering freight in the urban area.

1.2 Project Objectives

The overall aim is to research a hybrid electric powertrain for a light-duty truck. The study is to build a hybrid electric vehicle model for the light-duty truck and an appropriate control strategy for the particular duty cycles to minimise fuel consumption with either the same or a better performance than that of the corresponding conventional truck.

The objectives can be summarised as follows.

1. Study the advantages and the disadvantages of different hybrid architectures and study how to define the component for the light-duty truck, in order to meet the vehicle performance requirement.
2. Investigate the function of the HEV controller and optimise the controller to achieve better fuel consumption and performance.
3. Examine the battery behaviour during the drive cycle in order to maintain the target range.
4. Evaluate the improvement of the fuel economy through various simulations on a number of drive cycles.

1.3 Structure of thesis

The thesis is made up of seven Chapters describing the work conducted during the project. The first and the second Chapters are concerned with the background, objectives, and the literature review. From these Chapters, the aim and the methodology of this research are set up.

The architecture and the power capacity of the components for the HEV are determined in the third Chapter. This is done through a comparative study and calculations based on vehicle performance.

The fourth Chapter is devoted to the component modelling with detailed information and data for each component. These models are built in AMESim. The basic function and performance of each component are verified by the component test without any controller.

The fifth Chapter describes the controller. The control strategies and the structure of the sub-controllers are presented. In addition, this Chapter describes the tuning of the controller to improve the charge-sustaining strategy. After that, the component model and the controller are integrated with the plant model.

The sixth Chapter deals with the simulation results. In order to verify the function and the performance of the integrated HEV model, the simulation on a basic drive cycle is carried out. After validating them, a variety of simulations on a number of drive cycles are performed to study the effect on the fuel economy and the battery SoC. Finally, the vehicle performance and the fuel economy of the LD hybrid electric truck are compared to that of a conventional truck.

The seventh Chapter provides the conclusion and the summary of this study. Moreover, it suggests future work to improve this research further.

2 Literature review

As shown in the first Chapter, a light-duty truck with a GVW below 7.5t is a promising vehicle type for the hybrid electric system, because its portion in the urban area and the sales volume are quite big, compared to other kinds of commercial vehicles. The detailed description and sales volume are presented in the third Chapter.

However, relatively few studies on hybrid trucks were conducted, compared with hybrid city buses. Therefore, this literature review is focused on the hybrid electric system for commercial vehicles. Considering the driving conditions and the vehicle weights, many researches on the hybrid bus should be very relevant for trucks.

There are various research subjects and publications on hybrid vehicles that describe the development of each sub-system, for example the electric motor and battery, parametric optimisation, control strategy optimization, and modelling & simulation. However, key technologies and data related to the hybrid system have been kept confidential by automotive manufacturers trying to maintain competitiveness over their rivals. In particular, in the field of commercial vehicles where the hybrid system is not popular yet, data are even more limited than those of passenger cars.

2.1 Overview of hybrid electric vehicles

HEVs are defined as a vehicle in which propulsion energy is available from two or more types of energy store, sources, or converters and at least one of them can deliver electrical energy. This technology allows the vehicle to draw upon the benefits from both propulsion sources. The three main potential advantages of a hybrid system are as follows [6]:

1. Energy normally lost in braking can be recovered and stored for later use.
2. The size of the primary engine power source can be reduced.

3. The primary power source operates at a more constant load, which benefits the optimisation process and leads to higher efficiency.

Taking these features into consideration, it is advisable to apply this hybrid system to the vehicles which use the urban drive cycle to maximise the effect of the hybrid electric system, such as city buses or light-duty trucks. It means, therefore, that the advantages of the hybrid electric vehicles depend on the vehicle type and drive cycle.

2.2 Types of hybrid electric powertrains

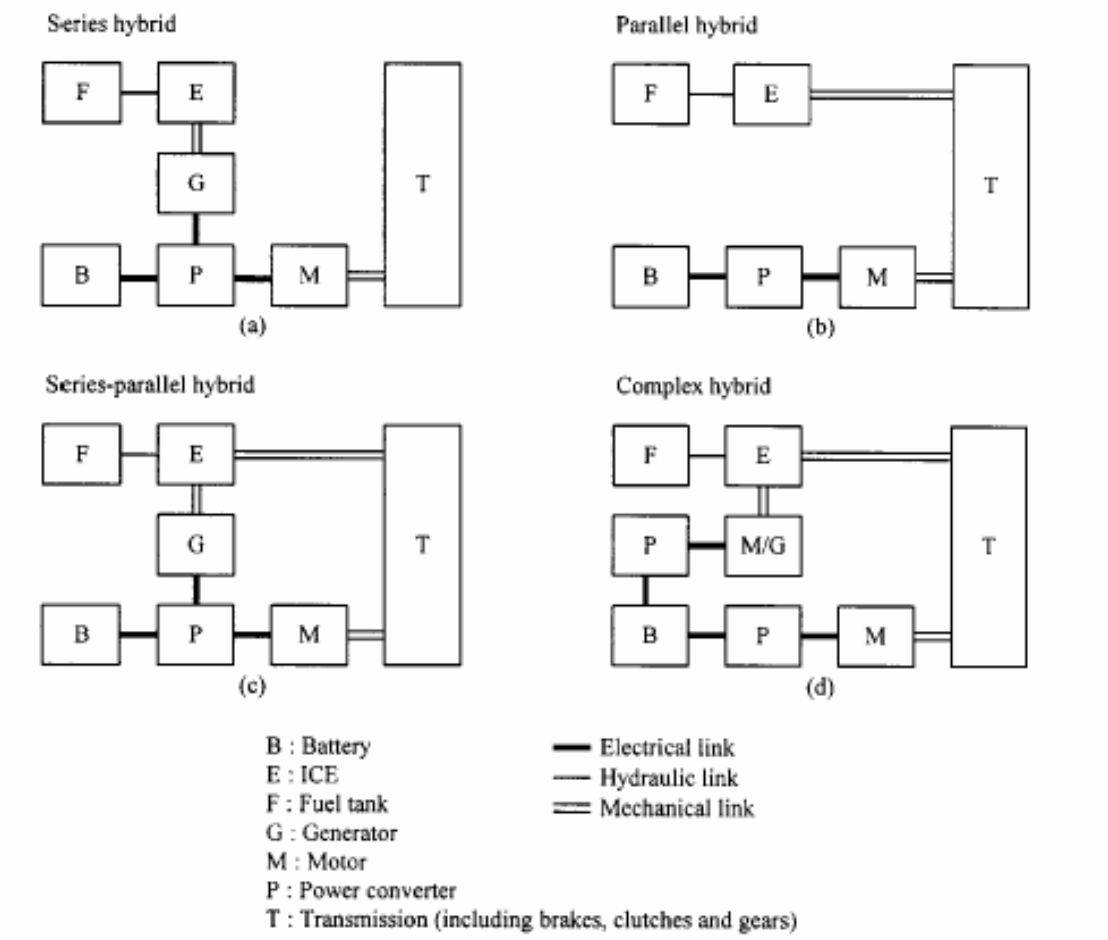

Figure 2-1 Types of hybrid electric powertrains (source: [7])

HEVs are classified into four types according to their architecture: series hybrid, parallel hybrid, series-parallel hybrid, and complex hybrid. Figure 2-1 shows the corresponding functional block diagrams [7]. The engine and the battery can be replaced by other types, such as the fuel cells as primary power source and ultracapacitors for the secondary source.

HEVs can be classified by the power source, too, i.e., battery-electric hybrid system, flywheel hybrid system, fuel cell hybrid system. In this thesis, battery-electric hybrid vehicles will be the main area of concentration.

Among them, the series type or parallel configuration is usually applied to the commercial vehicle, as discussed in Section 2-4. However, the structure of series hybrid powertrains is quite simple, because all the power is transmitted to the drive wheels through the EM, and there are few variants for the type. Hence, the detailed variations for the parallel configuration are described in the next section.

2.3 Configuration of parallel hybrid electric drive trains

A parallel hybrid drive train is a drive train in which the engine supplies its power mechanically to the wheels as in a conventional ICE-powered vehicle. It is assisted by an electric motor that is mechanically coupled to the transmission. The power of the engine and electric motor are coupled together by mechanical coupling. The parallel HEVs can be divided into several configurations by the position or type of the mechanical coupling.

The mechanical coupling may be a torque or speed coupling. Whilst the torque coupling adds the torques of the engine and the electric motor together, the speed coupling deals with the rotary speed. The speed coupling is usually important to power plants such as the Stirling engine and the gas turbine engine, in which their efficiencies are sensitive to speed and less sensitive to torque. The configurations of torque coupling are considered in this study based on a diesel engine.

Although several different configurations for the torque coupling parallel HEV can be constructed, there are four kinds of architecture for trucks in general, depending on the position of the transmission: pre-transmission double-shaft combination, pre-transmission single-shaft combination, post-transmission combination, and separated axle torque combination [8, 9].

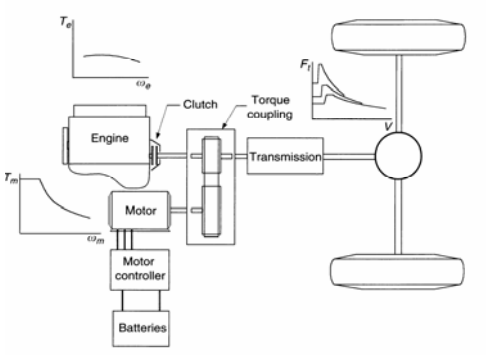

(a) Two-shaft pre-transmission

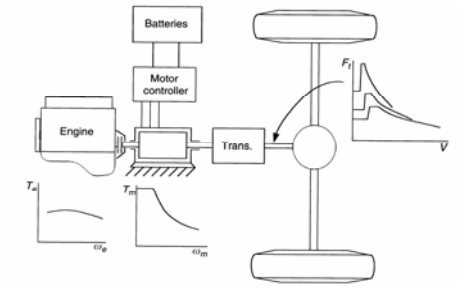

(b) Single-shaft pre-transmission

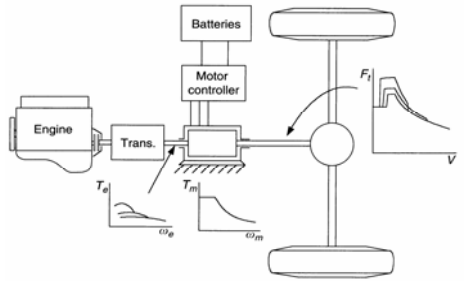

(c) Post-transmission

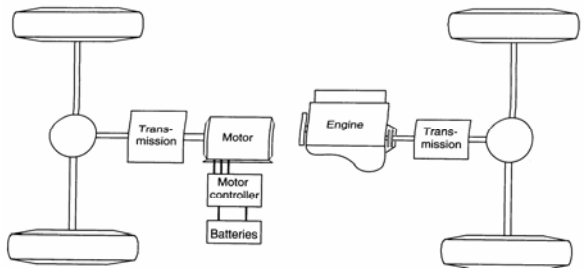

(d) Separated axle combination

Figure 2-2 Configurations of parallel hybrid system (source: [8])

As shown in Figure 2-2, the pre-transmission configuration has the gearbox located between the torque coupling and the drive shaft. This means that the torque from the two power sources can be added before the transmission. Therefore, the gear selected and shift changes have an effect on the performance of the electric machine as well as the engine. This configuration is regarded as the most favourable solution nowadays, because the conventional electric machine is adequate to deliver hybrid function and this type does not need big changes compared to the existing vehicles. However, it is

reported in [8] that this configuration requires relatively more complex control than post-transmission systems in which the existing control strategy for engine and gear shift is not changed compared to the current vehicle. This type is classified into two shaft configuration and single shaft configuration. The former is suitable in the case when a relatively small engine and electric motor are used, and the latter is usually used in the case of a small motor.

On the other hand, the torque coupling occurs behind the transmission in the post-transmission configuration. This means that the transmission can only affect the engine torque to improve engine operating efficiency while the motor torque is directly delivered to the driven wheels. So the electric machine requires very high torque levels to deliver the tractive force. This type is appropriate for a large electric motor so that this architecture is more difficult to be applied to the real vehicle than the single shaft pre-transmission type. That is because this type needs a completely different packaging layout and a much larger battery to operate the large electric machine.

The separated axle torque configuration is shown in Figure 2-2 (d), in which one axle is powered by the engine and another is powered by the electric motor. The original engine and transmission can be kept and the EM can be added in this configuration. However, the EM and the two transmissions occupy considerable space and the available space may be reduced.

Table 2-1 Features of the hybrid architectures

Configurations	Advantages	Disadvantages
Two-shaft pre-transmission	- The ICE and the EM can have different speed range.	- Relatively complex architecture : Two shaft structure - Complex control
Single-shaft pre-transmission	- Simple & compact architecture - Appropriate for a relatively small engine and electric machine	- The ICE and the EM must have the same speed range - Relatively complex control
Post-transmission	- Simple & compact architecture - The existing control strategy can be kept	- Requires the large EM with a very high torque - Needs big change of packaging layout
Separated axle combination	- the original engine and gearbox can be kept	- Available space maybe reduced

Table 2-1 shows the summary of the features of the hybrid architectures. Each configuration has advantages and disadvantages. In the matter of the feasibility of production, single shaft pre-transmission type and post-transmission configuration are preferred to others, because they need relatively small changes to be applied to the conventional vehicle.

A comparative study between pre-transmission and post-transmission configurations based on the two control strategies, 'thermostat' and 'power split' concepts were performed by Texas A&M University [10]. The former, so-called 'Engine on/off' strategy, is one of the simplest control strategies and turns on and off the engine based on the state of charge of the battery. For the power split controller, a variety of strategies have been suggested but the 'electrically assist' algorithm was applied. In this paper, the post-transmission hybrid gives worse fuel consumption at a smaller hybridisation rate, 30%, than the pre-transmission system. This is because the electric machine of the post-transmission configuration operates with a single gear reducer and is unable to meet the larger drive torque demands. On the other hand, the mutual 5-gear transmission in the pre-transmission hybrid reduces the drive torque of the motor and increases efficiency. However, both post- and pre-transmission hybrids offer almost similar fuel economy with higher hybridisation rates.

As a result of this study, it was found that the pre-transmission single shaft configuration is favourable for smaller hybridisation rates.

2.4 Hybrid electric systems for commercial vehicles

This section explains the real HEV examples of commercial vehicles. As the HEV examples for the truck are not as many as passenger cars, all the cases studied are presented regardless of the vehicle type, i.e., bus and truck.

2.4.1 Buses

Regarding the hybrid electric systems of commercial vehicles, city buses have been researched well and have already been marketed. They have many advantages: no major infrastructure investment, higher efficiency and lower air/noise pollution in urban areas. So a number of in-service evaluations have been undertaken around the world [6].

Orion VII buses equipped with the BAE SYSTEMS Hybridrive TM propulsion system had successfully completed reliability tests by 2003 in New York. After that, more than 300 units were produced and introduced in revenue service, and 700 more units are expected to be delivered as of October 2005. A series hybrid electric system with Cummins 5.9L diesel engine and lead-acid battery was applied to the low floor buses, and a catalysed diesel particulate filter was adapted to reduce emissions.

In Europe, various hybrid bus configurations were proposed and demonstrated in several European cities with the support of the European Union's 'THERMIE' programme. As an example of this programme, there were operational trials of hybrid battery-electric buses in Italy. The buses, produced by Iveco and operated in Terni between 1997 and 1998, were equipped with a Sofim 2800 diesel engine, three-phase 164 kW electric motor, and lead-acid battery. The remarkable finding is that 37% of the electrical energy supplied to the traction motor was recovered by regenerative braking [6].

One of the most important hybrid bus projects within Thermie is the Sagittaire project, aiming to introduce hybrid buses in nine European cities. Bossche [11] explained the hybrid buses under the programme, concentrating on hybridisation degree and battery types. Various combinations of ICE and EM by hybridisation degree from 22% to 125% were applied and several kinds of battery, including lead-acid, VRLA, Na/NiCl, Ni/MH batteries, were used for the bus application.

In Asia, research and development of a hybrid bus has been conducted by a number of projects. As an important case, Mitsubishi Fuso Truck & Bus company [12] developed a

series hybrid low floor city bus and tested in Japan. It downsized the conventional 13 litre diesel engine to an 8.2 litre engine, and applied 100 kW of generator and 300 kW of electric motor and the newly-developed lithium-ion battery.

2.4.2 Trucks

There are some difficulties in applying hybrid electric systems to trucks, in particular a lack of space for package layout. So relatively little research has been conducted for hybrid electric trucks and few trucks are produced or ready to market.

Some positive results on fuel economy and NOx emissions of light-duty hybrid trucks were presented by Takada et al. [13] who verified the improved effect of a light-duty parallel hybrid truck by carrying out tests with various payloads on roads. On the urban trip and the suburban trip, the fuel economy was improved by 23 to 28% as compared with the base truck, and NOx emissions by 26 to 34%. In this publication, however, the control strategy was not explained, even though the main specifications on components were presented. These data will be tackled in the next Chapter.

FedEx Express collaborated with the environmental advocacy group Environmental Defense to announce the Future Vehicle Program, with the goal of developing significant improvements in emissions and fuel economy for the W700 parcel delivery vehicle. Nellums et al. [14] described the development activities and good test results of a Class 4 hybrid electric truck for a particular FedEx modified test cycle submitted to this Program. Unfortunately, major changes of main components and control strategy were not presented in detail. Japanese manufacturers, Isuzu and Mitsubishi Fuso truck, have developed a similar configuration of hybrid truck. These vehicles will be presented in more detail in the third Chapter.

For other types of energy storage system, Nissan Diesel [15] has developed a parallel hybrid medium-duty truck with a high performance capacitor, which has a total 583Wh of energy density with 2 modules. It consists of a conventional 152 kW diesel engine

and an automated manual transmission system. Test results in M15 mode show a 50% improvement in fuel economy. It also demonstrated that the capacitor type storage system is suitable for this type of application.

2.4.3 Discussion

As shown in the examples above, mainly the basic types of hybrid system, i.e. series and parallel, were equipped in the commercial vehicles.

The series configuration has a relatively simple connection of the electric motor and the internal combustion engine. As shown on the Figure 2-1, even though it has the simplest configuration, it needs three power devices and more energy conversion, i.e., the overall efficiency is lower in general. The parallel hybrid system allows both the ICE and the electric motor to deliver power in parallel to drive the wheels. Its efficiency is better than that of a series configuration in general [7]. However, it needs a more complicated control strategy.

The general trends of efficiency related to the type of hybrid powertrain for heavy-duty transit buses were presented by comparative simulation analysis. When the power capacity of the ICE and the EM is selected to maximise the fuel economy, the fuel economy of the parallel type is better [16]. A similar study was carried out by An et al. [17].

As shown in [16] and [17], the efficiency of parallel HEV is generally higher than that of the series type, because the latter configuration needs more energy conversion to drive the vehicle [7]. In addition, a smaller ICE and a smaller electric motor can be used for the parallel type to obtain the same performance until the battery is depleted. Therefore, in this thesis, a parallel configuration will mainly be studied.

As to the type of transmission, this research will be concentrated on automated manual transmissions, because there are some limitations to applying other types of automated

transmissions to heavier commercial vehicles: AT and CVT which are usually adapted in passenger hybrid cars. An AT has the disadvantage of a large amount of power loss as its capacity is increased, and CVT can be applied only for small-sized passenger cars at present. However, AMT can be easily applied to commercial vehicles assisted by pneumatic actuators [18].

2.5 Component sizing and control strategies

System integration and optimisation are key factors in developing HEVs. That is to say, 'software' as well as 'hardware' should be optimised. Hardware means the components of HEVs and software is the control strategy. A variety of methods for the optimisation are presented in 2.5.2 and 2.5.3.

The most suitable powertrain depends on the drive cycle, the available technology, the cost of fuel, and other demands or conditions. In particular, the drive cycle is so important that it can be used as a criterion of hardware/software optimisation in terms of fuel economy as well as emissions.

HEV design methodology may use a selective or general approach in defining vehicle specifications. In 'selective' designing, the hardware specifications of a HEV are optimised by selecting the minimum size of EM and ICE with a single gear transmission system to operate efficiently in a specific driving pattern. The control strategy is selected according to the requirement of the particular driving behaviour. The 'general' approach customises the hardware and software specifications of the HEV so that it performs reasonably well under diverse driving patterns. This approach, of course, will not give optimum results for any particular drive cycle [19].

2.5.1 Drive cycles

Drive cycles for vehicle research were initially introduced to measure fuel consumption and emissions. As they are changed by the driving conditions and the vehicle types,

various drive cycles have been developed according to regional driving conditions. These standardised cycles were presented [20] and used for simulating vehicles, especially in the field of passenger cars.

Unfortunately, it is hard to find out the standard drive cycles for heavier trucks. For example, there is no standard cycle for the heavy duty vehicles certified by the EU; they just provide the cycles for evaluating heavy duty engines. Many countries have provided the regional standard cycles for commercial vehicles. Many researchers have used these cycles for studying commercial vehicles by choosing some cycles or modifying the existing cycles, including the standard cycles for the different classes of vehicle. For instance, Nellums et al. [14] use the modified 1975 FTP test cycle to design a Class 4 hybrid truck.

Some drive cycles for light duty trucks are presented in Table 2-2. The maximum speed ranges from 32kph to 90kph and the idling portion is between 15% and 52% according to the driving area, i.e., urban or suburban. The maximum acceleration is in the range between 1 and 2 m/s^2, except for the CBDTRUCK cycle. These factors are closely concerned with fuel economy and the optimisation strategy can be changed according to the target drive cycle. It is very hard to fix the target drive cycle to develop the vehicle. Therefore, it is advisable to verify the vehicle performance and the fuel economy through various drive cycles in the stages of computer simulation.

Table 2-2 Drive cycles for the trucks

Region	Driving Cycles	No of Stops	Dura -tion (s)	Total Distance (km)	Timing Idling (%)	Max Speed (kph)	Average Speed (kph)	Max Acc. (m/s^2)
USA	NYTRUCK	20	1016	3.43	52	54.7	12.2	1.96
	CBDTRUCK	14	850	3.51	19	32.2	14.9	0.36
EUROPE	TRL LGV	17	1155	6.3	15	46.8	19.7	1.52
JAPAN	JE05	12	1829	13.8	25	87.6	27.3	1.59

In this research, the drive cycles shown in Table 2-2 are mainly used for simulation. NYTRUCK and CBDTRUCK cycles are presented to represent the driving conditions in the USA.

For European real drive cycles, the TRL LGV drive cycle is taken into consideration measured by TRL. TRL Limited [21] was commissioned by the Charging and Local Transport (CLT) Division of the Department for Transport (DfT) to undertake a project (UG214) to address the gaps in the understanding of operational profiles and emissions with respect to traffic management. So they measured operational profiles for four vehicles: two LDVs – a car and a light goods vehicle, and two HDVs – a heavy goods vehicle and a bus in six cities in the UK. This means these drive cycles reflect the latest driving conditions.

Japanese 2005 emission standards introduced the new emission test cycle, JE05, for heavy vehicles of GVW above 3,500 kg which became effective in 2005. This cycle is a transient driving schedule of total duration of approximately 1800 seconds with 88kph of maximum speed.

Among the drive cycles presented, NYTRUCK is excluded from the computer simulation study, because the idling time is over 50% and it can distort the fuel consumption severely when compared to the general driving condition. Therefore, the simulation is carried out on the other three drive cycles.

2.5.2 Component sizing

One of the most important issues in developing an HEV is the feasibility to be commercialised which includes considerations of vehicle price and performance. Component sizing, such as the capacity of the ICE and electric motor and battery capacity, is very important from this point of view because it is concerned with the cost of vehicles and performance directly.

A practical method to configure the powertrain for the parallel hybrid vehicle was presented based on the performance requirement in [22] and [23]. That is, according to the required maximum speed, acceleration time, grade ability, and other constraints, the power for steady driving related to ICE and the power capacity for dynamic load concerned with EM were determined. After that, the gear ratios of final drive and transmission were calculated. The battery capacity is determined by two factors: power requirement by electric motor and energy requirement and is verified for the particular drive cycles. In this study, however, little attention is given to the transmission, which has only two gear ratios and could be further developed to improve the fuel efficiency.

Similar studies have already been conducted by Texas A&M University to develop an Electrically Peaking Hybrid Electric Vehicle (ELPH) [19]. In this study, required maximum speed and maximum specific energy were calculated by using diverse urban drive cycles and used to determine the power capacity for ICE, EM and battery capacity to assign the dynamic peaking power by electric motor. Four parallel HEVs were designed for four urban driving patterns according this concept. However, this resulted in a bigger motor size compared with produced parallel HEVs. Because using small size motors generally brings about lower battery weight and volume, smaller motor size is preferred in the automotive industry if the motor produces enough power to meet the performance and efficiency requirements.

On the other hand, Hellgren el al. suggested Driveline Synthesis (DS) for choosing powertrain configuration and sizing components in HEVs [24]. This method considers the various conditions such as fuel price and tax as well as the requirement for the particular drive cycle, and suggests the most cost-effective solution. It consists of optimisation and evaluation which employ a dynamic simulation in large time steps and a cost calculation. However, the main drawback with this method is that it is difficult to know if the optimal solution really has been found and the evaluation is not based on an optimal control. It is also a time-consuming method.

In this thesis, a method to select the parameters based on the performance requirement will be applied, because there are few cost data and the three methods above are very similar from a technical point of view, except for cost consideration.

2.5.3 Control strategies

Due to constraints for the design of the main components, such as the astronomical amount of investment, and limitations of choosing a hybrid system type, optimisation of software or control strategies are becoming more important nowadays. In the automotive industry, it is regarded as one of the key technologies to keep their edge [25]. It is very important to take advantage of all possible situations to achieve maximum efficiency under limited conditions.

Usually the control objectives are (1) meet the power demand of the driver, (2) operate each component with optimal efficiency, (3) recapture braking energy as much as possible, and (4) maintain the state-of charge of battery [8]. There are two basic types of control strategies: Maximum SoC-of-PPS control strategy which aims to meet the power demand and maintain the SoC at the same time, and is proper for a frequent stop-and-go driving pattern, and Engine On-off control strategy which is used for long charge-sustaining driving with a low load on the highway.

In the matter of hybrid types to which control strategy is applied, a parallel type of hybrid system offers more possibilities to optimise control strategies in fuel economy and exhaust emissions, whilst a series hybrid drive train features more energy conversion losses so as to limit the control actions. The control of the parallel hybrid drive train is more complex than that of a series hybrid drive train, due to the mechanical coupling between the engine and the driven wheels.

More advanced optimal control strategies have been presented for the parallel hybrid powertrain. They can be divided into three categories [26].

The first method is heuristic rule-based control strategy. This methodology known as load levelling to force the ICE to act at or near either its peak point of efficiency or its BSFC curve at all times is presented by Baumann et al. [27]. A fuzzy logic controller is adapted to accomplish the strategy. Although it is not basically able to optimise fuel economy, it is likely to be applied to the real vehicle easily and can get reasonably good results by the strategy constructed.

The second approach is based on static optimisation methods. Paganelli et al. suggest the supervisory control strategy in charge-sustaining HEVs based on an instantaneous equivalent energy consumption minimisation strategy (ECMS). In other words, the electrical power flow is converted into equivalent fuel consumption to calculate and optimise the overall fuel economy [28]. A similar concept of optimisation was presented for the parallel HEVs with CVT by Kim et al. [29]. This approach is generic in nature and can be readily applied to any arbitrary driving pattern. However, as this method does not consider the remained capacity of the battery and that the equivalent consumption ratio does not reflect the real driving condition and can be changed by the SOC, it is not able to optimise the efficiency, either. This problem has already been pointed out [30]. Although the fuel economy was improved by using this concept, it is not considered to be effective to the real efficiency because the SOC became much lower after simulation. Additionally, in order to make this strategy more reliable, the coefficients for the equivalent ratio have to be verified through tests for various conditions in advance.

The third category is dynamic optimisation methods. The control strategy for a medium-duty parallel hybrid electric truck using Dynamic Programming (DP) was reported [31]. Even though this approach provides the exact optimal solution, the resulting policy is not applicable to the real driving patterns, except given drive cycles, because it requires the knowledge of future driving conditions. So the applicable rule-based control strategies, e.g. power split strategy and charge-sustaining strategy, have to be established by benchmarking the result of dynamic optimisation. In addition, it takes too much time to determine the optimised strategy.

The control strategy for a series hybrid powertrain is more simple. As the system has only one way of power transmission, the overall control strategy concentrates on the improvement of ICE itself except for the efficiency of each component and power transmission. Consequently, two basic type of control approach are known: 'Engine on/off' control and 'Optimum line or continuous' control. These two different basic control strategies were studied for a series hybrid city bus. As can be expected, the 'Continuous' strategy results in better fuel economy [32].

Aside from the kinds of control strategy, the remained battery SOC is another issue after a simulation. Although the fuel economy is greatly improved as a result of the optimised strategy, if the battery gets much lower at the final stage, it is not applicable. In addition, the improved fuel economy is depreciated by the final SOC. So the charge-sustaining strategy is important.

To build an applicable control strategy is a target of this research. To this aim, the control strategy considering the final SOC will be built. Therefore, the actual effect of improving the fuel economy can be evaluated.

2.6 Simulation tools

Because computer simulation provides a cost-effective design, it has been developed for all kinds of vehicles. Especially for EVs and HEVs which have more complex architecture and control compared with the conventional vehicle, the importance of simulation is often emphasised.

Simulators can be divided into two categories: backward and forward type [33]. The former uses a given drive cycle as input and requires no driver behaviour. Force required to accelerate the vehicle is calculated and translated into torque. The procedure is repeated at each stage from the vehicle/road interface until the fuel consumption is calculated. For example, SIMPLEV from the DOE's Idaho National Laboratory, and MARVEL from the Argonne National Laboratory, and ADVISOR from the National

Renewable Energy Laboratory apply this type. The latter, forward simulator, requires the drive model and takes a given drive cycle as the velocity that the driver intends to keep. By comparing the actual vehicle velocity with the desired velocity, the simulator generates acceleration and brake commands. The fuel consumption is calculated from the accelerator angle given from the driver. For instance, this method was adapted in V-ELPH from Texas A&M University, OSU-HEVSIM from the Ohio University, all the simulators of which are written in Matlab/Simulink code. The forward simulation is near to realistic driving conditions so that it could be more useful in designing the different control algorithms and calculating vehicle performance, whilst the backward type is often faster and less complicated.

As can be seen from the examples above, Matlab/Simulink is the most popular simulation program which is a software package for modelling, simulating and analysing dynamical systems. In addition, it offers a graphical user interface (GUI) through Simulink for models as block diagrams which makes it much easier to build the models. As most automotive engineers have tried to find easy-to-use and accurate simulation tools, it became the essential software in the field of automotive control. However, in order to build models by using this software, mathematical models for all the systems are needed. This means that even the frequently-used models have to be analysed into the mathematical model by all the users. In automotive engineering, these kinds of models, such as engine and gearbox, can be found easily.

So many simulation programs provide the built-in models in advance. Advanced Modelling Environment for performing Simulation of Engineering System (AMESim) is one such advanced simulation software available with a modern graphical interface to display the simulation process. This tool offers a variety of built-in models and can be used for modelling and developing an optimal control strategy of powertrain easily, regardless of powertrain types [34]. It was used for not only developing an optimal powertrain control of the conventional vehicle with CVT [35], but also modelling of HEVs [25]. Moreover, it has a feature to be able to interface with Matlab/Simulink.

When these two simulation tools are interfaced with each other, the modelling and simulation can be completed conveniently except for the interface problems. This allows the user to easily change the program according to the research aim. So these two tools are used for this research.

3 HEV architecture & component sizing

As a consequence of the initial study and literature review, it was found that there are many hybrid architectures which have different features. As the configuration types have a direct effect on the driving efficiency, the appropriate architecture has to be chosen for the selected vehicle. In this sense, the comparative study of the existing HEV examples is very meaningful.

After deciding the hybrid architecture, the component sizing should be followed. It provides the vehicle with the best compromise in performance.

This Chapter will explain how the HEV architecture for this research is selected and the main components defined.

3.1 Specification of the base light-duty truck

To begin with, the specifications of the conventional light-duty truck are presented. These data are very important and are used as criteria to fix the HEV architecture. Based on this information of the base vehicle, the main components of HEV are selected according to the performance requirement.

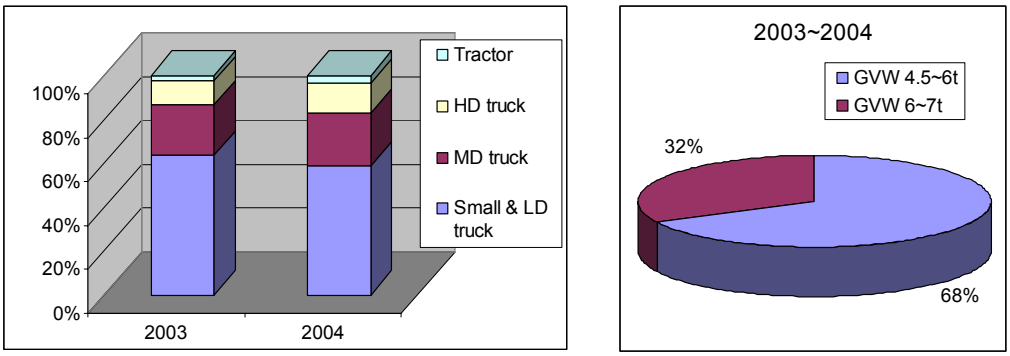

(a) Trucks in Japan **(b) LD trucks in Korea**

Figure 3-1 Truck market status of East Asia

Light-duty truck is usually defined as the truck with a GVW of 4.5 ton to 7.5 ton and a payload of 2 ton to 3.5 ton. The base conventional vehicle is selected in this range. Figure 3-1 illustrates the truck market status of East Asia. In Japan, the small and light duty truck (GVW 3.5t-7.5t) occupies about 60% of the truck market. In addition, as the market of the LD truck has been studied, GVW 4.5t-6t truck has a 68% share in Korea. Therefore, it can be assumed that the truck with GVW 5.5t is the promising variant for the hybrid vehicle.

Figure 3-2 Quarter view of the light-duty truck

Table 3-1 Specification and performance of the base truck

		Base model	Remarks*	
			Isuzu Elf	MMC canter
Gross vehicle weight(kg)		5,500	5,015	5,865
Overall length(mm)		6,175	6,080	6,235
Overall height(mm)		2,030	2,195	1,930
Wheel base(mm)		3,375	3,365	3,350
Engine		4.3litre/ 103 kW/520Nm	4.8L/118 kW /425Nm	4.9L/ 103 kW
Transmission		5 forward speed manual	Automated Manual	5 speed manual
Perfor-mance	Maximum speed(kph)	120	-	-
	Acceleration (s, 0-80kph)	24	-	-

*** These vehicles do not represent the base truck of the developed hybrid trucks. They are the specifications of the existing conventional trucks selected.**

The typical quarter view, detailed specification, and performance of the base light-duty truck are shown in Figure 3-2 and Table 3-1. This vehicle has a 4.3 litre engine and 5 forward speed manual transmission with a GVW of 5.5 ton. This vehicle data will be referred to in the parametric design and modelling of the conventional vehicle. Also, this vehicle has similar specifications to the same class of Japanese truck shown in Table 3-1.

3.2 Comparison of the existing light-duty hybrid trucks

As can be seen in the literature review, there are only a few hybrid examples for light-duty trucks. However, detailed study of the architecture and the main components of those examples is very useful for component selection. Although the number of samples is not many, it provides a good guideline for designing the LD hybrid trucks, because these vehicles have been launched or produced as prototypes.

This comparative study is limited to the same class of light-duty truck with a GVW of 4.5 ton to 7.5 ton as the base vehicle, and 4 examples, i.e., 3 Japanese trucks and 1 USA vehicle, are presented.

3.2.1 HEV architecture

Figure 3-3 shows the HEV architectures of the LD hybrid electric trucks. All the trucks have similar architecture and adapt the single shaft pre-transmission configuration, in which a smaller hybridisation results in better fuel economy. This means that the lower hybridisation rates are preferred in the LD truck category. It is closely concerned with the current status of market, i.e., needs from the customers and difficulty of package layout. As the required volume for the LD hybrid truck is not large, a lot of investment cannot be spent to develop the vehicles.

The Isuzu truck is somewhat different in its architecture from others, in that it uses an existing PTO drive as a torque coupling device. However, this truck can be classified in

the single shaft pre-transmission configuration largely, because all the torques are added before the gearbox and transmitted to the differential through the same shaft.

<table>
<tr><td>Hino Dutro hybrid truck</td><td>Fedex delivery truck</td></tr>
<tr><td> 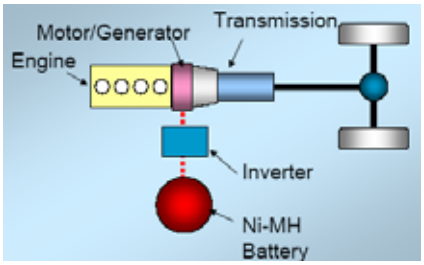
</td><td> 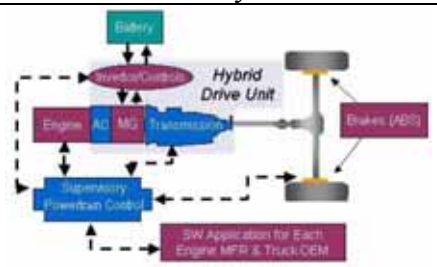
</td></tr>
<tr><td>Isuzu Elf hybrid truck</td><td>MMC Canter hybrid truck</td></tr>
<tr><td> 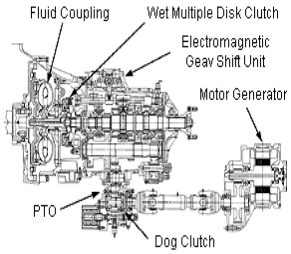
</td><td> 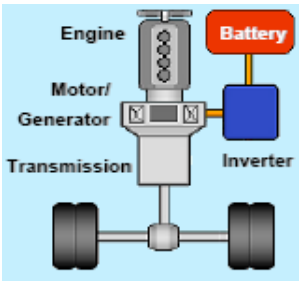
</td></tr>
</table>

Figure 3-3 Configurations of the current LD hybrid trucks (source: [14, 36-38])

As the production feasibility and a lower hybridisation ratio are considered, the general pre-transmission single shaft configuration, such as the Fedex truck, is chosen for this research.

3.2.2 Engine & Electric machine

After choosing the hybrid architecture, the next step is to decide the degree of hybridisation. However, it is very complicated work, because the hybridisation ratio is directly connected to the fuel economy, performance, cost of the vehicle. Therefore, various technical methods to decide the ratio have been reported, for example, approaches based on vehicle performance [19, 22, 23, 39], cost function [24], and computer simulation [10]. Comparative study of competitive LD hybrid trucks is another way to analyse the system technically.

The hybridisation ratio is defined as the ratio expressed in percentage between the electric power and the total propulsion power [10].

Hybridisation ratio = $P_m/(P_m+P_e)$

where P_m and P_e are the maximum power of the EM and the ICE, respectively.

Table 3-2 shows the detailed specification of the engines and electric machines for the same category vehicles as the base truck.

Table 3-2 Comparison of Engines & Electric machines

		Hino Dutro	Isuzu Elf	MMC Canter	FedEx
GVW(ton)		4.8	4.5-5.5	5.5(estimated)	7.2
Engine	Model	N04C-6A	4HL1-HE11	-	OM904
	Type	I4 Diesel	←	←	←
	Displacement(litre)	4	4.8	3.9(estimated)	4.3
	Peak Power(kW)	110	96	90	127
	Peak Torque(Nm)	392	333	-	569
Motor/ Generator	Type	3-phase AC	PM Synchronous	←	←
	Rated Output(kW)	23	25.5(29)	35	44
	Max torque(Nm)	243	274	-	420
Degree of Hybridisation(DOH)		17%	21%	28%	26%

All the vehicles are equipped with a 4 cylinder diesel engine as a primary power source and the engine power rating varies from 90 kW to 127 kW by the total weight of the vehicle. The displacement of the engine is decided between 3.9 litre and 4.8 litre which is enough to produce the required power.

Figure 3-4 reveals that the appropriate engine power rating for the base truck with a GVW of 5.5 ton ranges from 90 kW to 100 kW. This power rating will be confirmed in section 3.4.

It was found that the permanent magnetic synchronous motors are applied mainly as electric machines, because they have several advantages. Permanent magnets provide a loss-free excitation in a compact way without complications of connections to the external stationary electric circuits. So the PM motor can be potentially designed with high power density, high speed, and high operation efficiency, and it is easy to be controlled and cooled. The only drawback is the high cost of permanent magnets due to the rarity in the earth. As of now, this type of motor is the most promising candidate for EV and HEV application.

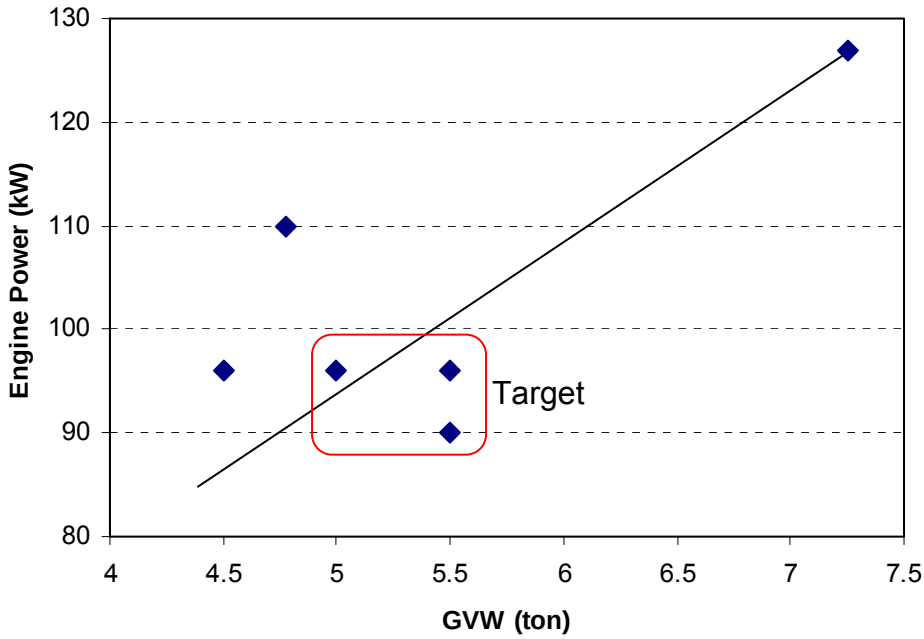

Figure 3-4 Engine power rating vs. GVW

The power rating of the EM for these vehicles ranges from 23 kW to 44 kW and the hybridisation degree is designed below 30%. As these factors usually depend on the HEV concept, the trend can be changed easily. However, this range and trend seem to be an appropriate reference for the LD truck, because all the vehicles were constructed and tested.

3.2.3 Energy storage systems

As shown in Table 3-3, the energy storage system applied in the light-duty hybrid truck is mostly the battery pack system. The other kinds of storage system are excluded from this report considering the rarity of the system in the field of the LD hybrid truck and the range of this research.

Table 3-3 Comparison of Battery pack

		Hino Dutro	Isuzu Elf	MMC Canter	FedEx
Battery Pack	Type	Ni-MH	Lithium-Ion	Lithium-Ion	Lithium-Ion
	Voltage(V)	273.6	173	173	288
	Capacity(Ah)	6.5	3.6	5.5	3

The Hino Dutro hybrid truck has an Ni-MH battery pack, and others are equipped with Lithium-Ion type batteries. The battery capacities are chosen differently, depending on the power capacity of electric machines and driving condition.

Table 3-4 Properties of Battery (source : [40])

Battery type	Specific Energy (Wh/kg)	Specific Power (W/kg)	Energy Efficiency (%)	Cycle Life	Self-Discharge (% / 48h)	Estimated Cost (US$/kWh)
Lead-acid	35-50	150-400	80	500-1000	0.6	100-150
Nickel-cadmium	30-50	100-150	75	1000-2000	1	250-350
Nickel-metal-hydride	60-80	200-300	70	1000-2000	6	200-350
Aluminum-air	200-300	100	<50	?	?	?
Zinc-air	100-220	30-80	60	500	?	90-120
Sodimu-sulfur	150-240	230	85	1000	0	200-350
Sodium-nickel-chloride	90-120	130-160	80	1000	0	250-350
Lithium-polymer	150-200	350	?	1000	?	150
Lithium-ion	80-130	200-300	>95	1000	0.7	200

Table 3-4 shows the properties of several battery systems. In the past, lead-acid batteries have been frequently studied for their application to commercial vehicles due to the maturity of technology and the cheaper cost. However, as the specific power and energy efficiency becomes more important for HEV application, interest has turned to the advanced battery system, such as Ni-MH or Lithium-ion system, despite the high cost. As can be seen in Table 3-4, the performance and efficiency of the advanced battery are better than the conventional lead-acid battery. In particular, the Lithium-ion battery is considered to be the most favourable solution for the near future. Therefore, the lithium-ion battery is preferred.

3.2.4 Transmission

As mentioned before, the type of transmission is important in the pre-transmission configuration. This is because the gearbox has an effect on both engine torque and motor torque. When the transmission is operated automatically by the optimised map, better energy efficiency is expected. So all the trucks presented in Table 3-2 are equipped with automated manual transmissions.

3.3 Component sizing

The next step is to define the parameters of HEV. This component sizing is performed based on the performance requirement and the result will be confirmed by the boundary condition discussed above.

The vehicle power sources must be sized for the vehicle weight, load condition, and performance goals. This is because the vehicle propulsion system traction is set by the vehicle mass and acceleration performance. So, first of all, the target performance and the required constraints are presented for the design of HEV drive train parameters. These data are based on the specification and performance of the base conventional truck. The overall parameters and target performance are as follows.

- Vehicle mass (GVW) 5,500kg
- Rolling resistance coefficient 0.01
- Aerodynamic drag coefficient 0.6
- Front area $3.73m^2$
- Air density $1.205kg/m^3$
- Rolling radius of driven wheels 0.367m
- $\eta_{t,e}$ 0.9
  (the transmission efficiency from engine to drive wheels)
- $\eta_{t,m}$ 0.95
  (the transmission efficiency from motor to drive wheels)
- Target performance based on the performance of the conventional vehicle
  - Vehicle maximum speed 120km/h (33m/s)
  - Acceleration performance (0-80kph) 24s

The transmission efficiency from engine to drive wheels is assumed to be lower than the motor transmission efficiency, because it is transmitted through the EM.

3.3.1 Design of engine power capacity & final drive ratio

As the grade effect is neglected which is not included in all the standard drive cycles, the total power of vehicle can be expressed as:

$$P_{\max} = \frac{v_{veh}\left(M_v g f_r + \frac{1}{2}\rho C_d A v_{veh}^{\ 2} + M_v \delta \frac{dv}{dt}\right)}{1000\eta_t} \qquad (3\text{-}1)$$

where P_{max} - Vehicle maximum power (kW)
v_{veh} - Vehicle speed (m/s)
M_v - Vehicle weight (kg)
g - Acceleration of gravity (m/s^2)

f_r - Rolling resistance coefficient

ρ - Air density (kg/m^3)

C_d - Coefficient of air drag

A - Front area of the vehicle (m^2)

η_t - Transmission efficiency

δ - Correction coefficient of rotating mass

As the power of HEV is supplied by the ICE and EM, the engine power can be calculated from the steady state portion of the power, while the dynamic load is related to EM. Thus, the engine power, related to the steady load, is:

$$P_e = \frac{v_{veh}\left(M_v g f_r + \frac{1}{2}\rho C_d A v_{veh}^{\ 2} \right)}{1000\eta_{t,e}} \tag{3-2}$$

where P_e is the engine power and $\eta_{t,e}$ is the transmission efficiency from the engine to the drive wheels.

It is seen that an engine power of 75.5 kW is needed for the target performance. The 10% power is considered as spare power to charge the battery. Therefore, the final engine power capacity is finally estimated:

$P_e = 75.5 \text{ kW}/0.85 \times 1.1 = 97.7 \text{ kW}$

where 0.85 is the average charge efficiency.

In order to determine the final drive gear ratio based on the maximum speed requirement, the highest gear ratio of transmission is needed. The light-duty trucks generally have 5-forward or 6-forward speed transmission with overdrive ratio. The highest overdrive ratio is usually between 0.7 and 0.75. The appropriate transmission for this engine, which is combined with it in the conventional truck, is the 5-forward speed gearbox with the highest gear ratio of 0.722 and this ratio is considered to be the same as the hybrid electric vehicle.

The vehicle speed is proportional to engine speed and inversely proportional to the total gear ratio.

$$v_{veh} = 0.377 \times \frac{R_{whl} N}{i_g \times i_{fd}} \tag{3-3}$$

where R_{whl} - Rolling radius of the drive wheels(m)

N - Engine speed (rev/min)

i_g - Gear ratio

i_{fd} - Final drive ratio

The final drive ratio can be determined as 4.625 for a hybrid vehicle with a maximum speed of 120km/h, according to the overall parameters, the rolling radius = 0.367m, the max engine speed = 2900 rev/min, the highest gear ratio 0.722.

3.3.2 Design of electric machine & battery

From the equation (3-1), the equation for the EM concerned with the dynamic load can be represented as follows:

$$P_m = \frac{M_v \delta}{2\eta_{t,m}\, t_a}\left(v_f^2 + v_b^2\right) \tag{3-4}$$

where P_m - Motor power (kW)

δ - Correction coefficient of rotating mass, 1.04

$\eta_{t,m}$ - Transmission efficiency from motor to the drive wheels

v_f - Final high speed to which the vehicle is accelerated from 0 speed (m/s)

v_b - Velocity speed corresponding to the base speed of the motor (m/s)

t_a - Acceleration time (s)

According to the parameters of the light-duty truck and the permanent magnet motor with the maximum speed of 4000 rev/min and the base speed of 1100 rev/min, the peak power of motor is calculated as 61.7 kW. However, it should be noted that the motor power obtained is overestimated, because the engine has some remaining power to help acceleration. So the motor power has to be determined as smaller than that calculated above.

Figure 3-5 shows the remaining engine power at the fifth gear ratio. To calculate the average remaining engine power, the Matlab program is used. The program code is presented in Appendix #1. The average remaining power of the determined engine is obtained as 31.8 kW. Hence, the final motor power capacity can be determined as 30 kW.

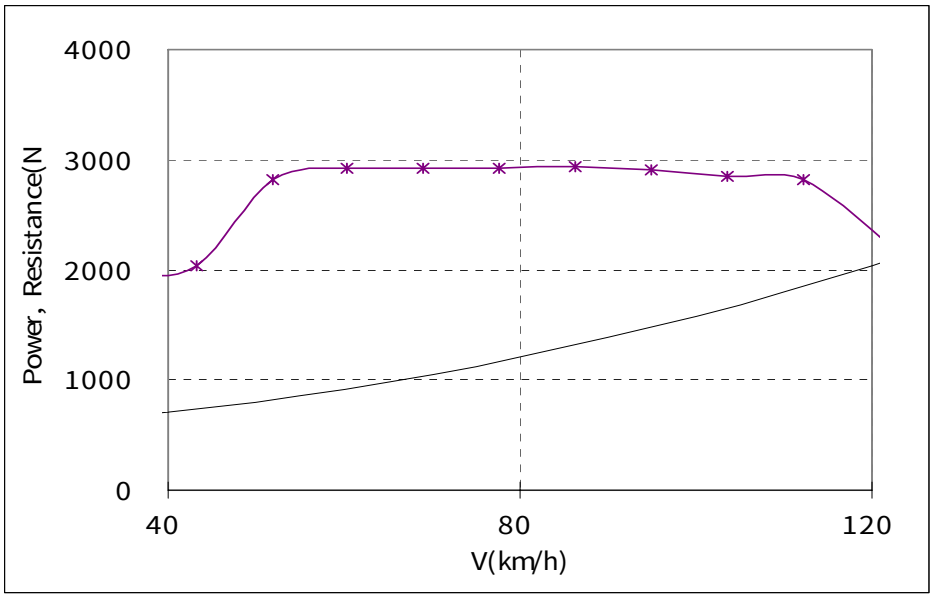

Figure 3-5 Engine power vs. resistance

Battery design is mainly concerned with two factors: power and energy capacity. Although the power capacity can be determined by the equation (3-4), the energy capacity design is closely associated with the drive cycles.

So as it is a somewhat complicated issue, it is hard to generalise the way to design battery. A more practical method is to apply the same grade of battery with the same class of vehicle with a similar capacity of motor and to verify the capacity using simulation later. For this reason, the battery capacity is determined based on the battery of the Isuzu Elf hybrid truck, which has 173V and 3.6Ah of Lithium-ion battery, as important is to give estimated weight.

3.4 Discussion

Table 3-5 shows the results of the comparative study on the existing LD hybrid trucks, the rough boundary of the HEV system, and the component definition which is based on the performance requirement. The results are similar but can be varied for the target market and drive cycle. It is seen that the motor size is relatively smaller than that of the engine, i.e., a lower hybridisation ratio (17-28%). This means that the power capacity for a steady state load, in other words the engine capacity is more important than that for a dynamic load related EM, or acceleration performance.

Table 3-5 Summary of HEV architecture and component

	Comparative study	Component sizing
Configuration	Single shaft pre-transmission	-
Engine power rating	90 kW - 100 kW	97.7 kW
Electric motor capacity	23 kW - 44 kW	30 kW
Battery	Lithium-Ion battery	
Transmission	Automated manual transmission	

4 Component modelling

This Chapter is for the modelling of the mechanical components. It explains the major component modelling and the data related to each component. The control strategies are presented in the next Chapter. After modelling each component, a simple component test without control concept is performed to verify the function and data.

Through this methodology, the control variables can be determined or the related data can be modified by the targeted control variables. In the case of the engine modelling, there are many kinds of ways to do this, according to the control input and outputs. If the torque demand as an input signal and torque output as an output signal are selected, the data for torque and engine speed are needed. If the fuel consumption of the engine is considered to be an output, the fuel consumption map will be needed. Hence, the required data can be changed according to the control variables and the type of model.

As can be seen, in order to build a reliable model, a lot of information on each component is needed. The more accurate data secure the appropriate operation and results but it is very difficult to obtain the exact data for all the main components. So the information on the needed data and parameters were derived from many paths. The data were obtained from the literature, such as journal papers and reports, the Internet, and other modelling tools. Some information is inserted in each model but others were changed and modified by the related models. Sometimes calculation and reasonable assumption are needed. The more details are presented in the modelling of each component.

As two models are built for a comparative study between the light-duty conventional truck and the hybrid electric truck, some components need two values. These data are presented in order of component.

All the components, except for the controller, are modelled on the basis of the AMESim simulation tool. It has many built-in models with related mathematical relations inside.

Therefore, the appropriate model has to be selected for the control variables and the data met the AMESim data format should be entered. The features and mathematical models for each built-in model are referred to from the manual [41].

There are five special data formats which are very widely used in this software: 1D table, 2D table, 3D table, table of 1D table, and XYs table. Each component model requires different types of data formats. In order to operate the selected model properly, the data format has to be considered as well as the accuracy of the data.

4.1 Overview of vehicle models

Figure 4-1 shows the mechanical models of the light-duty hybrid electric vehicles built in AMESim. It consists of 6 parts largely, engine, clutch, transmission, motor/generator, battery, and vehicle dynamics and has some small sensors and torque coupling devices, too. These components are now explained and the related data presented.

The model for the conventional vehicle is not presented here but is shown in the next Chapter, because it is quite simple compared with the hybrid electric vehicle. However the related data are tackled here.

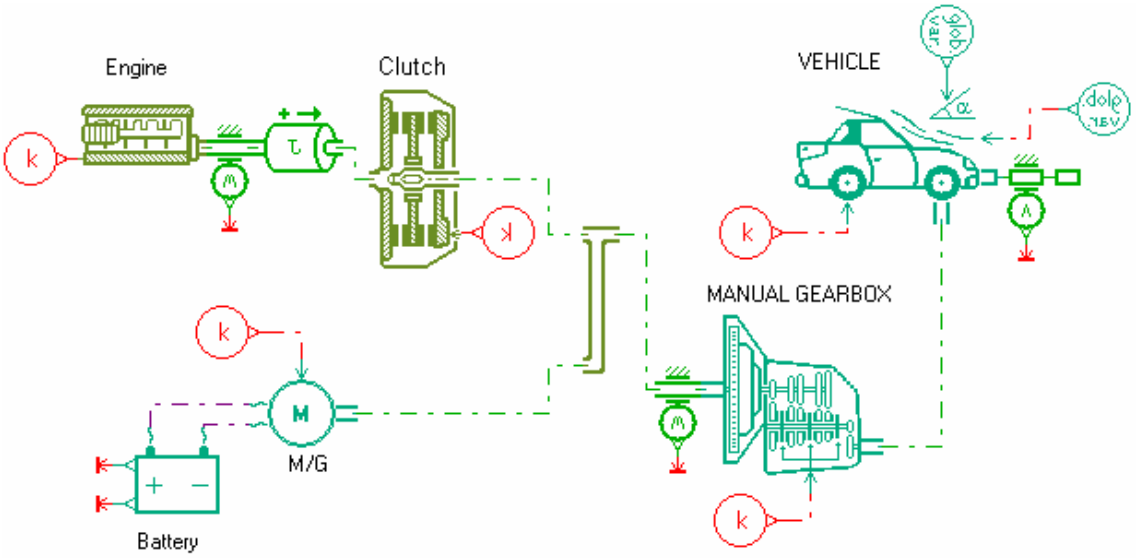

Figure 4-1 Overview of the mechanical part of the hybrid electric vehicle

4.2 Engine model

The engine is very important in the hybrid vehicle, in that it acts as the primary power source. In other words, the engine is concerned with the basic performance and fuel economy of the vehicle. In this respect, the engine model has the output variables related to output torque by the torque demand and engine speed. So the torque map and fuel map are required.

There are two basic built-in engine model series in AMESim. One is TREN series which is simple and generates the torque and engine speed by the torque demand. The other is DRVICE00A which is more complex and considers the calculation of emission and fuel economy as well as output torque. It considers the thermal combustion mode, too.

Because the emission effect is not considered in this research, the emission maps are not needed and the simple TREN series, is therefore enough for this research. In more detail, although four kinds of TREN series are provided by the data format or variables, TREN0B has been selected for this study.

Figure 4-2 Engine model

This model represents the engine with the output torque defined by ASCII file T=F(w, teta) and can be controlled by the throttle position. The shaft speed (rev/min) is input at port 1 and a dimensionless signal is input at port 2 which can be interpreted as the throttle position, as shown in Figure 4-2. The output torque (Nm) is computed as a function of the two inputs defined in a data 2D table and output at port 1.

Table 4-1 Engine specifications

	Conventional	HEV	Remarks
Weight(kg)	395	364	- 31kg
Type	In-line 4 cylinder Diesel	In-line 4 cylinder Diesel	
Displacement(litre)	4.3	3.9	Downsizing : 0.4litre
Peak Power(kW/rpm)	100	103/2900	
Peak Torque(Nm/rpm)	520/1600	372/1800	

Table 4-1 summarises the general specification of the engines for the conventional truck and the hybrid electric truck. As the engine power is determined as 97.7 kW on the basis of the vehicle performance estimation, this engine with slightly more power is selected. This engine is a diesel engine with 4 cylinders. Even though these two engines have the same range of power rating, the torque of the HEV engine is much lower than that of the base one due to the downsizing of displacement. However, this lack of torque can be compensated for through the electric machine in the hybrid electric vehicle. So the downsizing does not have an effect on vehicle performance.

Figures 4-3 and 4-4 depict the maximum engine torque and the fuel consumption map of the conventional engine and the downsized engine for the hybrid electric vehicle respectively. As the required data formats are 1D and 2D table for torque and fuel consumption map, the data were rearranged.

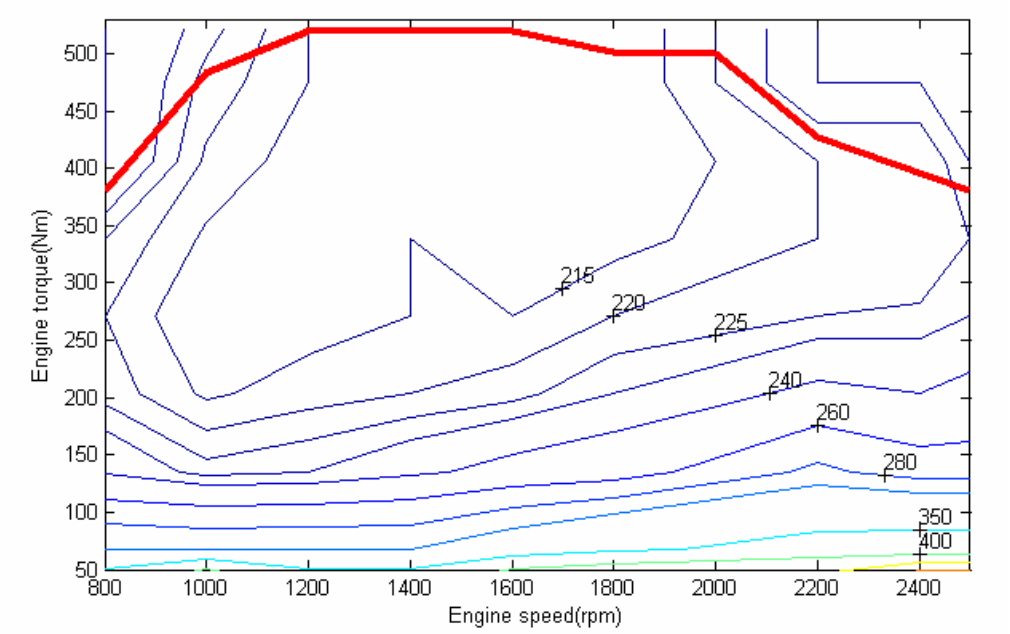

Figure 4-3 Maximum torque and fuel consumption map for the conventional vehicle

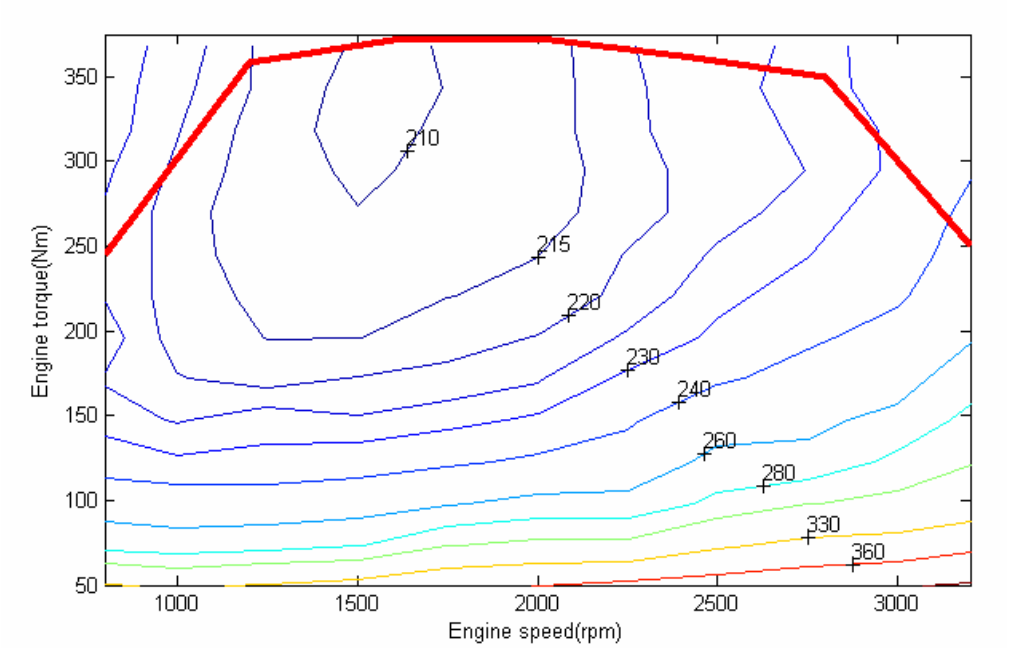

Figure 4-4 Maximum torque and fuel consumption map for HEV

The remaining data for the engines are the engine friction loss, or zero torque command. They are not common and hard to obtain. It is presumed that the engine friction loss is proportional to the piston displacement. As the engine loss data for the 1 litre and 4.8 litre engines were presented [25, 37], the friction loss could be obtained through a

simple Matlab program using interpolation. The program is presented in Appendix #2. As a result of the interpolation, the engine friction loss data for the modelled engines appear in Table 4-2.

Table 4-2 Engine friction data (Nm)

Speed (rev/min)	800	1000	1200	1400	1600	1800	2000	2200	2500	2900	3200
3.9 litre	-32	-36	-40	-43	-45	-47	-49	-53	-56	-64	-68
4.3 litre	-36	-40	-45	-48	-50	-52	-54	-58	-63	-	-

4.3 Transmission

Although various transmissions can be built by using many sub-models, there are 5 kinds of built-in transmission model in AMESim: 3 kinds of manual transmission, an automatic transmission, and a CVT model. As the transmission types were decided, a manual gearbox is needed for the conventional vehicle and an automated manual transmission is needed for the HEV. So only the details for manual transmission models are referred to here.

- DRVMG0A - n-ratio gearbox (included clutch)
  This model can be used to achieve a simple dynamic modelling of an n-ratio manual gearbox and includes the clutch.

- DRVMG0B - n-ratio gearbox (without clutch)
  This model is a simple dynamic model without clutch. So the clutch should be modelled and combined to this model later.

- DRVMG0C - n-ratio gearbox (without clutch)
  This model is similar to DRVMG0B but considers the thermal effect.

These three models have the same functions basically and the same outputs can be obtained if the inputs are chosen properly. As the thermal effect is not considered in this study and the complicated control strategy is applied later, DRVMG0A has been selected. In addition, this model can be used in the hybrid electric vehicle as an automated manual transmission if the appropriate controller is built and combined as well as in the conventional truck.

The external variables of transmission appear in Figure 4-5. If the gearbox control signal is entered at port 1, the input torque at port 3 from the engine is transmitted to port 2 after applying the gear ratio and the final drive ratio given. The rotary velocity is transmitted in the opposite direction. These relations can be represented as follows:

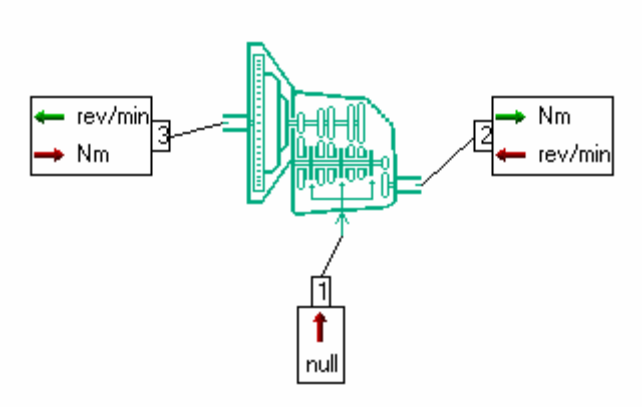

Figure 4-5 Transmission model including clutch

The torque transmitted by the synchronizer T_s is

$$T_s = T_{slip} \times \tanh\left(2 \times \frac{\omega_{rel}}{\omega_{thr}}\right) \tag{4-1}$$

where T_{slip} - Maximum Coulomb friction torque (Nm)

ω_{rel} - Relative rotary velocity (rad/s)

ω_{thr} - Rotary velocity threshold (rad/s)

The primary shaft torque T_p is deduced as follows:

$$T_p = \frac{1}{\eta_g} \times \frac{-T_s}{i_g} \tag{4-2}$$

where η_g - Efficiency of the engaged gear

i_g - Transmission ratio of the engaged gear

Finally, the rotary velocity s and the torque t2 transmitted by the powered are calculated.

$$\omega_s = -\omega_2 \times i_{fd} \tag{4-3}$$

$$T_2 = -\eta_{fd} \times T_s \times i_{f\,d} \tag{4-4}$$

where ω_2 - Input rotary velocity (rev/min)

i_{fd} - Final drive ratio

η_{fd} - Efficiency of the final drive axle

T_s - Torque transmitted by the gearbox

The transmission data are obtained from the transmissions matched with the modelled engine in the conventional vehicle. The summary of data is shown in Table 4-3.

Table 4-3 Transmission data

			Base truck	HE truck
Type			5-forward speed manual	5-forward speed automated manual
Gear ratio & Efficiency	1st	90%	5.37	5.38
	2nd	90%	2.97	3.028
	3rd	90%	1.66	1.77
	4th	93%	1.00	1.0
	5th	90%	0.74	0.722
Maximum Coulomb friction torque			10000Nm	←
Rotary velocity threshold			100	←
Final drive ratio			3.727	4.625

4.4 Electric machine

In general, the EM and battery serve as a secondary power source to assist the primary power source, usually ICE, in parallel hybrid configuration. So these two models have to be considered simultaneously. It is a motor or generator, irrespective of whether the battery is included. In motor mode, the appropriate torque has to be produced by the input torque and the battery is discharged according to the consumed energy. On the other hand, if the minus input torque is given in generator mode, the battery is charged through the generator. Hence, the basic function of the electric machine is to convert the electric energy to the mechanical energy or the reverse operation.

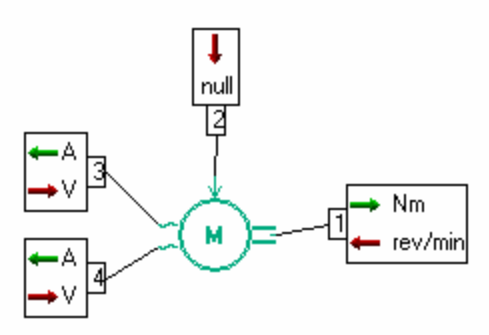

Figure 4-6 Electric machine

The electric machine model provided in AMESim is shown in Figure 4-6. This model uses the data files to calculate the outputs. It can be operated as a motor or generator according to the input torque demand. Its function is quite simple. When the input torque demand is given at port 2 and the voltage from the battery at port 3 and 4 in motor mode, the output torque can be computed and produced at port 1 by using torque and loss data files. So it is able to be used for all electric machines, regardless of the type of the electric machine and the converter. In other words, this model is independent from the motor and its converter.

The mathematical relations for this model are as follows. The motor torque is determined from the limited reference torque by a first order transfer function.

$$T_m = \frac{1}{1+\tau s} T_{\lim} \tag{4-5}$$

where T_m - Torque on the shaft of the motor at port 1 (Nm)

τ - Time constant (s)

T_{lim} - Limited torque (Nm)

The electric machine has friction loss and the electric power of the machine is composed of the mechanical power and the loss power. P_{el} is greater than P_{mech} in motor mode, but P_{el} is less than P_{mech} in generator mode. The power loss of the EM, P_{lost}, includes the loss by the power electronics, because the converter is not needed for the designed EM model in AMESim. So the total power loss data are considered.

$$P_{el} = P_{mech} \pm P_{lost} \tag{4-6}$$

The electric power and the mechanical power can be calculated by these simple equations.

$$P_{el} = VI \tag{4-7}$$

$$P_{mech} = T_m \times \omega \tag{4-8}$$

where P_{el} - Electric power (W)

V - Voltage at port 3 (V)

I - Current at port 3 (A)

P_{mech} - Mechanical power (W)

T_m - Motor torque at port 1 (Nm)

ω - Rotary velocity at port 1 (rad/s)

However, as the sign convention of AMESim is reverse to the classic convention, equation (4-6) has to be calculated carefully. In motor mode, as the signs of the torque and the rotary velocity are reversed, so $P_{mech}<0$, the lost power has to be subtracted. In generator mode, P_{mech} becomes greater than zero.

The motor capacity was estimated as 30 kW in Chapter 3 and the motor is required to have a lower rotary speed considering the speed of the diesel engine. However, it is very difficult to find out the motor data to meet the requirement accurately. Hence, after obtaining information on the motor with a similar speed range, scaling to meet the power requirement is needed.

In that sense, the motor of the Isuzu Elf truck is available [37]. This motor has a speed range between 0 and 4000 rev/min and 25.5 kW of peak power. The base speed is 1100 rev/min. In order to meet the required power, i.e. 30 kW, scaling is carried out. Figure 4-7 is the modified power and efficiency after scaling.

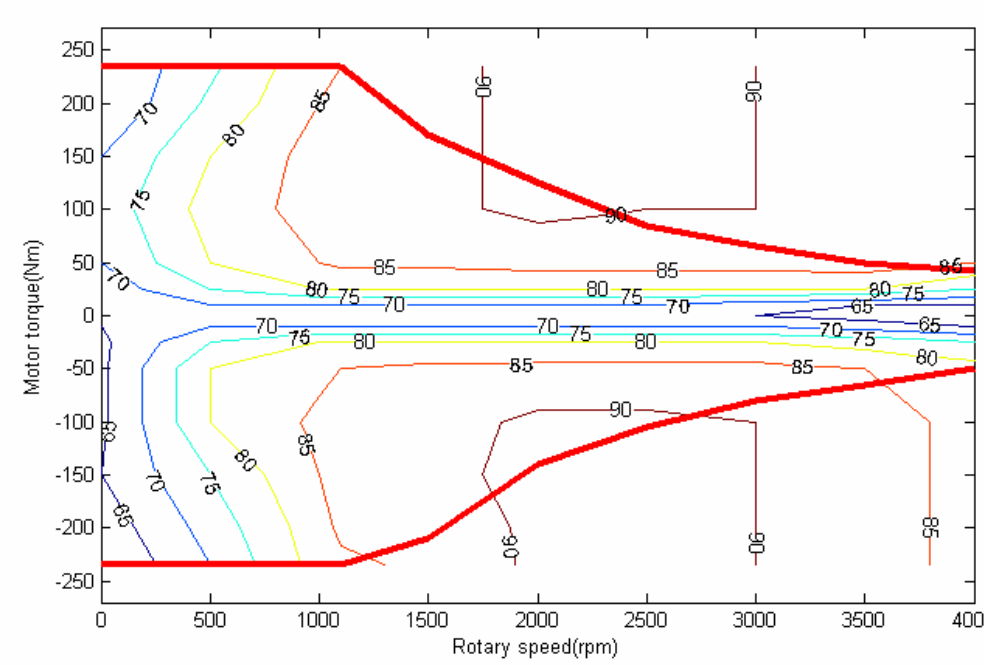

Figure 4-7 Motor efficiency map

P_{lost} can be expressed in general by using input and output power:

$$P_{lost} = P_{in} - P_{out} \tag{4-9}$$

By using the equation (4-8) and considering the efficiency, the output power in motor mode is calculated.

$$P_{out} = T_m \times \omega = \eta_m \times P_{in}$$

Thus $$P_{lost} = P_{in} - P_{out} = T_m \times \omega(1/\eta_m - 1) \quad (4\text{-}10)$$

In generator mode, P_{in} is P_{mech}. That is:

$$P_{in} = T_m \times \omega = 1/\eta_m \times P_{out}$$

As P_{lost} should be always positive and the torque is negative in this mode,

$$P_{lost} = | P_{in} - P_{out} | = | T_m \times \omega(1 - \eta_m) | = T_m \times \omega(\eta_m - 1) \quad (4\text{-}11)$$

Finally, the P_{lost} can be obtained from equations (4-10) and (4-11) by using the efficiency map above. The loss of the power electronics are included by considering the average efficiency, 0.9. Because it needs a lot of interpolation and calculation, the power loss data are obtained though Matlab programming. The program source is presented in Appendix #3.

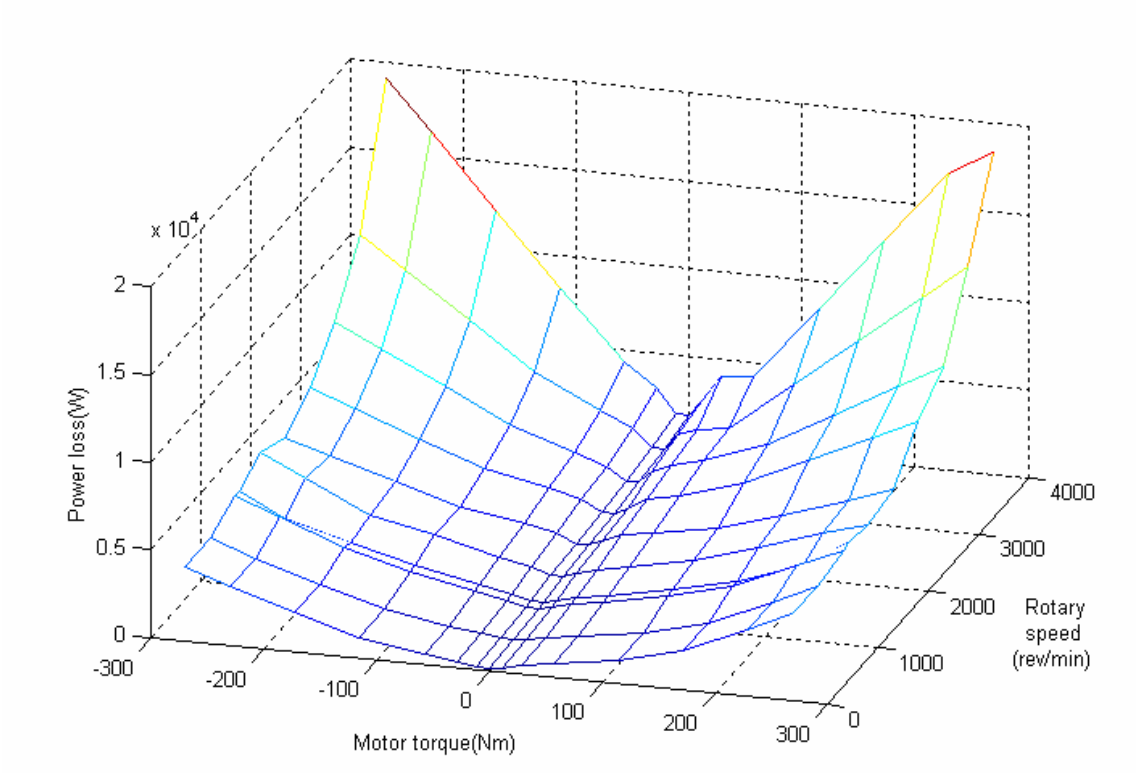

Figure 4-8 Power loss data

During the programming, more problems occurred. When the rotary speed of the motor is zero, the torque cannot be calculated by using the efficiency map, because its input power, $T_m\omega$, becomes zero. However, there is apparently loss at 0 rev/min. In order to solve this problem, the same method as ADVISOR is applied. The nearest loss data at 500 rev/min is copied to the place at zero speed. Although not exact, it can be considered to be reasonable, because the operation at this zone occurs very rarely in the drive cycle. For the zone of zero torque, the same method as ADVISOR is applied, too. Figure 4-8 shows the power loss calculated from the motor efficiency map. As the magnitude of the torque increases, the power loss increases.

4.5 Battery

The battery system is closely associated with the electric machine, as this is used as a power source and energy accumulation system. That is to say, it has to provide enough electrical energy to the motor in motor mode and charge the mechanical energy from the electric machine in generator mode.

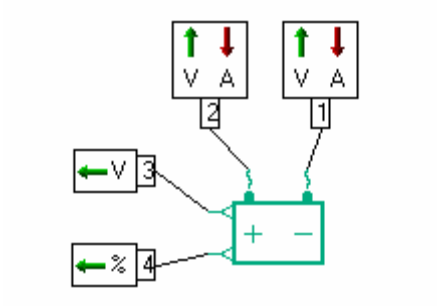

Figure 4-9 Battery model

This submodel is an internal resistance model and can be defined by the open circuit voltage and an internal resistance. As Figure 4-9 indicates, there are 4 ports. Port 1 and 2 are battery terminals which can be combined with the electric machine for charging and discharging. Port 3 generates the open circuit voltage as an output and Port 4 gives the state of charge.

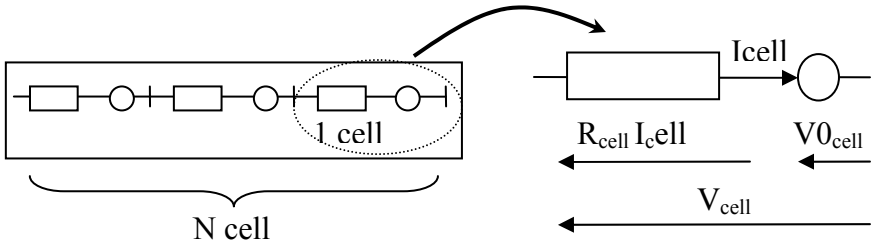

Figure 4-10 Structure of battery bank and cell

This battery is made up of banks in serial and parallel arrangements and each battery bank consists of cells. Figure 4-10 depicts a structure of a battery bank. As the output voltage of one cell is calculated by the equation (4-12), the voltage of a bank is decided by the number of cells per banks.

$$V = V_o - R \times I \tag{4-12}$$

where V - Output voltage (V)

V_0 - Open circuit voltage (V)

R - Equivalent internal resistance (ohm)

I - Input current (A)

In the same way, the total terminal voltage of battery (V_{tot}) can be calculated easily by the number of banks in serial arrangement.

$$V_{tot} = V_{bank} \times S_{bank} = V_{cell} \times N_{cell} \times S_{bank} \tag{4-13}$$

where V_{bank} - Bank output voltage (V)

S_{bank} - Number of battery banks in serial arrangement

V_{cell} - Cell output voltage (V)

N_{cell} - Number of cells in series per bank

The state of charge (SoC) at port 4 is calculated by subtracting the depth of discharge (DoD) from 100% and DoD is expressed in per cent as follows:

$$DoD = \frac{q}{Q_{nom}} \times DoD_0 \qquad (4\text{-}14)$$

where q - Charge used by the load (As)

Q_{nom} - Rated capacity (As)

DOD_o - Initial depth of discharge (%)

As the battery system type and the capacity were decided in Chapter 3, the related data are obtained. ADVISOR provides the open circuit voltage and the internal resistance for a cell of a lithium-ion battery.

The internal resistance is different for charging and discharging and this is considered in ADVISOR. However, in the AMESim model, the difference is not considered and only one resistance data has to be inserted. Hence, it is assumed that the charging phase occurs in the same period as the discharging phase and the average resistance is used in the battery model.

The input data for the battery model are shown in Table 4-4 and Figure 4-11. To meet the required voltage, the number of cells per the battery bank is set to 3 and the number of the bank is set to 32 in series.

Table 4-4 Parameters of battery system

	Parameters
Rated capacity of the battery	6 Ah
No of cells in series per battery bank	3
No of battery banks in parallel	1
No of battery banks in series	32
Total terminal voltage	346 V

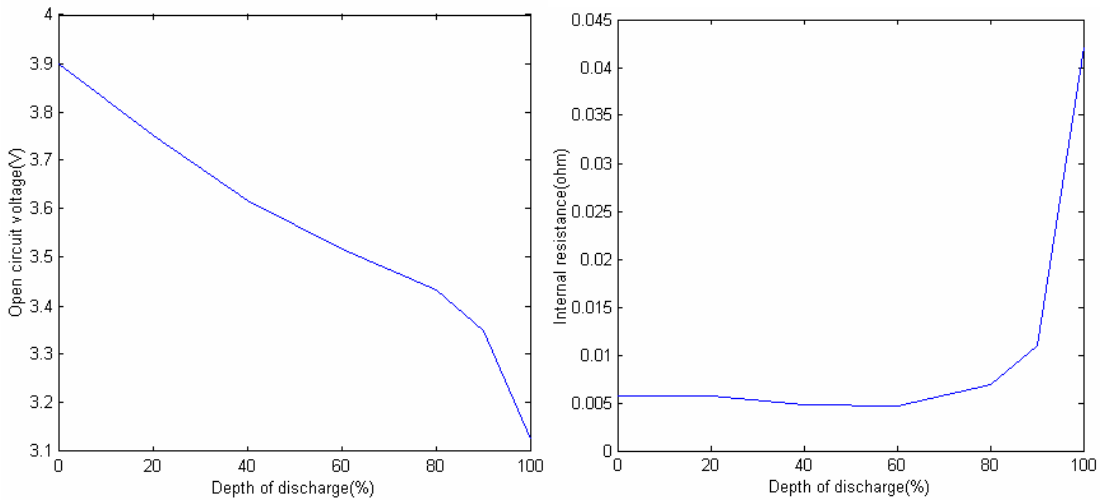

Figure 4-11 Open circuit voltage and internal resistance of a cell of the battery

4.6 Clutch

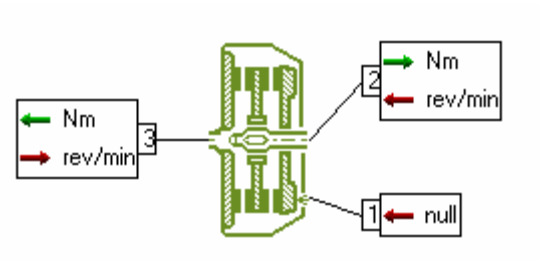

Figure 4-12 Open circuit voltage and Internal resistance of battery

The clutch model is used in the modelling of the hybrid electric truck to engage or disengage the engine torque in this research. There is no necessity to apply this model to the conventional vehicle, because the transmission including clutch is used.

Figure 4-12 depicts the external variable of the friction torque transmission clutch model. This represents the one-dimensional motion of two inertias under the action of frictional force. When the clutch control signal between 0 and 1 is given at port 1, this clutch will be engaged or disengaged. The meaning of the signal is somewhat strange. Note that 1 signal means not engagement but disengagement.

This model's mathematical relation is as follows:

$$F_{fric} = F_{dyn} \times \tanh\left(2 \times \frac{v_{c\_rel}}{v_{c\_thr}}\right)$$

where F_{fric} - Friction force developed between the two plates

F_{dyn} - Coulomb friction force modulated by the command input and the velocity threshold

v_{c_rel} - Relative velocity between the shafts

v_{c_thr} - Velocity threshold

The used parameters for this model are shown in Table 4-5.

Table 4-5 Parameters of clutch

	Parameters
Maximum Coulomb friction torque	465 Nm
Rotary velocity threshold	1 rev/min

4.7 Vehicle model

In order to simulate the acceleration behaviour and the fuel consumption in a drive cycle, the longitudinal resistance is the only interest for the vehicle. So the vehicle has to be modelled to show the vehicle performance against the resistance. The resistance includes the rolling resistance, the aerodynamic drag, and slope resistance. In other words, this model predicts the vehicle performance and behaviour, such as the velocity and the acceleration performance, for the given torque and the rotary speed from the powertrain.

The vehicle model to reflect these resistances is provided in AMESim as illustrated in Figure 4-13.

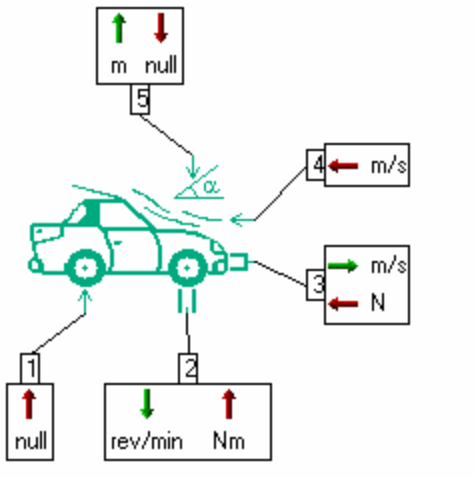

Figure 4-13 Vehicle model

This model does not consider any lateral behaviour and there in no difference between left and right wheels. The signal input at port 1 is a braking control which is between 0 and 1. Signal 1 means the maximum braking torque demand. Port 2 is for the torque input from the powertrain. Port 3 is used to evaluate the longitudinal vehicle velocity and can be used to add a resisting force from the outside. Ports 4 and 5 are the wind velocity input and the road slope respectively. Therefore, when the output torque through the driveline is given at port 2, the vehicle velocity, displacement, and acceleration performance can be calculated considering the given driving condition.

The mathematical relations for this model are as follows. The equivalent mass in linear motion is calculated by considering the rotating mass.

$$M_{equ} = M_v + \frac{J}{R_{whl}^2} \tag{4-15}$$

where M_{equ} - Mass of the vehicle (kg)

J - Inertia of the 4 wheels ($kg.m^2$)

R_{whl} - Wheel radius (m)

The rolling resistance F_{roll} is:

$$F_{roll} = M_{equ} \cdot g(f + kv_{veh}) \tag{4-16}$$

where f - Rolling friction coefficient

k - Velocity coefficient

v_{veh} - Vehicle linear velocity (m/s)

The aerodynamic resistance F_{aer} is:

$$F_{aer} = \frac{1}{2}\rho \cdot C_d \cdot A \cdot (v_{veh} + v_{wind})^2 \tag{4-17}$$

where v_{wind} - Head wind speed (m/s)

ρ - Air density (kg/m^3)

C_d - Coefficient of air drag

A - Front area of the vehicle (m^2)

The climbing resistance can be calculated but not considered in this research because the slope is assumed to be 0%.

Therefore, the global equation ruling this vehicle model can be expressed by using the first principle of mechanics.

$$a = \frac{1}{M_{equ}}\left[\left(\frac{T_2}{R_{whl}} - \frac{T_{brk}}{R_{whl}}\right) - F_{roll} - F_{aer} - F_{cl} - F_{ext}\right] \tag{4-18}$$

where a - Vehicle linear acceleration (m/s^2)

T_2 - Input torque at port 2 (Nm)

T_{brk} - Braking torque (Nm)

F_{roll} - Rolling resistance (N)

F_{aer} - Aerodynamic drag (N)

F_{cl} - Climbing resistance (N)

F_{ext} - Input optional force (N) at port 3

From the relations above, it is assumed that the climbing resistance and the optional force from the outside are zero. Additionally, the vehicle specification of the hybrid electric truck is the same as that of the conventional vehicle. The input parameters are shown in Table 4-6.

Table 4-6 Parameters of the vehicle model

Variables	Parameters
Mass of vehicle	5,500 kg
Tyre width	178 mm
Tyre height	75%
Wheel rim diameter	16 in
Inertia of the 4 wheels	3.22 kg.m^2
Maximum braking torque	13700 Nm
Rolling friction coefficient(f)	0.01
Coefficient in rolling resistance(k)	0
Aerodynamic drag coefficient(C_d)	0.6
Frontal area	3.73 m^2

4.8 Verification of component model

In order to verify the function and performance of each component, two basic models were built and some simple tests carried out. One model is for the mechanical component and the other for the electrical parts. The verification is conducted by entering a simple input signal without any driver model or controller.

4.8.1 Mechanical component model

The basic model to verify the function of the mechanical components is illustrated in Figure 4-14. This model does not include any electrical parts and consists of 3 parts: engine, transmission, and vehicle.

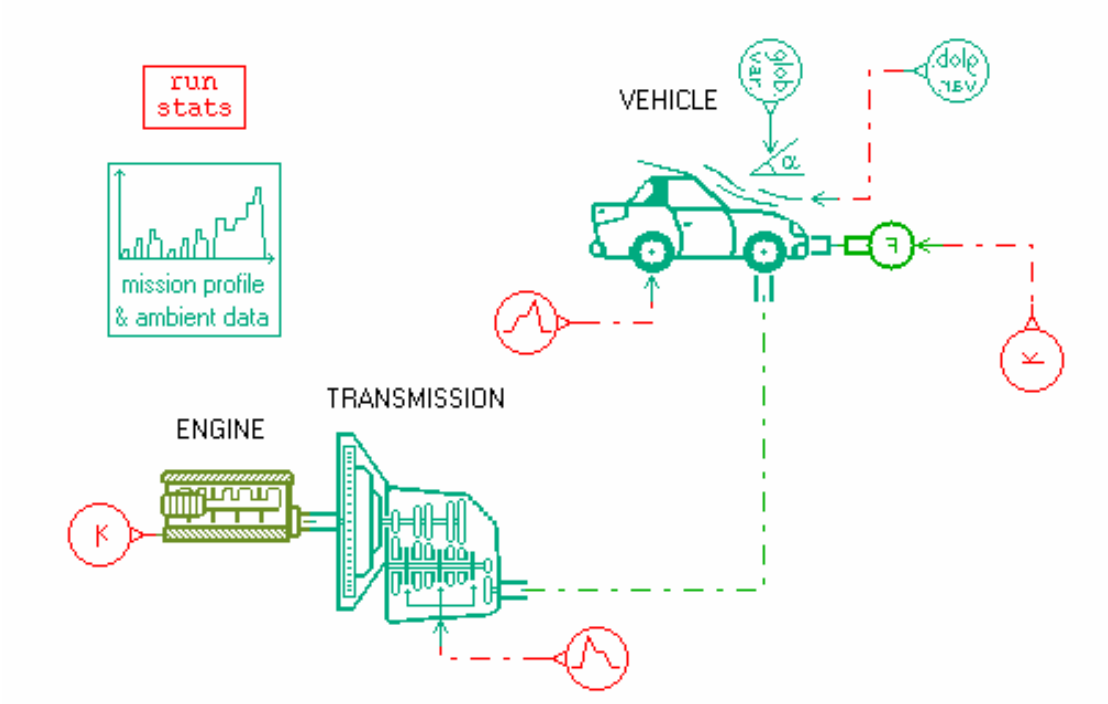

Figure 4-14 Mechanical component model

Most of all, when the throttle opening signal and gearbox signal are given, the output torque of the engine and the driving torque to the vehicle through transmission are verified.

The internal data are the same as the set-up data explained, and the test conditions are modified to meet the test purpose. The test conditions are as follows:

- Throttle opening signal : 0.01, 0.2, 0.5, 1.0

- Transmission
  - Gear signal: 1st gear during 15 seconds and 2nd gear during 15 seconds
  - Primary shaft inertia: 0.15kg.m^2

- Maximum Coulomb friction torque: 7000 Nm
- Rotary velocity threshold: 100rev/min

- Vehicle
  - No braking signal and no external force

Figure 4-15 shows the engine output torque according to the accelerator pedal command. As the input signal increases, the output torque increases. However, when the signal of 0.01 is given, the output torque is less than zero. This means that the signal is not sufficient to overcome the engine friction and the engine will stop. So an idling control is needed for the conventional vehicle. This controller is presented in the next Chapter.

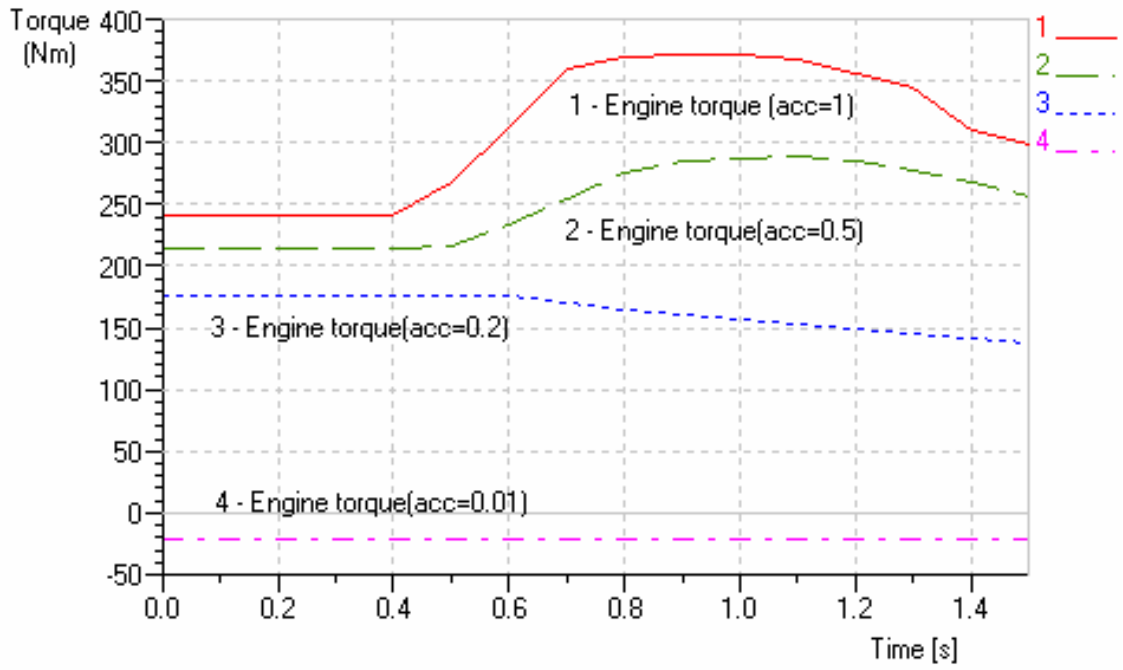

Figure 4-15 Engine output torque

Figure 4-16 depicts that the torque transmitted to the vehicle through the transmission and the powered axle when the gear signal is changed from the 1st to the 2nd gear. The output torque is affected by the gear ratio and the final drive ratio, and decreases by the difference of the gear ratio when the gear is changed.

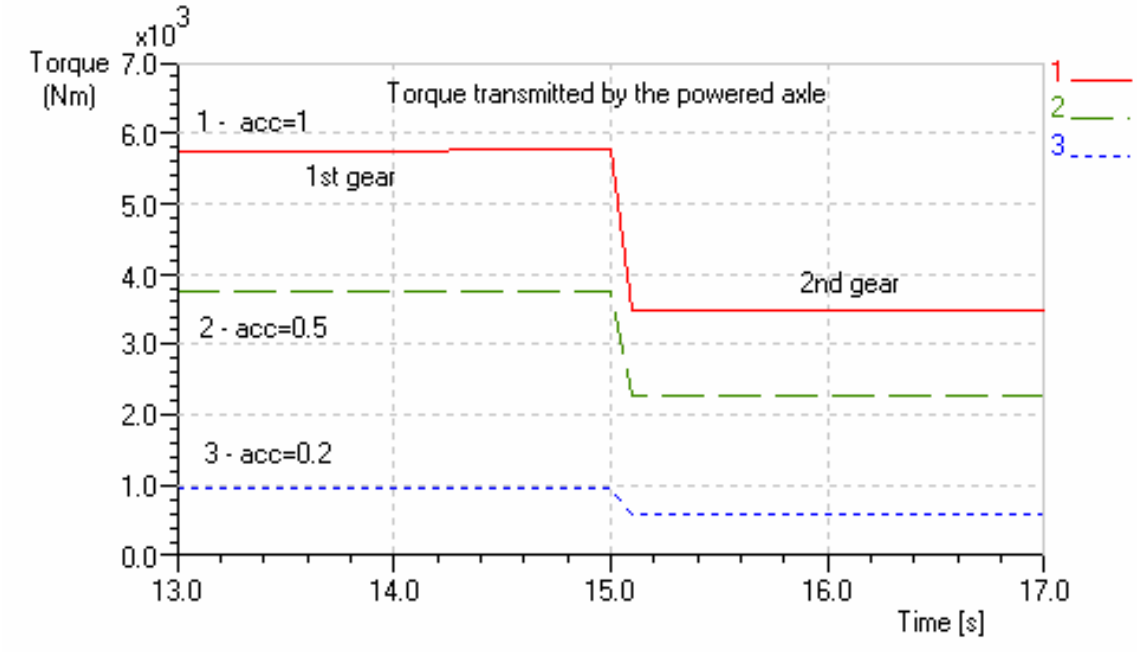

Figure 4-16 Torque transmitted through transmission and powered axle

The total resistance of the vehicles is shown in Figure 4-17. The rolling resistance is constant regardless of the vehicle velocity but the aerodynamic drag is rising in proportion to the square of velocity. It can be seen that the aerodynamic resistance become more important as the velocity increases.

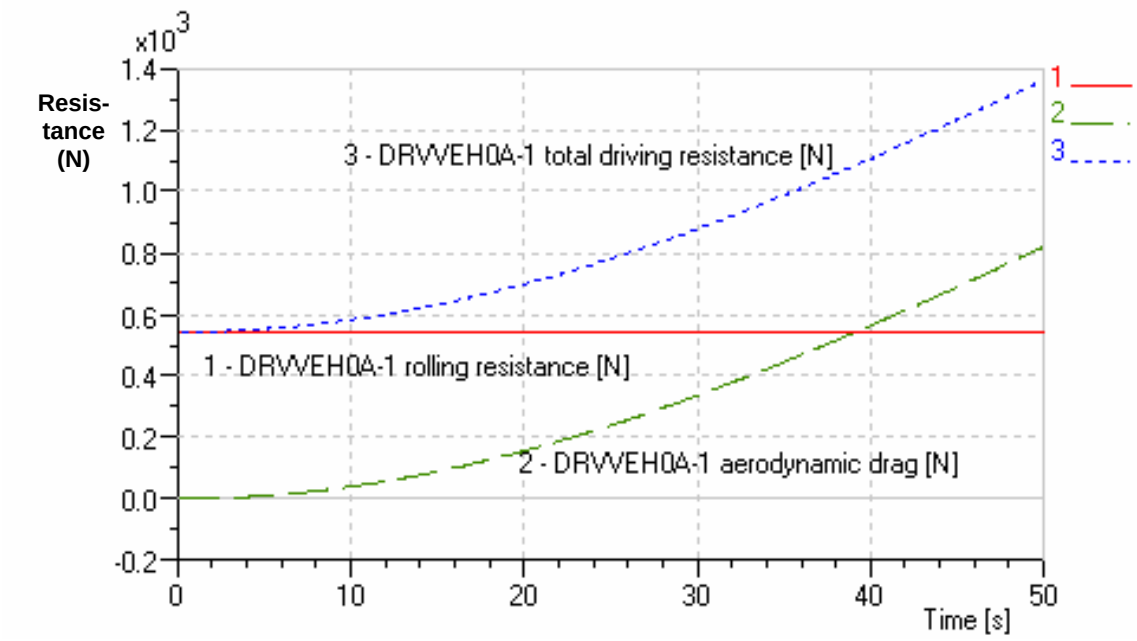

Figure 4-17 Vehicle resistance

4.8.2 Electrical component model

This basic model illustrated in Figure 4-18 is to verify the function of the electrical components: the EM and the battery. The same transmission and the vehicle model are added in this model as the mechanical component model, and the charging and discharging tests are conducted.

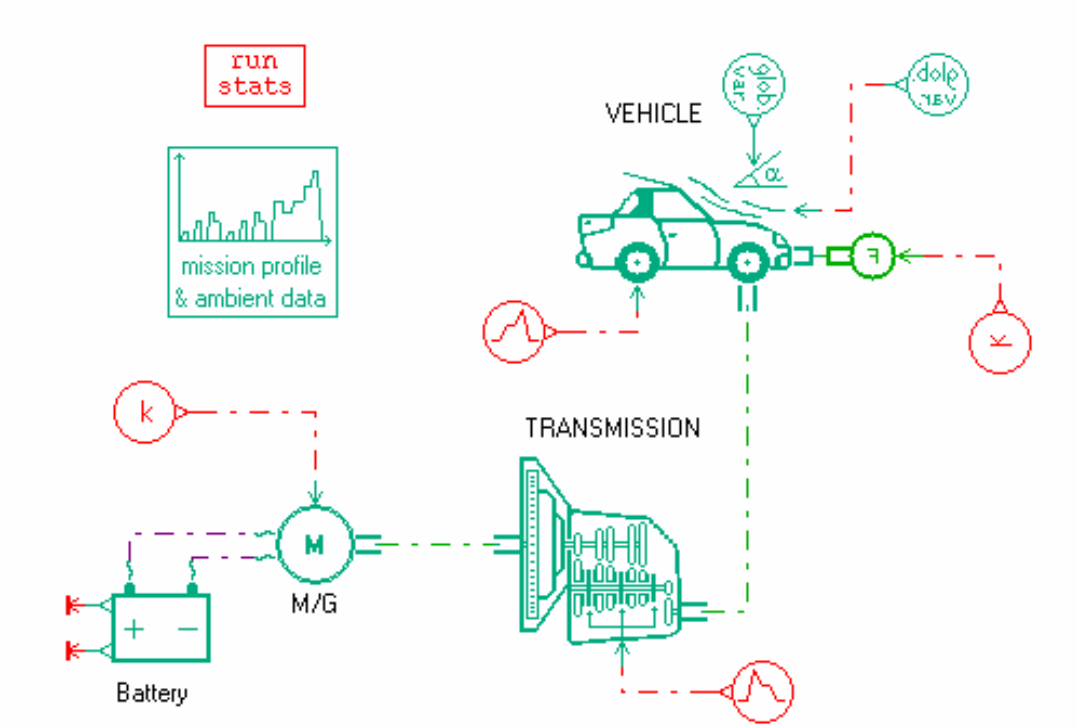

Figure 4-18 Electrical component model

The test conditions for the discharging test are as follows:

- EM Torque command : 100Nm, 200Nm, and 300Nm
- Battery initial SoC : 60%
- Transmission gear signal : 0 (no torque transmission)

The motor torque increases according to the torque demand but limits to the maximum torque at the given speed. The output torque cannot exceed the maximum torque limit of the EM, 270Nm, even though the torque command is 300 Nm, as can be seen in Figure 4-19.

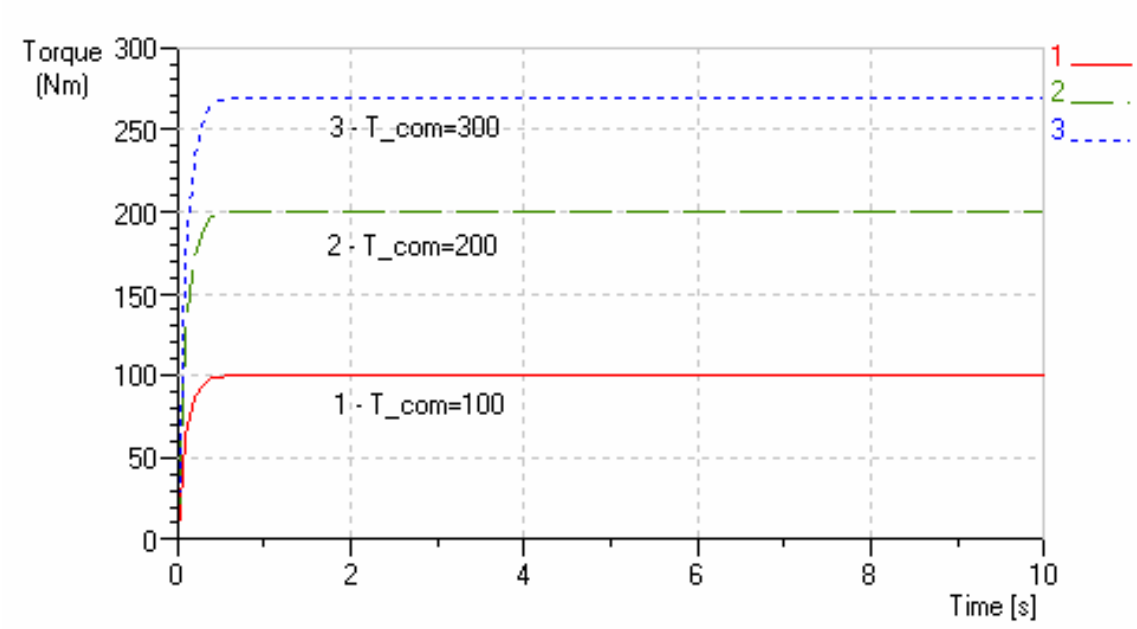

Figure 4-19 Motor output torque according to the torque command

The state of charge decreases steadily as the motor operates. So if the output torque from the motor increases, the SoC will decrease more rapidly. Figure 4-20 describes this trend. When the maximum torque command is given, the decreasing slope becomes the deepest.

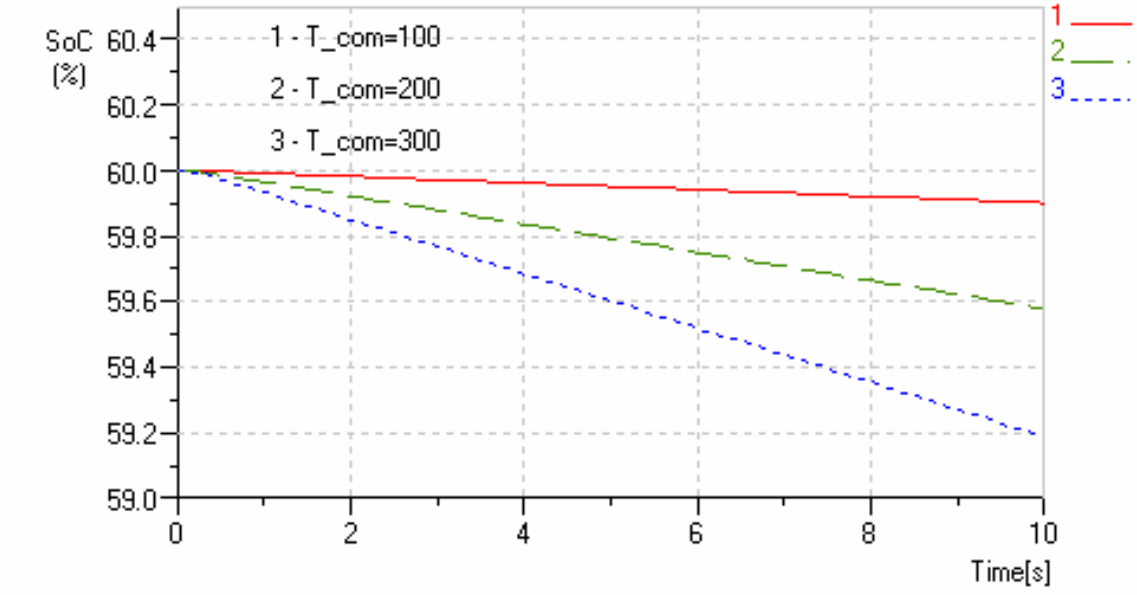

Figure 4-20 State of charge in discharging phase

Figure 4-21 represents the results of the charging test. When the regenerative torques are entered in the EM, for example from -100Nm to -300Nm in Figure 4-20, the battery will be charged. This trend is also affected by the input torque command but limited to the minimum torque of the generator. That is to say, although the absolute magnitude of the regenerative torque command increases too much, the charging capacity cannot be increased due to the limit of generator.

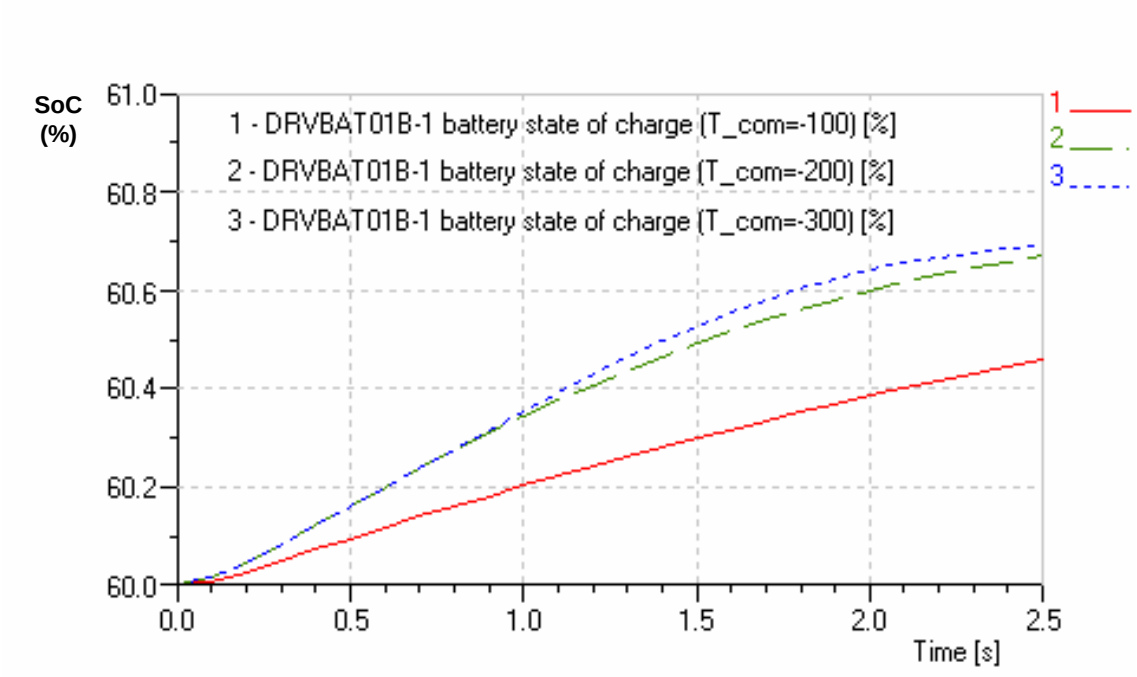

Figure 4-21 State of charge in charging phase

In order to verify the startability by the EM, the maximum torque command is given to the motor on the condition of 1st gear ratio. Figures 4-22 and 4-23 shows that this motor produces enough output torque to start and accelerate the vehicle at low speed zone without any assistance from the engine. That is to say, as the output torque is sufficient, the vehicle velocity becomes higher than the required speed, because it has no controller. In Figure 4-22, the output torque at the motor is transmitted to the vehicle in proportion to the total gear ratio. Figure 4-23 describes that the velocity speed by the maximum torque of the EM is much higher than the required vehicle velocity and it has sufficient torque capacity for the vehicle. The difference between the actual vehicle velocity and the required vehicle velocity can be reduced by using the motor controller.

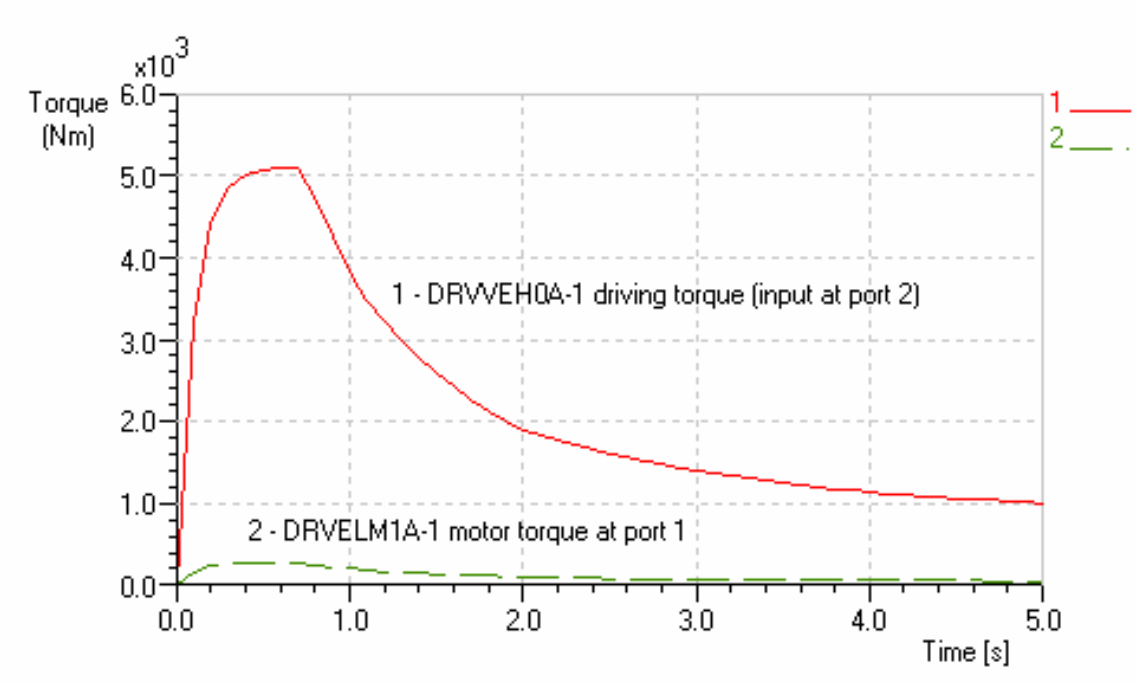

Figure 4-22 Transmitted driving torque vs. the motor output torque

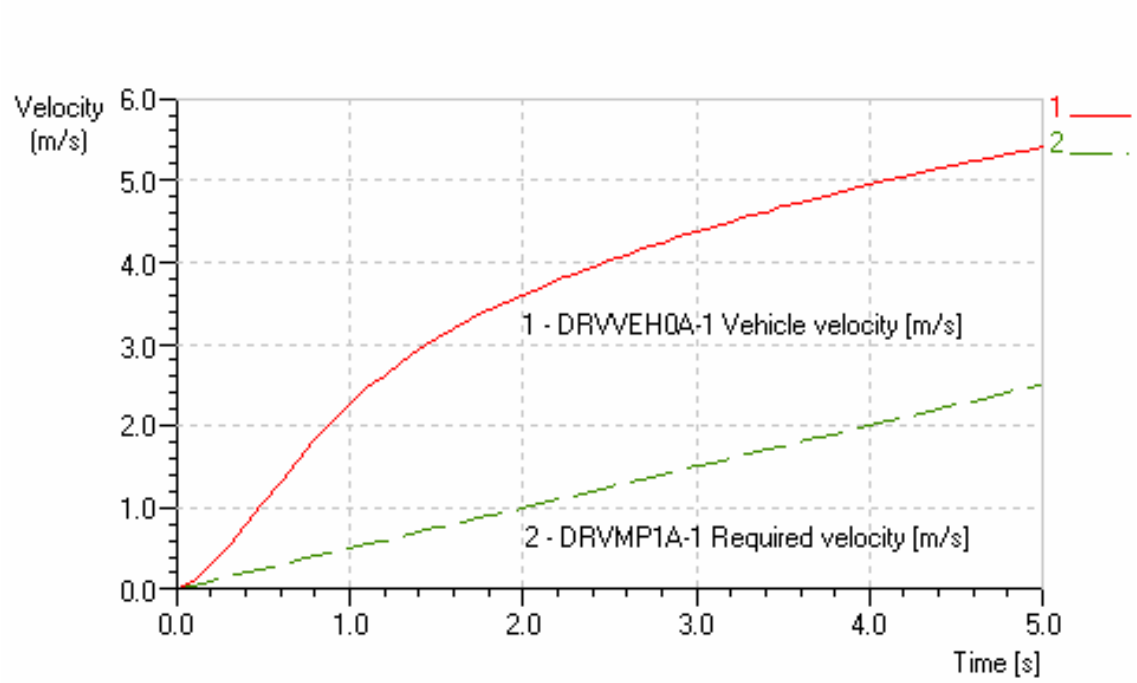

Figure 4-23 Vehicle velocity vs. the required vehicle velocity

5 Control strategy

The hardware for the light-duty hybrid electric truck has been described above. This Chapter discusses the design of the strategy to control the components. As the main objective to design the control strategy in this research is to develop the applicable controller in the real condition on the balance of the fuel economy and vehicle performance, this controller will be focused on these two aspects.

Two controllers are introduced here. One is for the conventional truck, and the other is to control the hybrid electric vehicle. Considering the relative feasibility of implementation in the real vehicle, regardless of the driving condition, the rule-based concept is adopted for the controller of the hybrid electric truck. This controller is improved through the basic simulation.

Whilst the components are modelled in the AMESim, the controllers are built by using Simulink/Stateflow, because AMESim provides the interface with Matlab/Simulink, and Simulink offers a variety of functions and convenience.

In this study, as the forward facing simulation is considered, a driver model has to be built. Fortunately, AMESim offers some kinds of driver models. Among them, a driver model is selected and applied as a basic controller to fit the component model built in the last Chapter.

5.1 Control strategy of the conventional LD truck

As a driver model is provided in the AMESim and the manual transmission is applied, only the basic controller is needed for the conventional vehicle. So this controller plays an active role as a driver to operate the vehicle manually. This means that this controller has no special control variables to be controlled electronically, except for the engine speed control. This controller consists of the driver model, the engine controller, and the transmission controller.

5.1.1 Driver model

Even though there are many built-in driver models in AMESim, they can be divided into two categories. One is related to the manual gearbox, the other is concerned with any kinds of automatic transmission, such as CVT and AMT. These models have similar functions. That is to say, when the vehicle control speed is given, this driver model serves as a PID controller to meet the target speed from the difference between the current vehicle speed and the required speed. By selecting the gains of this controller, it can be used as PI or PD controller.

As they can provide many kinds of input and output variables according to the configuration of the component model, for example the gearbox control and clutch control for manual gearbox, these driver models basically calculate the acceleration control and the braking control to control the vehicle speed. That is because a driver typically controls vehicle speed by depressing the accelerator pedal and the brake pedal and these driver models simulate the typical driver.

For the conventional vehicle with the manual gearbox, driver models for the manual transmission with or without clutch control are needed. However, in this study, the driver model for automatic gearshift, named DRVDRVA00A in AMESim has been chosen. Because most of the manual gearbox driver models require the gear control data file for drive cycles, it is hard for this to be applied to arbitrary drive cycles except for the standard drive cycle provided in the simulation tool. As discussed before, as there is no standard drive cycle certified internationally for heavier duty trucks, this simulation tool only offers the standard cycles for passenger cars. Therefore, the basic transmission controller is designed for the manual gearbox separately. In other words, a separate transmission controller is built and the driver model for the manual transmission is not needed any more.

Figure 5-1 illustrates the chosen driver model which calculates the acceleration control and the braking control. It does not include gearbox ratio and clutch controls. The

information on the vehicle control speed is supplied by the mission profile model. The output signals from this driver model can be interpreted as the driver's intention, or the angle of the accelerator pedal and brake pedal.

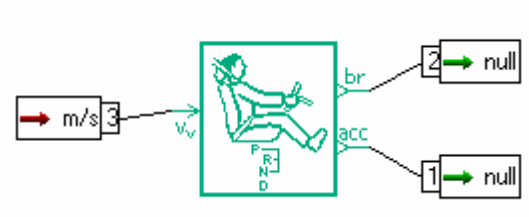

Figure 5-1 Driver model in AMESim

A simple block diagram for this driver is illustrated in Figure 5-2. The vehicle speed error is calculated as the difference between the control speed and the current speed. The two control outputs through the driver model are saturated in the range from 0 to 1 which means the angle of throttle position and the angle of brake pedal, respectively.

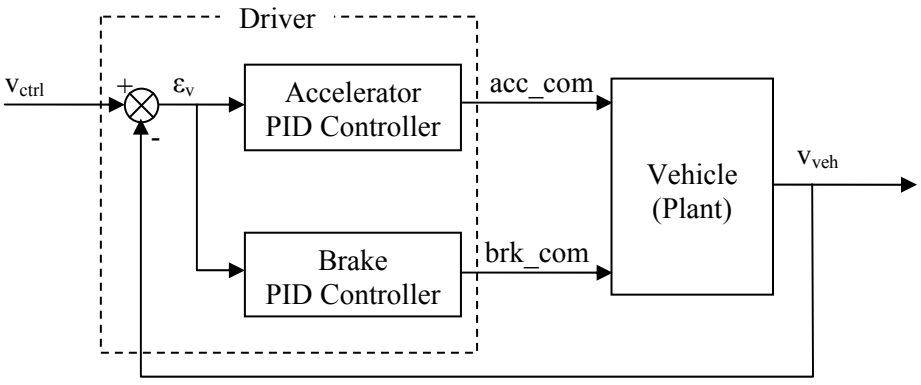

Figure 5-2 Block diagram of driver model

5.1.2 Engine controller

The driver model mentioned above does not output the detailed control for the engine. However, because the engine is the only power source in the conventional truck and it could not be stopped during the drive cycle, it needs some more controls. So the simple engine controller was built as shown in Figure 5-3.

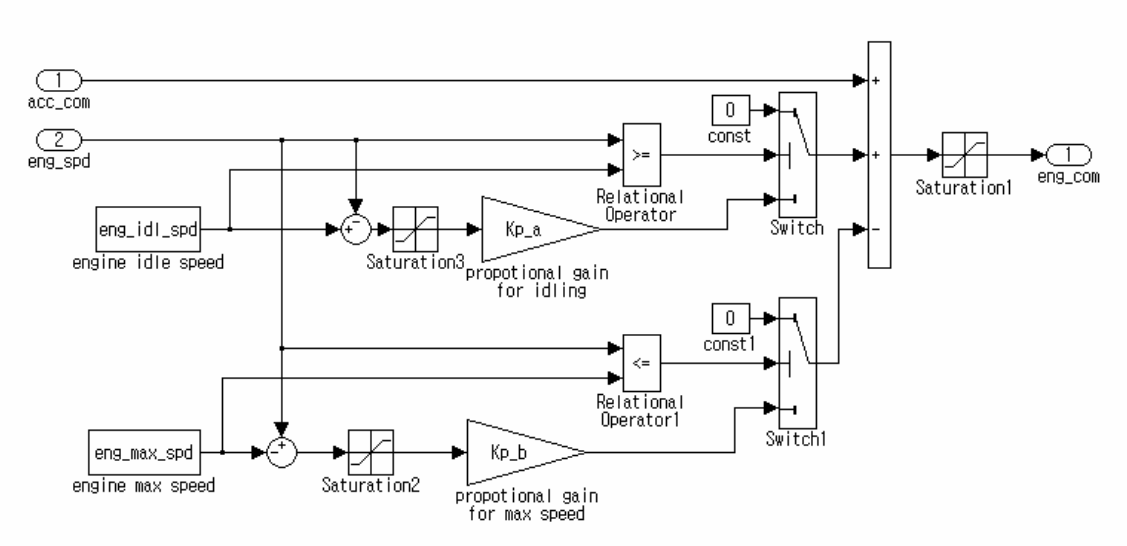

Figure 5-3 Engine controller for the conventional vehicle

It is a proportional controller to make the engine operate in the operating engine speed range without engine stop and it is composed of 2 parts: idling control and maximum engine speed control. When the engine is operating in a lower speed region than the idle speed, this engine will be stopped. To avoid this engine stop, the acceleration command has to be increased slightly. So, if the engine speed is lower than the idle control speed, the engine controller produces the signal to increase the engine speed and add to the original acceleration command. In the case of maximum speed control, the acceleration command decreases slightly.

5.1.3 Transmission controller

The gearbox controller for the manual transmission is built for applying any arbitrarily selected drive cycle. The driver usually changes the gear step of the manual transmission according to the engine speed and this controller shown in Figure 5-4 simulates this function. When the engine speed reaches the engine maximum speed, the controller will carry out the upshift, and will do the downshift at the peak torque rotary speed. If the vehicle control speed is zero, the gear will output the neutral signal, 0. This controller can be built easily by adding the simple gearshift map. The shift map is shown in Figure 5-5 and represents the vehicle speed along the engine speed. The solid

line describes the upshift map and the dotted line is the downshift map. This map can be obtained by using the equation (3-3).

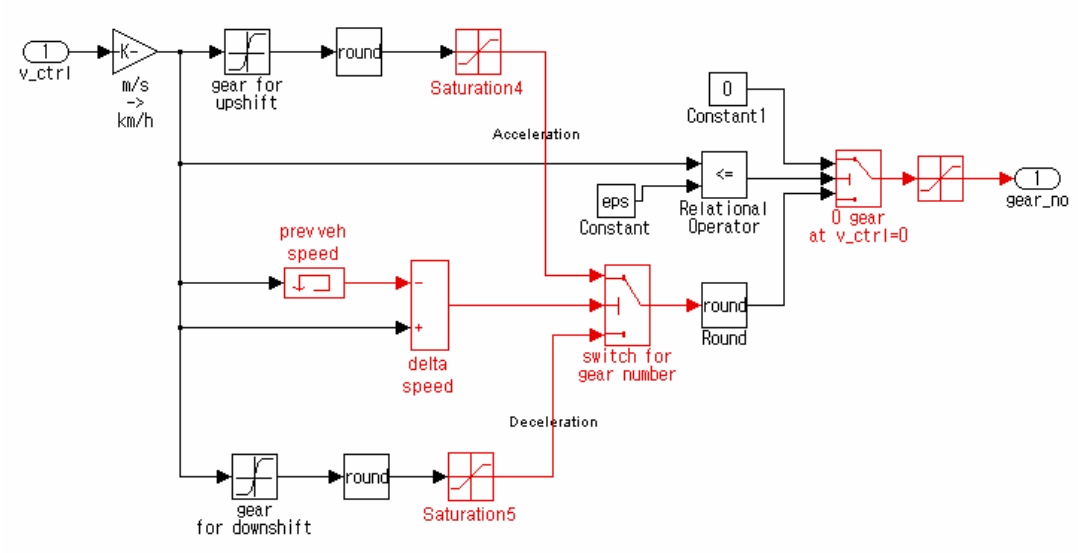

Figure 5-4 Manual transmission controller

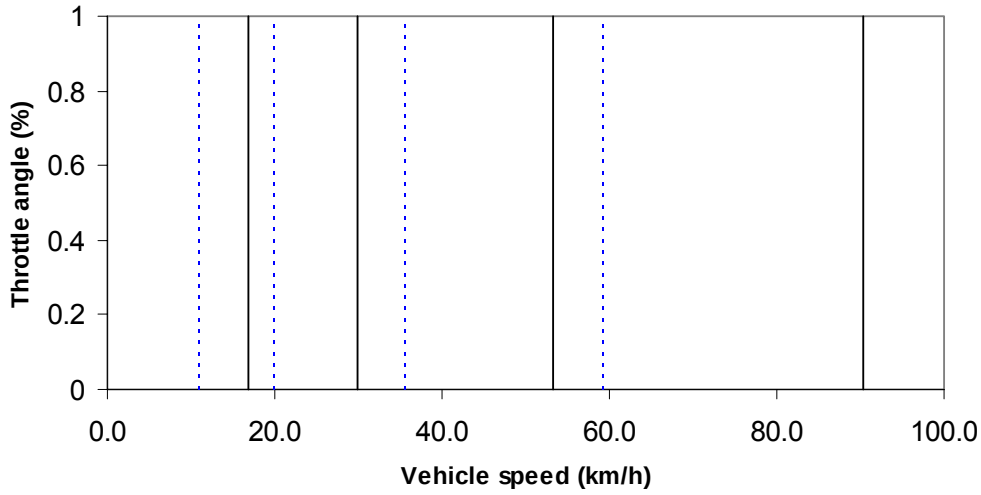

Figure 5-5 Shift map for the manual transmission

5.1.4 Completion of the conventional truck modelling

The component and the controller models are integrated and illustrated in Figure 5-6. Of course, this model will be simulated through the interface between AMESim for the component models and Simulink for the controller. In order to avoid the rapid changes

of the output commands which can not be realised in real driving, the first order lag blocks are added to the control signals. Time constant is set to 0.5s.

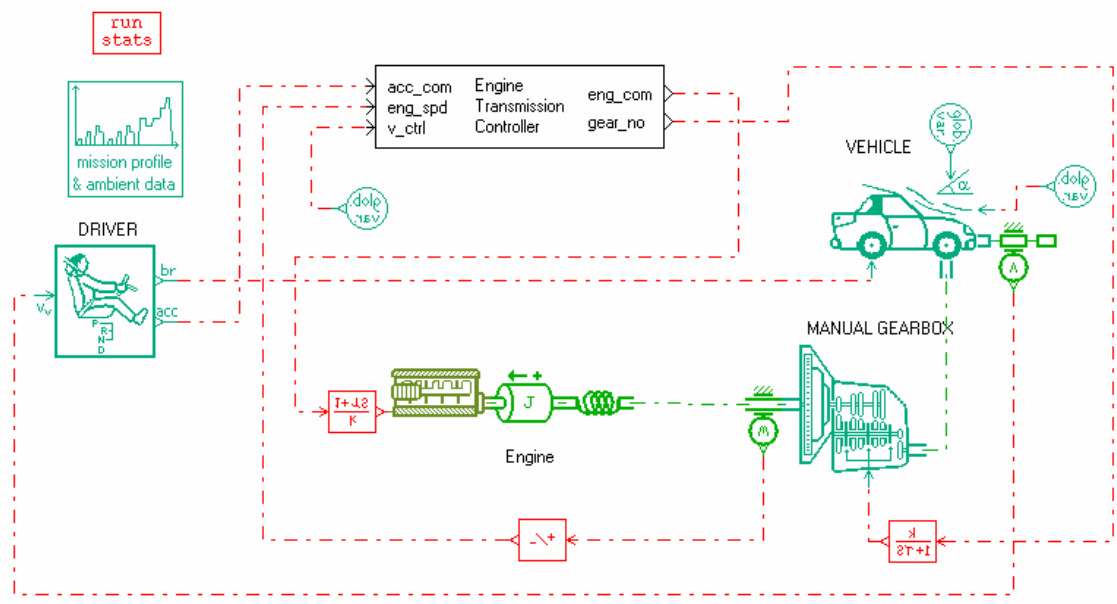

Figure 5-6 Complete model of the conventional LD truck

5.2 Control strategy of the LD hybrid electric truck

The key factor for the HEV controller is how to distribute the torque demand between the ICE and the EM. This controller has many control variables and is more difficult to be built compared with a conventional one.

The HEV controller built in this study is focused on the rule-based concept. This is because this concept is relatively convenient to be constructed and applied to the real vehicle at the initial stage of controller development without any special test data. In addition, if the optimised rule is added to the controller, this concept can produce great results.

Figure 5-7 depicts a overview of the HEV controller, which has two levels of scheme. At first, the higher level of mode selector decides the appropriate operation mode by

using many control inputs and a lower level of controllers, such as power split controller, clutch, and brake controller, which make the command to the each component. The gearbox controller operates separately.

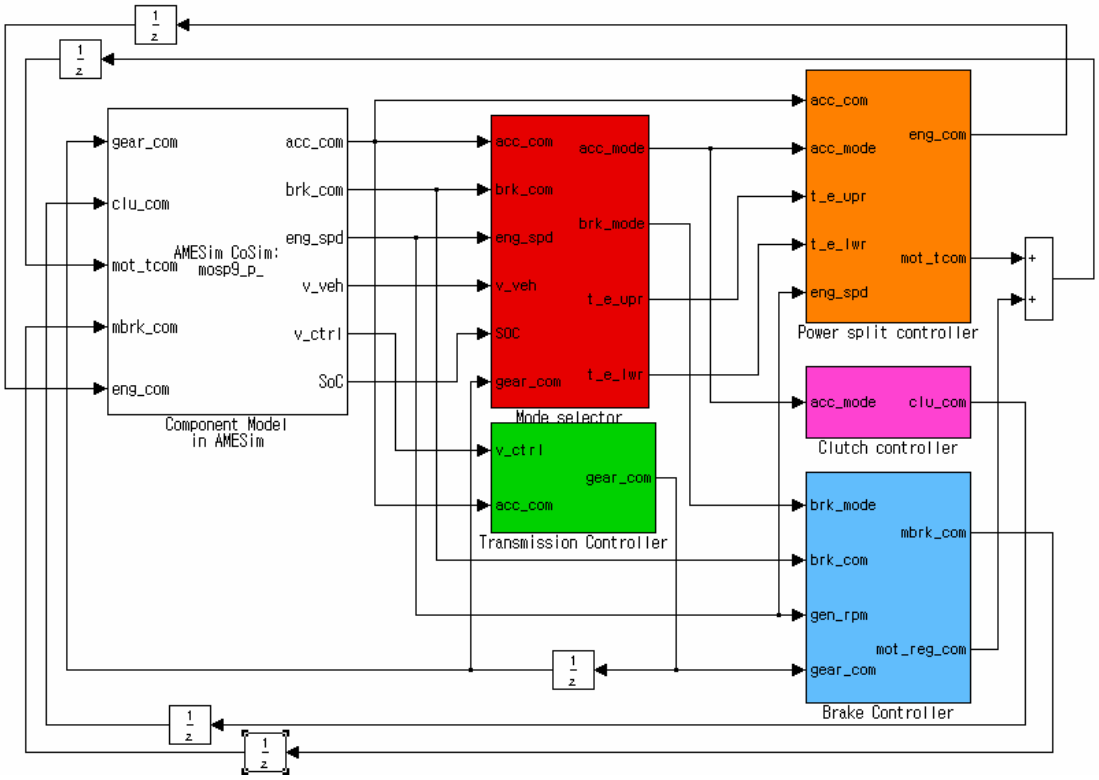

Figure 5-7 Structure of HEV controller

This HEV controller is made up of 5 sub-controllers as illustrated in Figure 5-7: the higher level of mode selector, the power split controller, the clutch controller, the transmission controller, and the brake controller. The detailed structure and the functions will be tackled in each controller section. The driver model is provided in AMESim and is not built in Simulink.

5.2.1 Basic control concept

First of all, the control variables have to be defined to make the HEV controller. These variables are input/output parameters to control the component models in Figure 4-1.

- Input variables
    - Vehicle control speed or required speed (m/s)
    - Vehicle current speed (m/s)
    - Engine rotary speed (rev/min)
    - Battery SoC (%)

- Output variables
    - Engine command or accelerator pedal position (0-1)
    - Motor torque/generator command
      (max generator torque - max motor torque, Nm)
    - Gearbox control (0-5)
    - Clutch control (0-1)
    - Mechanical brake control (0-1)

The basic control concept is an electric start at low rotary speeds where the ICE has worse efficiency and electric assist where the motor assists the primary power source, the ICE, as needed. The SoC is maintained in the reasonable range through charge from the ICE directly or the regenerative brake. In other words, the charge-sustaining strategy is taken into consideration. The basic rule-based control concept has been reported [8]. In this study, the control concept is modified and improved.

Figure 5-8 explains the control concept for the HEV controller built in this study when the battery SoC is over the minimum limit. According to the operating area and the battery SoC, the operation can be classified into 6 modes: the motor only mode, the engine only mode, the charge mode, the hybrid mode, the regenerative braking mode, and the mechanical braking mode. From these, the first 4 modes are related to the acceleration and the last two are called the braking modes.

The motor only mode is when the EM delivers the power to the driven wheels without the power from the ICE and represents region A in Figure 5-8. When the vehicle speed is lower than the preset vehicle speed and the vehicle starts, this mode can be applied. The preset vehicle speed is closely concerned with the engine speed and efficiency, and

can be set by the characteristics of the ICE. On the other hand, as the motor only produces the torque to start the vehicle in this mode, the startability of the vehicle has to be verified to use this mode. The startability is expressed as follows.

$$S_i = \tan\theta \times 100 \qquad (5\text{-}1)$$

where S_i : Startability (%)

θ : Maximum uphill grade

The engine only mode is applied when the required torque is less than the OOL (optimum operation line) of the ICE and the SoC is enough. In this case, the EM is stopped and the ICE becomes the only power source to the driven wheels. Point B in Figure 5-8 is a case of this mode.

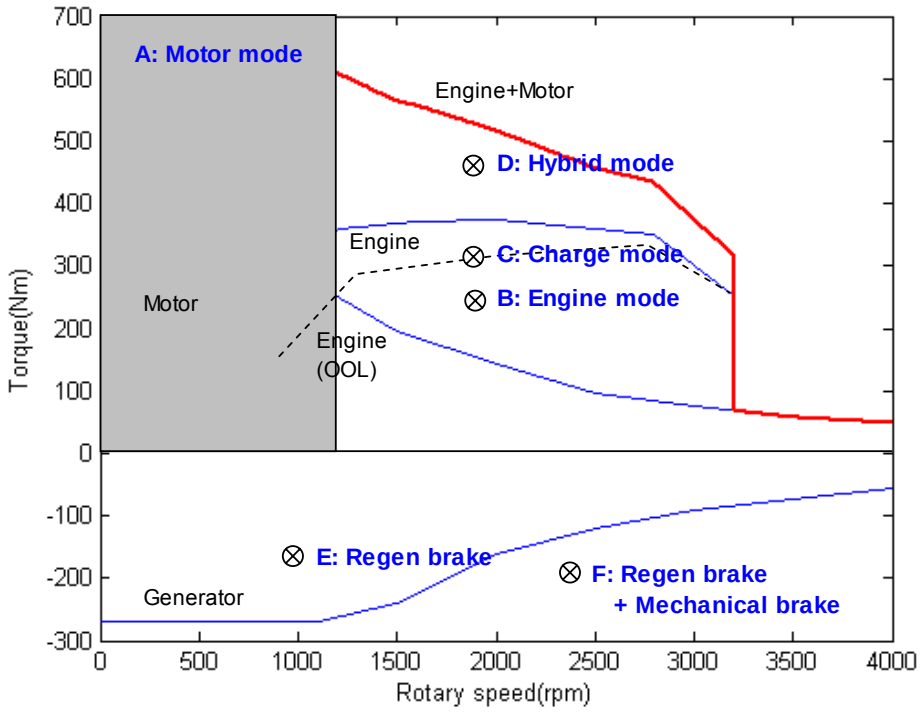

Figure 5-8 Basic control concept of HEV

The charge mode is regarded as a kind of engine mode. This mode is turned on when the total torque demand is less than the OOL of the ICE but the SoC needs to be charged. That is to say, the engine operates along the OOL like point C in Figure 5-8 to deliver the required power, and the difference in torque between the required torque and

the operating torque at the OOL is used for charge. So the efficiency of the ICE is maximised in this mode.

When the vehicle is accelerated, the maximum power of the HEV is demanded. Like point D in Figure 5-8, when the required torque is greater than the ICE can produce, both the ICE and the EM have to operate and produce the required power. This mode is called the hybrid mode.

With regard to the braking, the HEV can recover the braking energy by the conversion from the kinetic braking energy to the electrical energy which is stored in the battery through the generator. This operation is called the regenerative brake mode. The points E and F in Figure 5-8 represent this operation mode. When the demanded braking torque is less than the maximum limit of the generator, all the torque can be used to charge the battery. However, if the demanded torque is beyond the torque capacity of the generator, the mechanical brake as well as the regenerative brake must be applied to cover the total demanded braking torque. In this sense, the latter mode can be divided into another braking mode, so-called the hybrid braking mode. In this study, the mode is not divided but the same function is included in the brake controller.

Table 5-1 Driving mode of HEV

Mode	Application	Engine command	Motor torque	Mech. brake command	Remarks
Motor only	Vehicle start	= 0	≥ 0	= 0	
Engine only	Constant speed drive	≥ 0	= 0	= 0	
Charge	Low battery	≥ 0	≤ 0	= 0	Engine only
Hybrid	Acceleration	≥ 0	≥ 0	= 0	
Regenerative brake	Deceleration/Braking	= 0	≤ 0	≥ 0	Regen only, Hybrid brake
Mechanical brake	Deceleration/Braking	= 0	= 0	≥ 0	SoC>80

During braking, if the battery SoC reaches the top line, the battery must not be charged. So only the mechanical brake is used to stop the vehicle. This mode is the mechanical brake mode.

Table 5-1 shows the application case and the torque demand of the operation modes set up in this controller. With this basic control concept and the torque command, the controller will be built in detail in the next section.

The HEV controller is designed based on the forward facing simulation method and needs to apply the driver model. The same driver model as that of a conventional vehicle shown in Figure 5-1 is applied to this controller, because it is appropriate for the automated manual transmission which is equipped in the LD hybrid electric truck. The transmission controller is added with the different control logic from the conventional manual transmission.

The engine controller is not taken into consideration here. As the engine controller is used to control the idling speed and the maximum rotary speed of the ICE in the modelling of the conventional truck, it is assumed that the HEV does not have to control the rotary speeds due to the operating range of the EM. That is because the EM has a wider range of operating speed, from 0 to 4000 rev/min, and the EM is operating alone at low speeds according to the motor only mode.

5.2.2 Mode selection strategy

The mode selector is a higher level of controller against the other controllers, except for the gearbox controller. It judges the operation mode considering the given condition. The basic input variables are the accelerator command, the brake command from the driver model, and the battery SoC.

These operation modes can be divided into two categories by using the outputs from the driver model: the acceleration modes and the brake modes. The algorithms for these modes are presented.

5.2.2.1 Acceleration modes

The control flow chart for the acceleration mode selector is illustrated in Figure 5-9. The input and parameters are as follows:

- acc_com : Acceleration command from the driver model between 0 and 1.
- T_{acc} : Total torque demand calculated by using acc_com (Nm)
  This value will be explained in the next section.
- T_{e_opt} : Torque at the OOL of the engine (Nm)
- v_{set} : Preset vehicle speed below for the motor only mode (km/h)

The basic input signal is the acceleration command from the driver model. If this input signal is greater than zero, this controller selects the appropriate acceleration mode. If the input is zero or less than zero, it means that there in no power demand and the no acceleration mode is chosen.

This controller considers the charge-sustaining strategy without the external energy supply. While the SoC is below the minimum limit of the battery charge, 20%, the EM will not operate and the engine only mode or the charge mode can be selected according to the magnitude of the required torque.

If the SoC is enough to operate the EM, the motor only mode or the hybrid mode can be chosen. As the motor only mode is chosen for the low rotary speed zone, it can be determined by the preset vehicle speed. If the required torque is greater than the torque at the OOL of the engine, the hybrid mode will start. Of course, the engine mode or the charge mode can be applied according to the given condition.

The preset vehicle speed, v_{set}, is considered to be the minimum vehicle speed below which the engine cannot operate steadily. From the engine fuel map shown in Figure 4-4, the bottom engine speed is decided as 1200 rev/min which is below the most efficient speed of 1500 rev/min. The vehicle speed is calculated by the equation (3-3).

Starting in the first gear, the vehicle speed is 6.7 km/h. This speed is entered as the preset vehicle speed for the motor only mode.

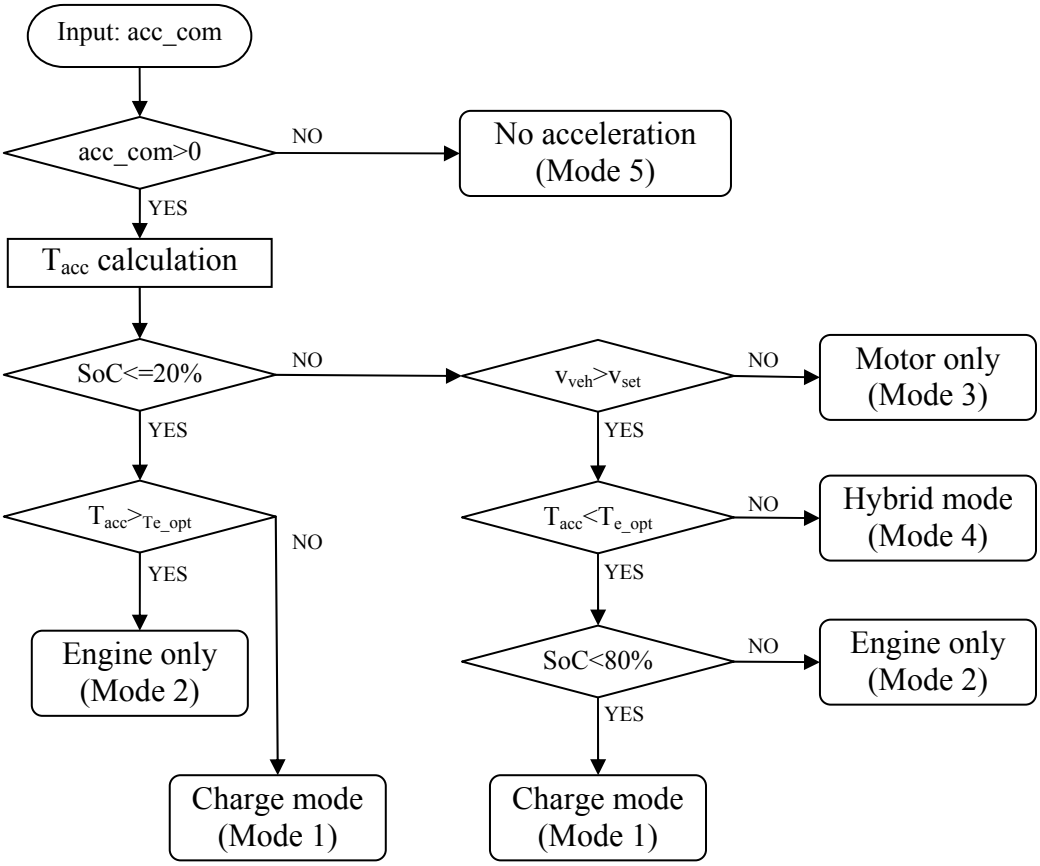

Figure 5-9 Algorithm for acceleration modes

5.2.2.2 Brake modes

The control flow chart for the brake mode selector is quite simple as shown in Figure 5-10. When the brake command, which represents the brake pedal position between 0 and 1, is entered to this controller, the braking torque will be produced to decelerate the vehicle. This torque can be covered by the generator or the mechanical brake. This controller decides to operate the regenerative brake through the generator, taking the SoC and the gear state into consideration. When the SoC is below the top limit of the charge capacity and the gear is not neutral, the controller will choose the regeneration brake mode which includes the so-called hybrid braking mode. In other cases in which the charge is not needed, the mechanical brake mode is selected.

The controller built under Simulink/Stateflow environment is illustrated in Figure 5-11.

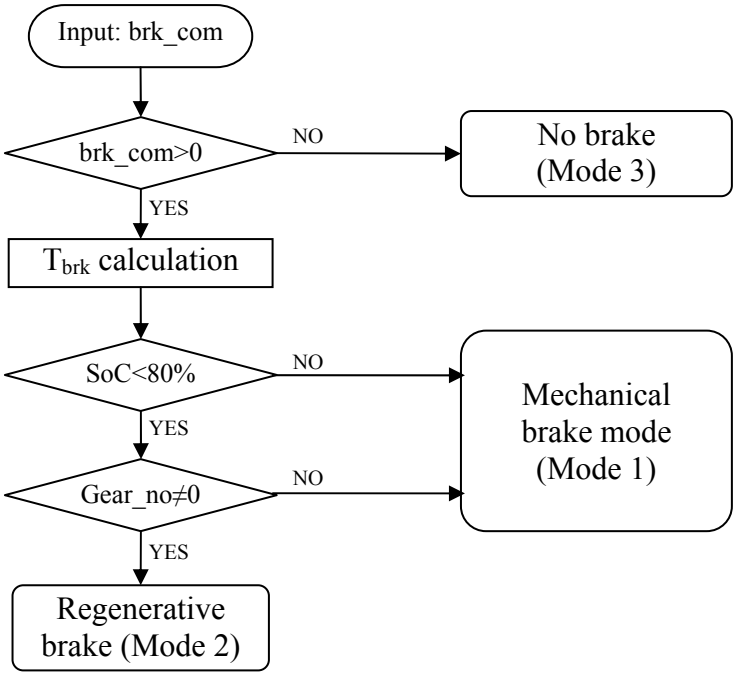

Figure 5-10 Algorithm for brake modes

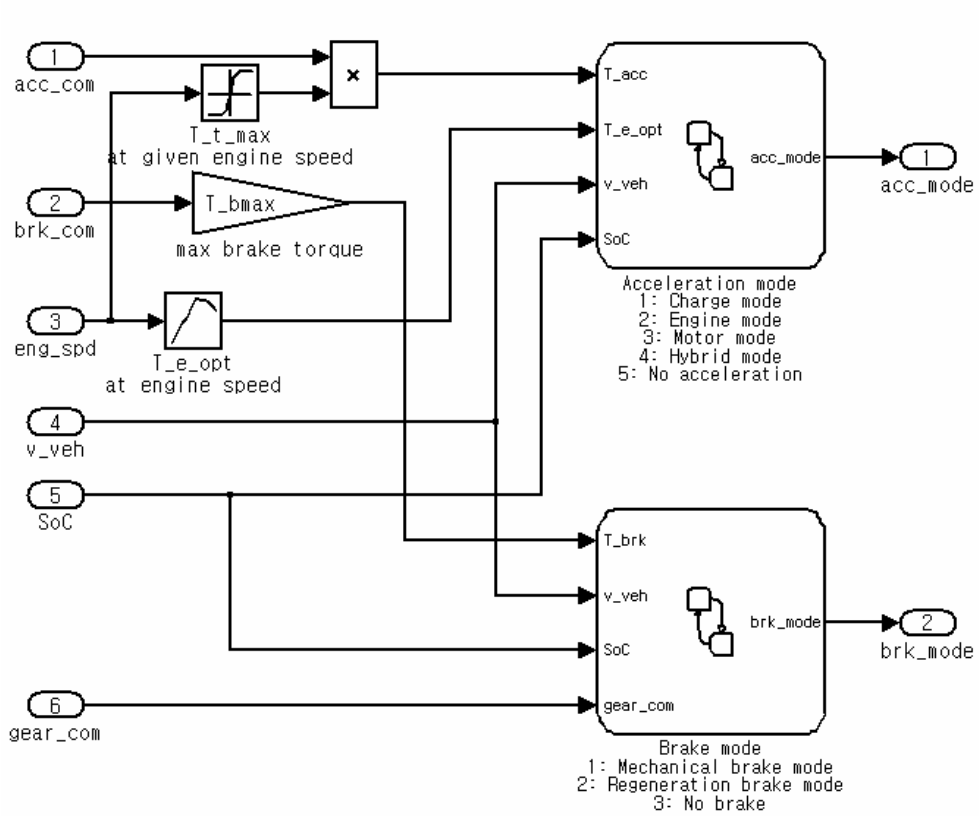

Figure 5-11 Mode selector for the hybrid electric truck

5.2.3 Power split strategy

This section explains how to distribute the total torque demand to the ICE and the EM based on the acceleration mode decided by the mode selector.

First of all, the total torque demand of the driver can be estimated from the acceleration command. The acceleration command is regarded as the signal of the accelerator pedal position and has a proportional relation with the torque demand.

$$T_{acc} = acc\_com \times T_{t\max} \tag{5-2}$$

where T_{acc} : Torque required by the acceleration command, acc_com.

T_{tmax} : Total maximum torque which can be produced from all the HEV power sources at current speed N, the ICE and the EM.

Based on this total torque demand, T_{acc}, and the SoC, the mode selector chooses an acceleration mode and the power split controller decides how to divide the torque demand. For example, in the engine only mode, all the torque demand is allocated to the engine and the torque command for the EM becomes zero. The torque demand is assigned to the EM in the motor only mode.

In the charge mode in which the battery SoC is not sufficient and T_{acc} is less than the torque at the OOL, T_{e_opt}, the engine command is increased to reach T_{e_opt} and the remaining torque, T_{e_opt}-T_{acc}, is used for charging. That is to say, the engine efficiency is increased.

In the hybrid mode, the engine torque at the OOL is assigned to the engine and the excess torque, T_{acc}-T_{e_opt}, becomes the motor torque command.

The torques of the ICE and the EM assigned by the power split controller have to be changed to the output commands. As modelled in the last section, attention should be paid to the type of the command. The input control variable for the ICE is the signal of the accelerator pedal position which is in the range between 0 and 1. A zero signal

means the fully released accelerator pedal and a 1 signal is the fully depressed pedal. However, the control signal for the motor is the torque command. So the torque allocated to the EM need not be changed.

Table 5-2 Output command of power split controller

No.	Mode	Torque Split	Output command
1	Charge	$T_e=T_{e\_opt}$ $T_m=(T_{e\_opt}-T_{acc})x-1$	eng_com =T_{e_opt}/T_{e_max} mot_tcom=T_m
2	Engine only	$T_e=T_{acc}$ $T_m=0$	eng_com =acc_com mot_tcom=0
3	Motor only	$T_e=0$ $T_m=T_{acc}$	eng_com =0 mot_tcom=T_{acc}/T_{m_max}
4	Hybrid	$T_e=T_{e\_opt}$ $T_m=T_{acc}-T_{e\_opt}$	eng_com =T_{e_opt}/T_{e_max} mot_tcom=$T_{acc}-T_{e\_opt}$
5	No acceleration	$T_e=0$ $T_m=0$	eng_com =0 mot_tcom=0

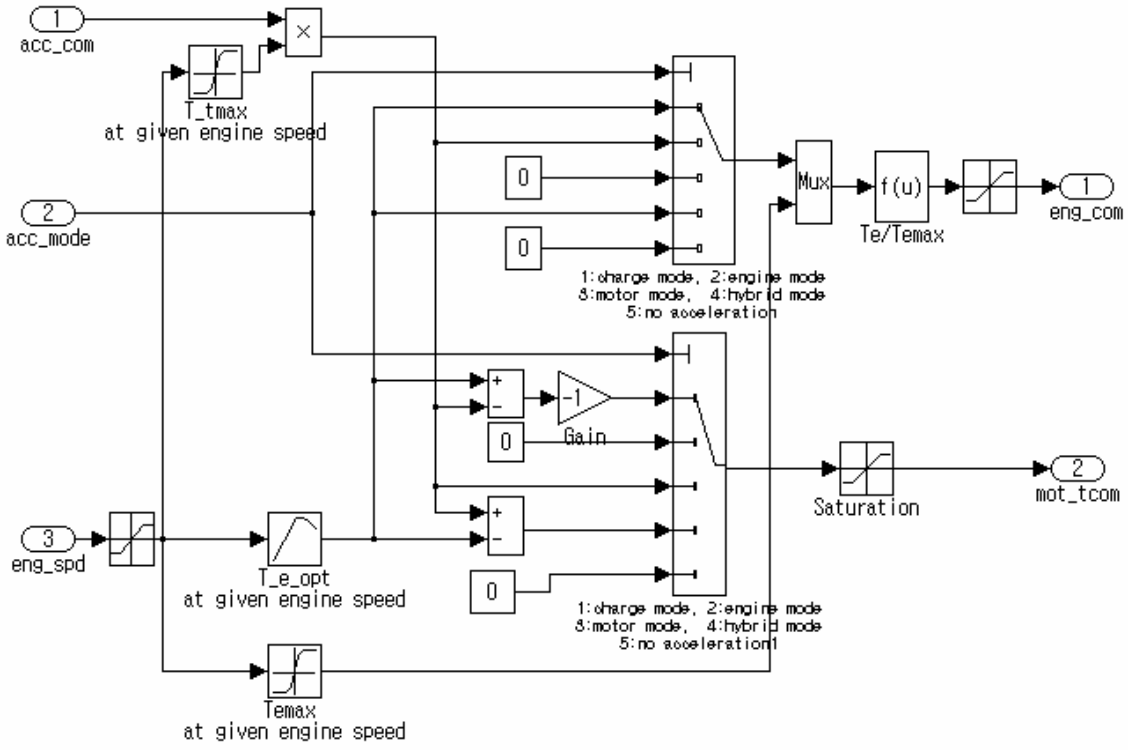

Figure 5-12 Power split controller for the hybrid electric truck

Table 5-2 shows the summary of the output commands of the power split controller along the acceleration mode. It should be noted that a sign of the EM torque demand changed to minus to operate the generator to charge the battery.

The power split controller is built in Simulink on the basis of Table 5-2 as shown in Figure 5-12. The engine command and the motor command are saturated in the accelerator position or torque capacity range before going out.

5.2.4 Braking strategy

The basic braking strategy in the HEV is to recover the regenerative braking energy as much as possible. However, it is not possible to recover all the braking energy due to the brake dynamics and the drive axle configuration. So, in order to estimate the maximum regenerative braking energy, the braking force at each axle has to be calculated in advance.

As the braking performance is directly associated with the vehicle safety and stability, the vehicle has the appropriate braking power capacity and the braking power has to be distributed to the front and rear wheels properly to maintain the vehicle direction. The braking power capacity is assumed to have the same capacity as the conventional vehicle. The braking power distribution can be calculated based on the brake dynamics. The regenerative braking torque is related to the braking torque at the rear wheels, because the modelled LD hybrid truck has the 4x2 FR configuration (front engine, rear drive).

In general, the braking torque required is much larger than the torque capacity of the EM. So the regenerative braking energy is limited to the torque which the EM can receive. The required torque over the EM capacity in the regenerative brake mode is dealt with by the mechanical brake.

5.2.4.1 Brake dynamics

In order to calculate the braking torque on the rear wheels to maintain vehicle stability, the ideal braking force distribution curve between the front and the rear wheels which is derived from the vehicle specification and the centre of gravity, has to be obtained. The curve may be obtained by using the general brake dynamics presented in [42] and [43].

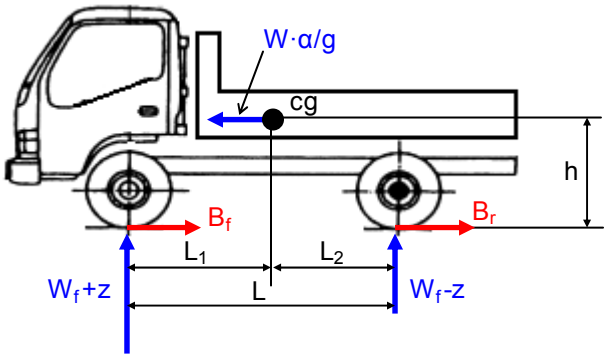

Figure 5-13 Schematic diagram for the braking power distribution

Figure 5-13 shows the schematic diagram for the braking power distribution. From the figure, the static weight on the front axle and the rear axle is expressed as follows:

$$W_f = W \times \frac{L_2}{L} \tag{5-4}$$

$$W_r = W \times \frac{L_1}{L} \tag{5-5}$$

where W : Weight of the vehicle (kg)

L : Wheelbase of the vehicle (m)

In addition, the general equation for braking performance may be obtained from Newton's Second law.

$$B_f + B_r + F_{aer} + W \sin\theta = \frac{W}{g} \cdot \alpha \tag{5-6}$$

where B_f : Front axle braking force

B_r : Rear axle braking force

F_{aer} : Aerodynamic drag

θ : Uphill grade

g : Gravitational acceleration

α : Linear deceleration

From the equation (5-6), because the aerodynamic resistance and the grade resistance are negligible when the vehicle is driving at low speed on a flat road, the total brake force is expressed as follows:

$$B = \frac{W}{g} \cdot \alpha \tag{5-7}$$

During braking, a dynamic load transfer from the rear to the front axle occurs such that the load on an axle is the static plus the dynamic load transfer contributions.

$$W_f^{'} = W_f + z = W_f + \frac{\alpha}{g} \cdot W \cdot \frac{h}{L} \tag{5-8}$$

$$W_r^{'} = W_r - z = W_r - \frac{\alpha}{g} \cdot W \cdot \frac{h}{L} \tag{5-9}$$

where z : Dynamic load transfer contribution, or moment of inertia by the total brake force, W·α/g

Then, the maximum brake force on each axle is given by:

$$B_f = \mu \cdot W_f^{'} = \mu\left(W_f + \frac{\alpha}{g} \cdot W \cdot \frac{h}{L} \right) \tag{5-10}$$

$$B_r = \mu \cdot W_r^{'} = \mu\left(W_r - \frac{\alpha}{g} \cdot W \cdot \frac{h}{L} \right) \tag{5-11}$$

where μ : Friction coefficient

The maximum brake force which varies differently at each axle is dependent on the deceleration and can be obtained when the friction coefficient, μ, equals the deceleration ratio, α/g.

$$B_f = \frac{\alpha}{g} \cdot \left(W_f + \frac{\alpha}{g} \cdot W \cdot \frac{h}{L} \right) \tag{5-12}$$

$$B_r = \frac{\alpha}{g} \cdot \left(W_r - \frac{\alpha}{g} \cdot W \cdot \frac{h}{L} \right) \tag{5-13}$$

where μ : Friction coefficient

From the vehicle specification, applying the following data to the equations from (5-4) to (5-13), the equations for the ideal brake force distribution curve may be obtained.

- Vehicle specification
  - Vehicle weight: 5,500 kg
  - Wheelbase, L : 3,375 mm
  - L_1 : 2,007 mm
  - L_2 : 1,368 mm
  - H : 912 mm

$$B_f = 21866 \cdot \frac{\alpha}{g} + 14578 \left(\frac{\alpha}{g} \right)^2 \quad \text{(N)} \tag{5-14}$$

$$B_r = 21866 \cdot \frac{\alpha}{g} - 14578 \left(\frac{\alpha}{g} \right)^2 \quad \text{(N)} \tag{5-15}$$

Using the equations (5-14) and (5-15), the ideal braking force and torque curve is drawn as shown in Figure 5-14.

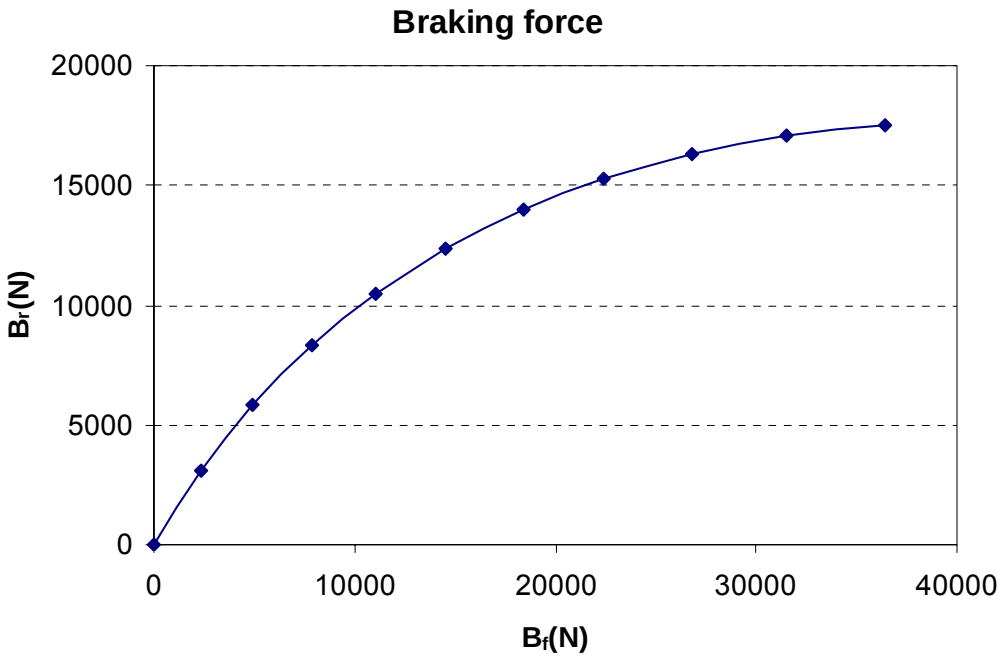

(a) Braking force distribution

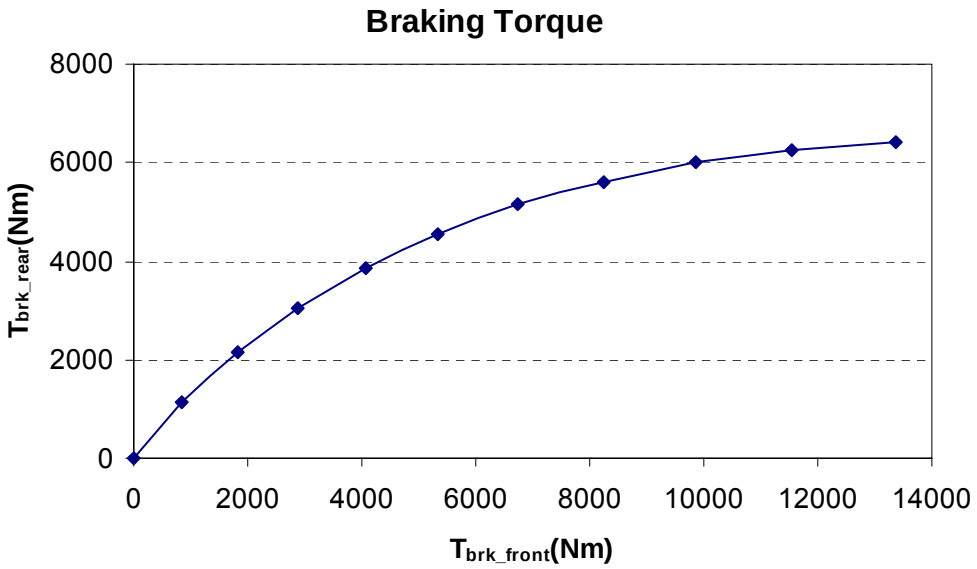

(b) Braking torque distribution

Figure 5-14 Ideal braking force and torque distribution

5.2.4.2 Algorithm for the regenerative brake controller

Now that the brake torque on each wheel is known, the capacity for the regenerative brake can be calculated. The algorithm and the mathematical relation for the regenerative braking are presented hereafter. Figure 5-15 shows the algorithm. It does not include the algorithm for the mechanical brake, because it is quite simple such that the brake torque demand from the driver is given to the friction brake.

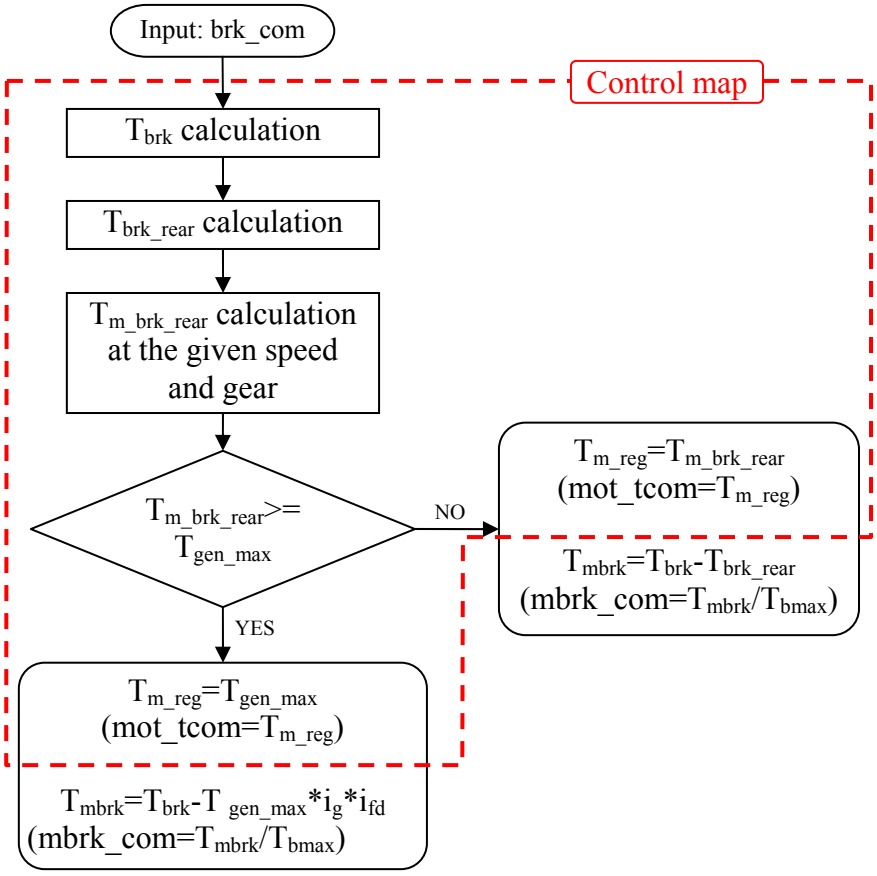

Figure 5-15 Algorithm for the regenerative braking

The total braking torque can be estimated by the braking command from the driver model, or the signal of the brake pedal position.

$$T_{brk} = brk\_com \times T_{b\max} \tag{5-3}$$

where T_{brk} : Torque required by the braking command, brk_com.

T_{bmax} : Maximum braking torque of the vehicle (Nm)

Based on the brake mode from the mode selector, the distribution of these braking torques is determined. In the mechanical brake mode, all the braking torque is assigned to the mechanical brake and the vehicle stopped by the friction brake without any assistance of the regenerative brake. In the regenerative brake mode, the required braking torque is allocated to the EM in the torque capacity range and the rest torque is handled by the mechanical brake. Therefore, the total torque can be divided to two parts:

$$T_{brk} = T_{mbrk} + T_{reg} \tag{5-4}$$

where T_{brk} : Total braking torque required by the brake pedal position

T_{mbrk} : Braking torque produced by the mechanical brake

T_{reg} : Regenerative braking torque at rear wheels

Alternatively, this total brake can be expressed by the torque on the front wheel and the rear wheels.

$$T_{brk} = T_{brk\_frt} + T_{brk\_rear} \tag{5-5}$$

As the braking torque on the rear wheels can be calculated from the equation (5-5) and Figure 5-14 (b), the regenerative braking torque in the generator, $T_{m\_brk\_rear}$, is obtained by the following euation:

$$T_{m\_brk\_rear} = \frac{T_{brk\_rear}}{i_g \times i_{fd}} \tag{5-6}$$

If this torque is greater than the maximum torque capacity of the generator at the given rotary speed, the maximum torque of the EM becomes the EM torque demand for the regeneration, T_{m_reg}, otherwise the calculated torque, $T_{m\_brk\_rear}$, becomes the EM torque demand.

Finally, the torque demand for the mechanical brake can be obtained from the equation (5-4), as the regenerative braking torque on the rear wheels, T_{reg}, is calculated by multiplying T_{m_reg} and total reduction ratio, $i_g \cdot i_{fd}$.

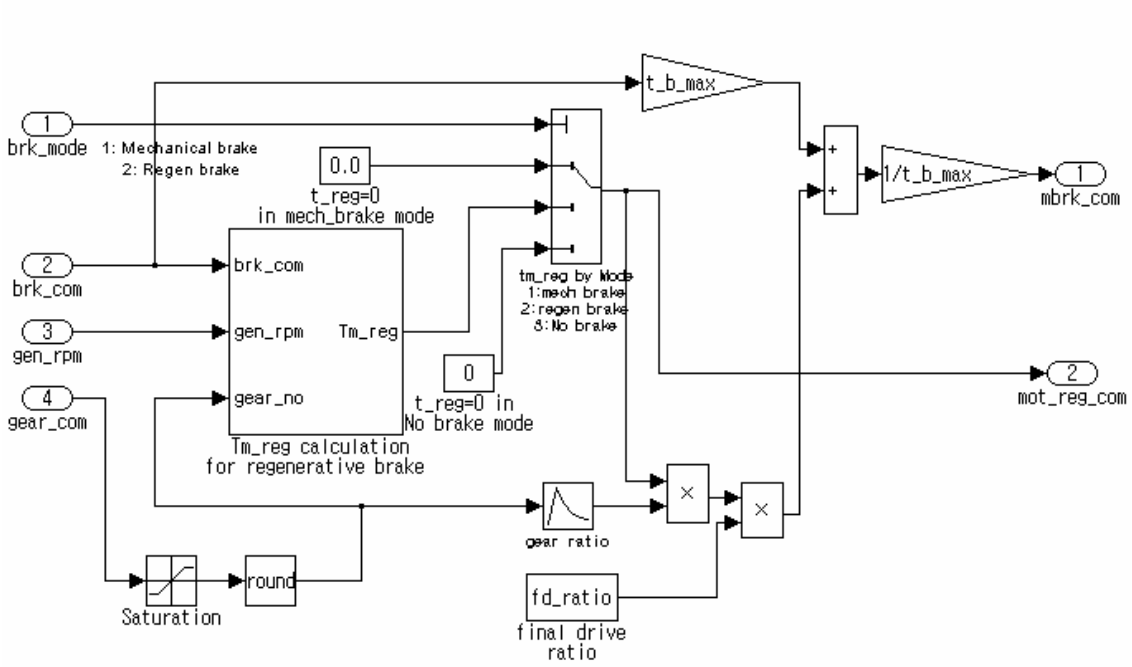

(a) Overview of brake controller

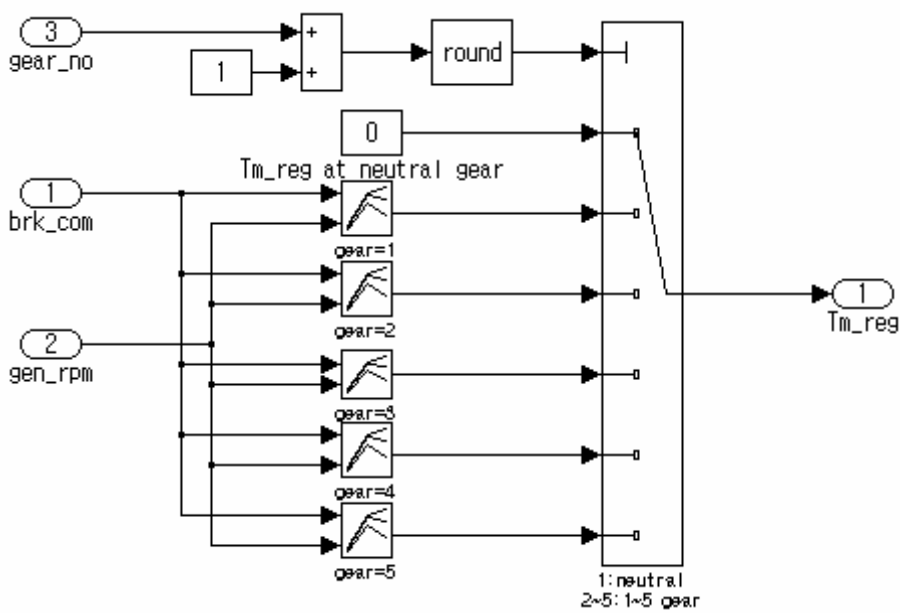

(b) T_{m_reg} map at the given condition

Figure 5-16 Brake controller built in Simulink

5.2.4.3 Brake controller built in Simulink

The brake controller built in Simulink is presented Figure 5-16, based on the algorithm represented in Figure 5-15. In order to make the controller simple and avoid the singularity problem, the part inside the dotted line in the algorithm is made as a type of map in Simulink. Therefore, the Matlab program is coded to make the regeneration torque demand map according to the given rotary speed and gear step. The program is presented in Appendix #4.

5.2.5 Clutch & Transmission controller

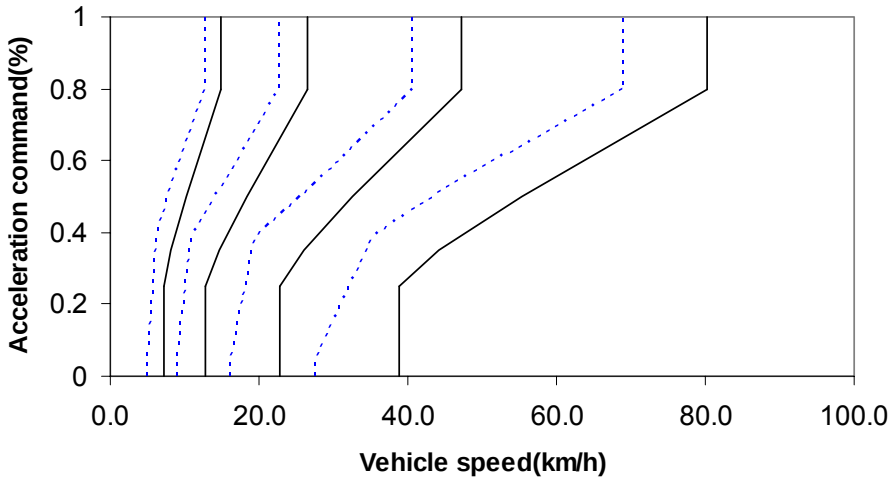

Figure 5-17 Gear shift map for the automated manual transmission

The controller for the automated manual transmission is similar to the manual gearbox transmission. However, the gear shift map is made considering the engine efficiency and the vehicle performance, and is therefore more complicated. Thus, the accelerator pedal position signal as well as the engine speed is needed as input signals to select the gear step. Figure 5-16 shows the gear shift map used in this controller. The solid line describes the upshift map and the dotted line represents the downshift map. During the upshift, the comparison with the previous gear step by using the memory block is carried out to avoid any hysteresis. That is, only if the next gear step is greater than the previous step during the upshift, the gear command is changed. If the vehicle control

speed is zero, the gear will output the neutral signal, 0. The final transmission controller built in Simulink is illustrated in Figure 5-17.

The clutch controller is quite simple. As the required clutch signal is 1 for the disengaged state and 0 for the engaged state, the appropriate signal outputs according to the operation mode are determined by the mode selector. Only in the case of the motor only mode, this controller produces the signal for the disengaged state, 1.

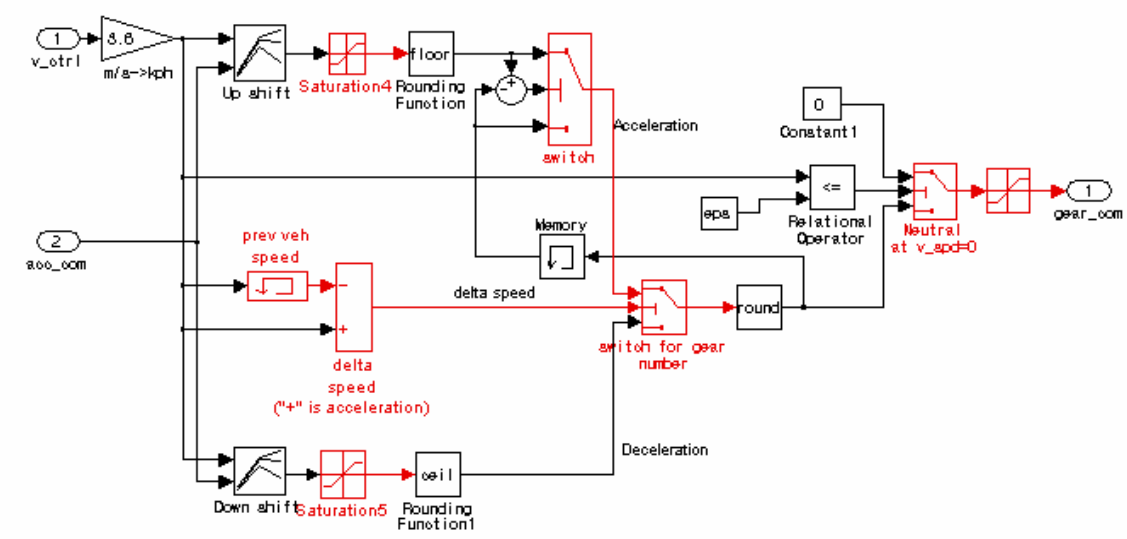

Figure 5-18 Automated manual transmission controller

5.2.6 Basic simulation and Improvement of the HEV controller

As a result of initial simulation with the basic controller, some problems were found. Firstly, this controller does not consider the remaining SoC after running the given drive cycles. As shown in Figure 5-19, the final battery SoC becomes completely different from 33% to 78% according to the drive cycles, although the initial SoC is set to the same value, 60%. This means that this controller is not applicable to the real driving condition and it is hard to evaluate the practical fuel economy due to the difference.

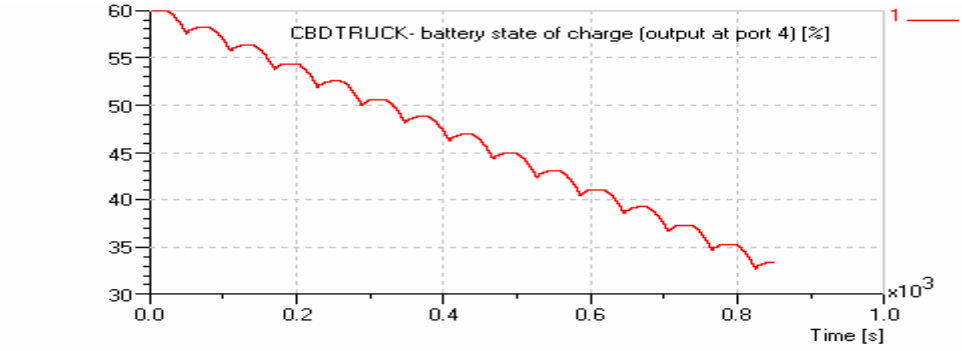

(a) CBDTRUCK

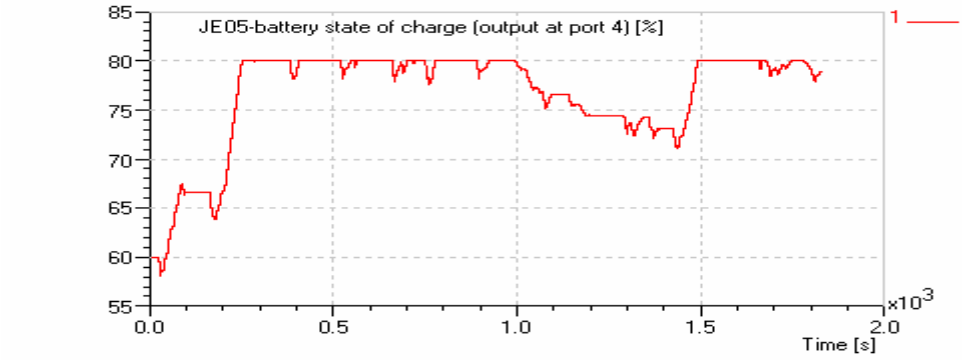

(b) JE05

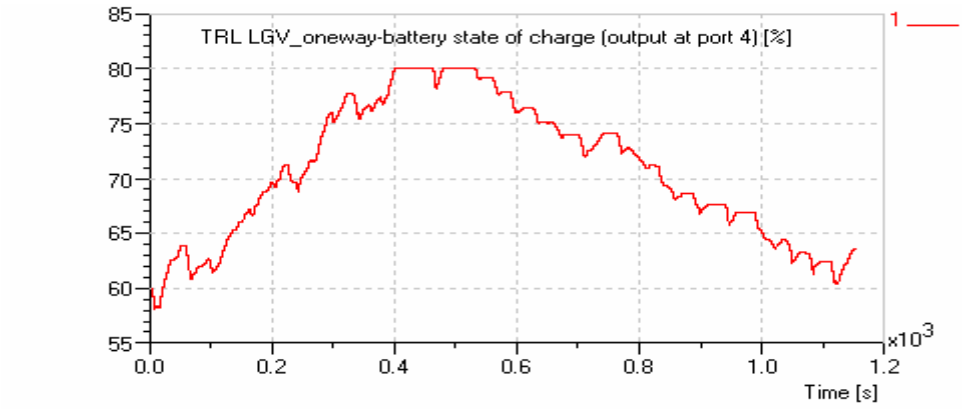

(c) TRL LGV oneway

Figure 5-19 Changes of Battery SoC after simulation with a basic controller

Secondly, the maximum power cannot be used from the control strategy, because the maximum power of the ICE is set to the OOL torque to improve engine efficiency. That is, the total power in the hybrid mode cannot reach over the maximum torque of the EM plus the torque of the ICE at the OOL. It can result in a drop in vehicle performance. Therefore, the basic controller needs to be modified slightly.

5.2.6.1 Improved charge-sustaining strategy

In order to maintain the battery SoC during the drive cycles, the engine operating zone is changed in the improved controller according to the current battery SoC, whilst the basic controller has a line of engine operating region (OOL). For this purpose, the engine operating zone is determined by using the upper threshold and the lower threshold. In case the target SoC is 60%, the normal operating limit is set to +/- 10%. As shown in Figure 5-20, the upper threshold is between the maximum engine torque and the OOL torque and the lower threshold is from zero to the OOL torque. These thresholds are changeable by the SoC. When the SoC reaches the upper limit, 70%, the upper threshold for the engine operating zone becomes the OOL and the lower threshold becomes the zero torque line. That is to say, the charge amount by the ICE decreases. On the other hand, as the SoC reaches the lower limit, 50%, the upper ICE operating threshold becomes the maximum torque line of the ICE, and the lower threshold becomes the OOL.

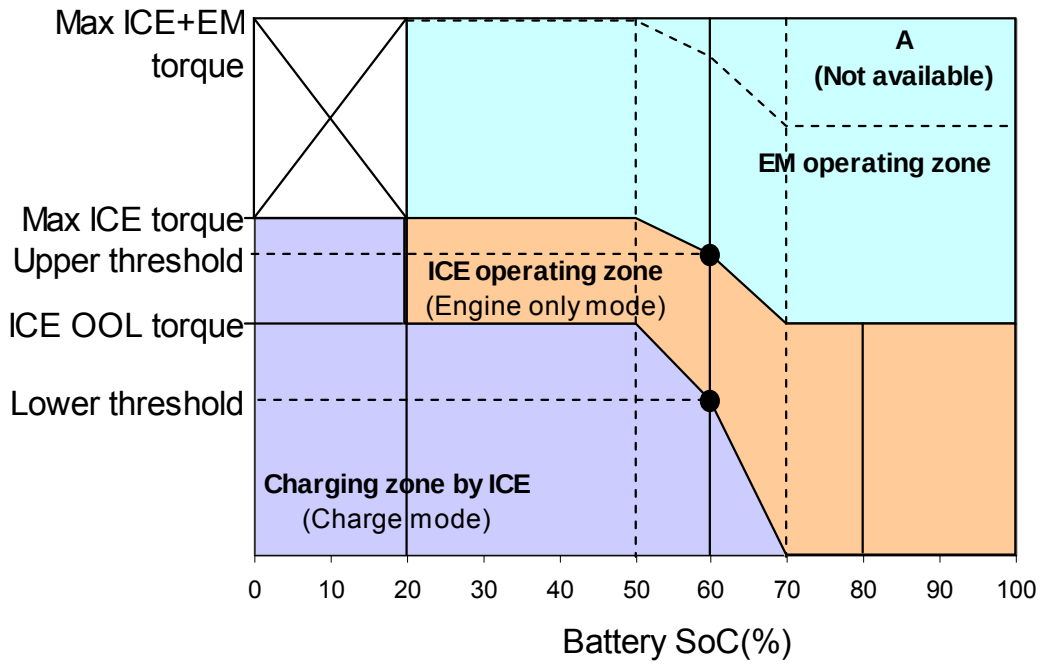

Figure 5-20 Improved charge-sustaining strategy

The second problem is about the maximum torque from the ICE and the EM. Like region A in Figure 5-20, the maximum torque cannot be obtained when the SoC is sufficient, even with the improved controller, because the upper engine operating threshold is set to the OOL or less than the maximum torque. So the modified algorithm is needed to improve the controller. If the required torque is greater than the maximum EM torque and the ICE torque at the upper threshold, the ICE will produce the maximum torque at a given rotary speed.

A new flow chart using this improved charge-sustaining strategy and power split strategy is presented in Figure 5-21 and Table 5-3. Figure 5-22 shows the improved controller built in Simulink based on the modified control strategy.

5.2.7 Completion of HEV model and co-simulation

Finally, the component models for the LD hybrid electric truck are integrated with the improved controller as shown in Figure 5-23.

Table 5-3 Power split strategy for the improved controller

No.	Mode	Torque Split	Output command	Remarks
1	Charge	$T_e=T_{e\_lwr}$ $T_m=(T_{e\_lwr}-T_{acc})x-1$	eng_com =T_{e_lwr}/T_{e_max} mot_tcom=T_m	
2	Engine only	$T_e=T_{acc}$ $T_m=0$	eng_com =acc_com mot_tcom=0	
3	Motor only	$T_e=0$ $T_m=T_{acc}$	eng_com =0 mot_tcom=T_{acc}/T_{m_max}	
4	Hybrid	$T_e=T_{e\_upr}$ $T_m=T_{acc}-T_{e\_upr}$	eng_com =T_{e_upr}/T_{e_max} mot_tcom=$T_{acc}-T_{e\_upr}$	
5	Max hybrid	$T_e=T_{e\_max}$ $T_m=T_{acc}-T_{e\_upr}$	eng_com =1 mot_tcom=$T_{acc}-T_{e\_max}$	T_{e_max}/T_{e_max}
6	No acceleration	$T_e=0$ $T_m=0$	eng_com =0 mot_tcom=0	

As the component model was built in AMESim and the controller was designed in Simulink, the interface between the two simulation tools is used. So the co-simulation of AMESim and Simulink is carried out for the simulation on a number of drive cycles.

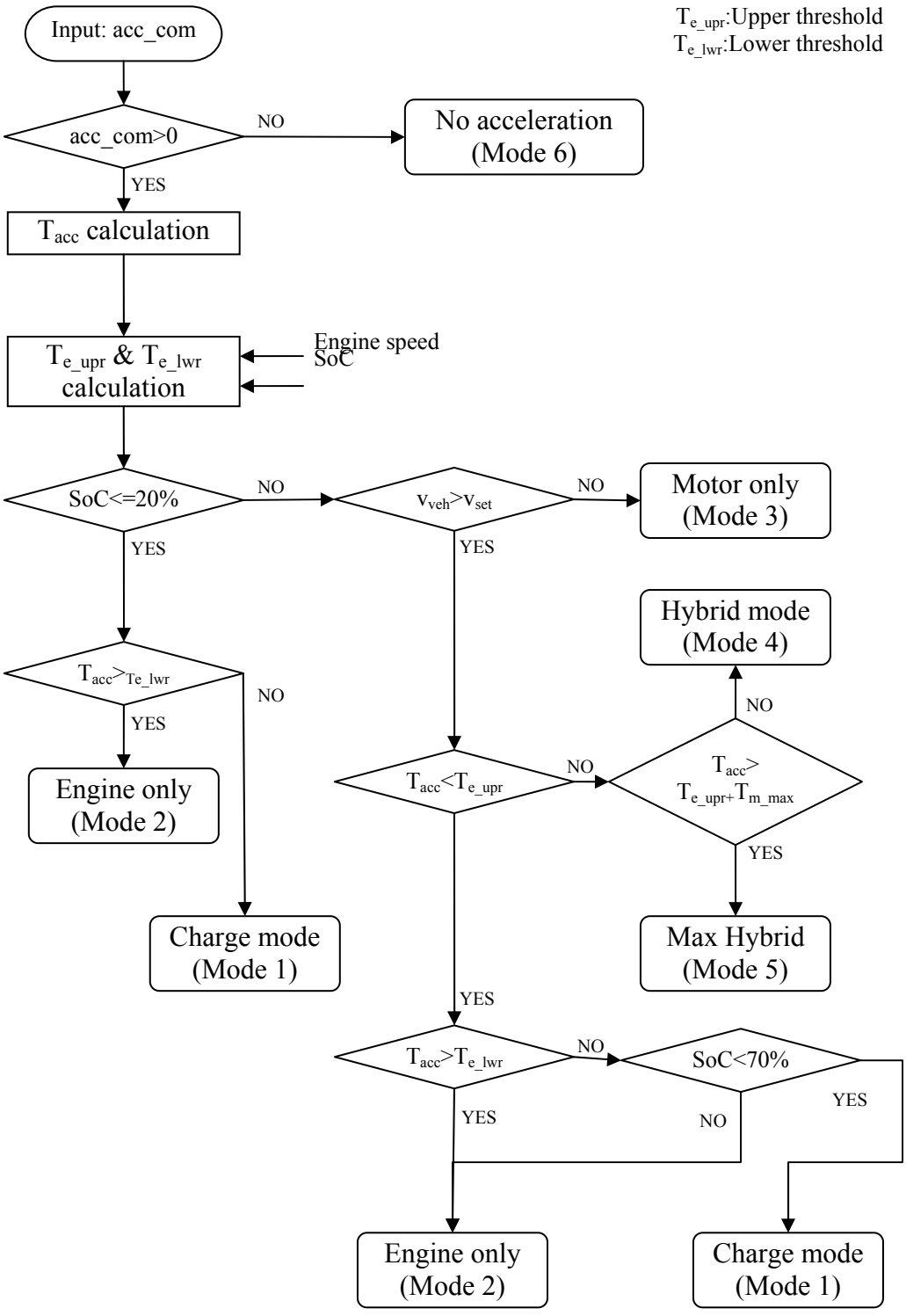

Figure 5-21 Improved flow chart for the acceleration mode selector

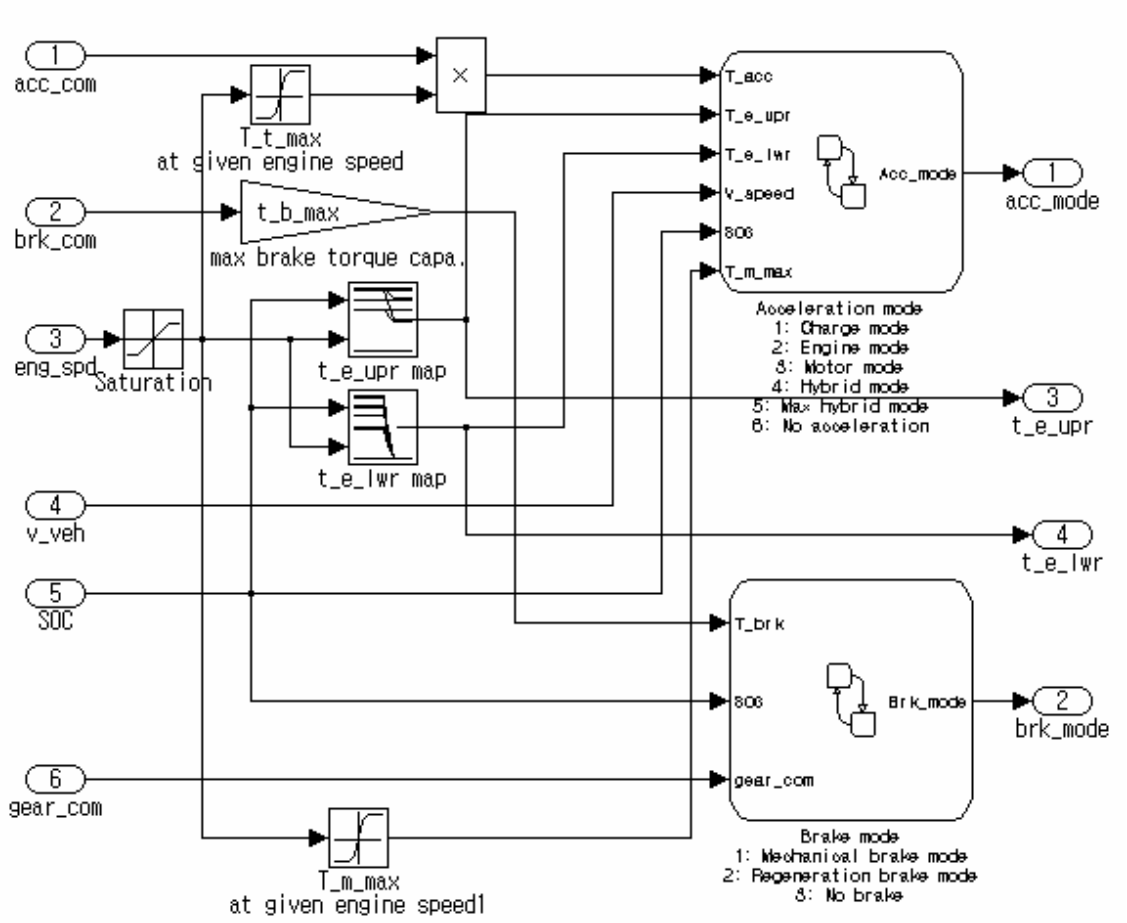

Figure 5-22 Improved mode selector

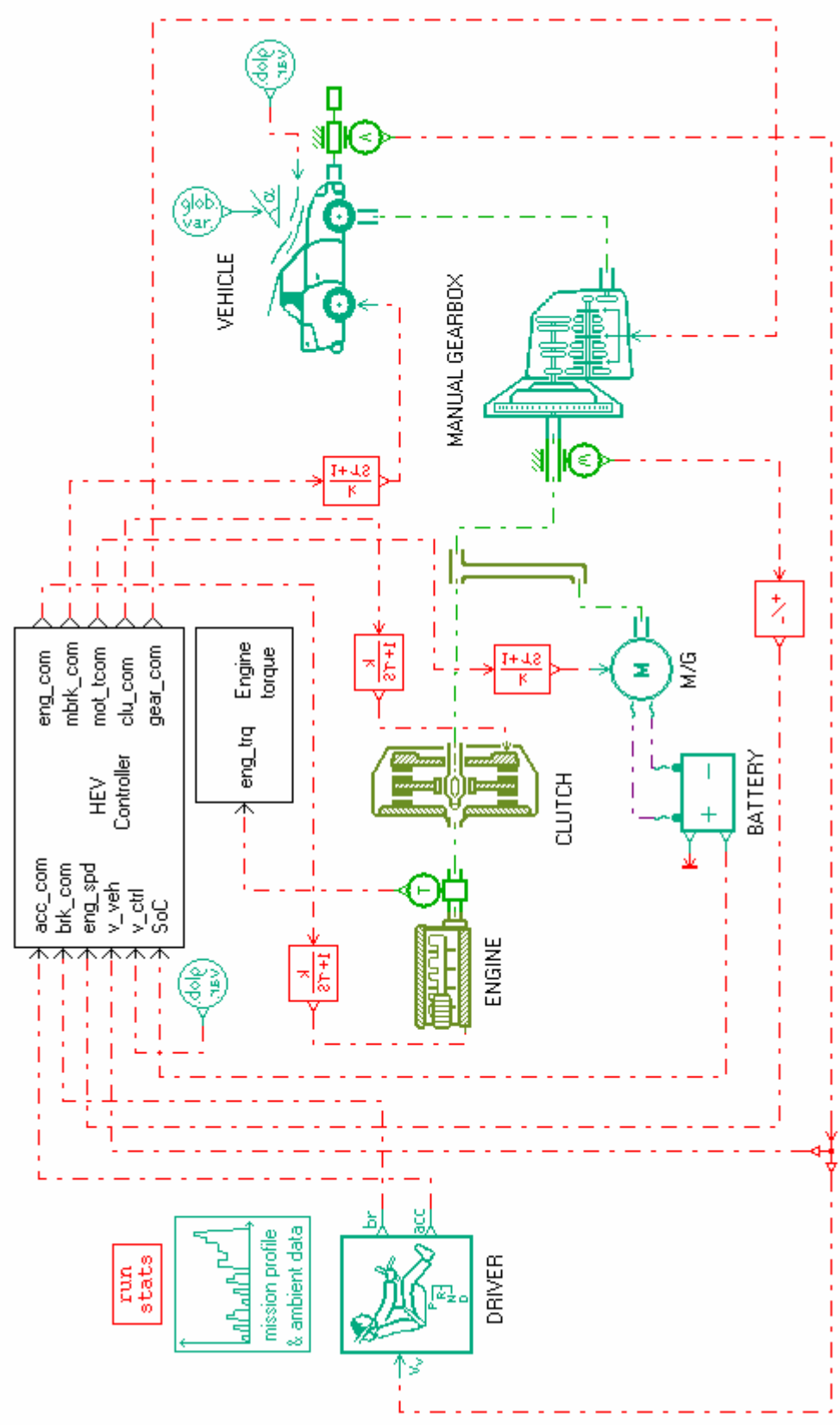

Figure 5-23 Integration of HEV model and controller

6 Simulation results

After the component models of the conventional truck and the hybrid electric truck and the controllers are integrated, the simulation to compare the operation and the fuel consumption is carried out. This Chapter summarises the simulation results. The simulation is implemented with selected drive cycles to compare the results. The order of simulation is as follows.

Firstly, the simulation for the basic duty cycle is performed to verify and understand the basic function of the built model and controller. Secondly, further optimisation of the controller concerned with the engine operating zone is made based on the remaining SoC and the fuel consumption. Thirdly, the effect on the change of the EM power capacity is studied. Finally, fuel consumption on a few duty cycles is compared. Most of the simulations are conducted on 3 drive cycles, as previously explained: CBDTRUCK for the USA, TRL LGV drive for Europe, JE05 for Asia.

6.1 Basic simulation

The basic simulation is carried out along the basic duty cycle composed of gentle acceleration, cruise speed, and gentle deceleration. The gentle acceleration is set to increase the vehicle velocity from zero to 20 m/s over 40 seconds and the cruise zone is set to 20 seconds. The deceleration zone is set to decrease the velocity to zero over 50 seconds. The simulation results for the conventional vehicle model and the hybrid electric model are presented in this order. This simulation is for verifying and understanding the different functions between the conventional truck and the hybrid electric truck.

6.1.1 Conventional vehicle

As the structure and the controller function of the conventional vehicle are not as complicated as those of the HEV, the simulation results are quite simple. Figure 6-1 compares the required velocity profile with that of the current velocity achieved by the built model over the drive cycle.

It is shown that the built vehicle model follows the vehicle control speed well except for the low velocity area. This is due to the idling control and accelerator pedal sensitivity. As the engine controller is designed to maintain the idling speed and the relation between the acceleration position and the engine torque is not linear, the ICE produces more power than is needed.

In the gentle deceleration phase, the negative torque, which is used to decelerate the vehicle, is produced by the engine friction loss, as shown in Fig 6-1 (b). However, it is not actually sufficient to do that. So the braking torque by the brake command occurs in this region, too. The torque spike that occurred around 120s in Figure 6-1 (b) is for the idle speed control. Because it is assumed that the ICE of the conventional truck is operating during the duty cycle, this occurrence is reasonable. Figure 6-1 (c) and (d) show that the engine speed is well managed between the idle speed and the maximum speed, and that the gearbox is controlled from the neutral position to 4^{th} gear along the vehicle speed. It should be noted that the engine speed is negative, because it is the sign convention of the rotary speed in AMESim.

6.1.2 Hybrid electric truck

As designed in the last Chapter, the LD hybrid electric truck has a complex architecture. The controller especially has a variety of functions and more control variables. So the function and operation of each component have to be verified before simulating the built model for full drive cycles.

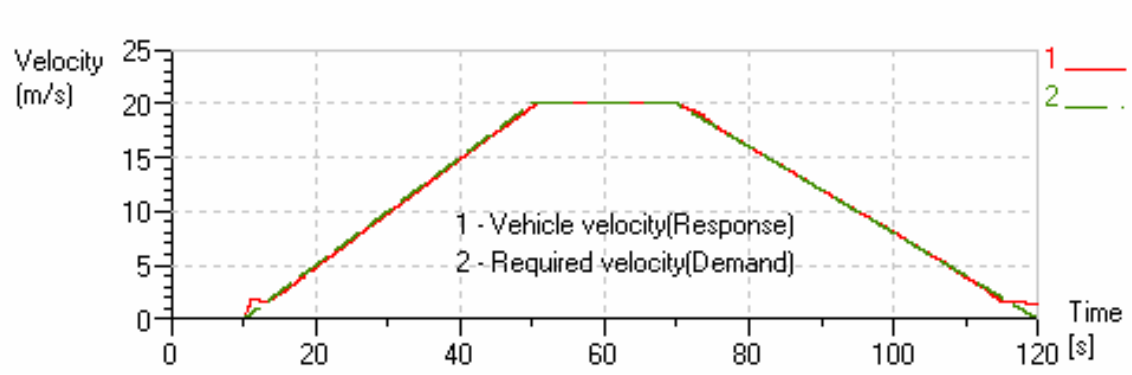

(a) Velocity profile

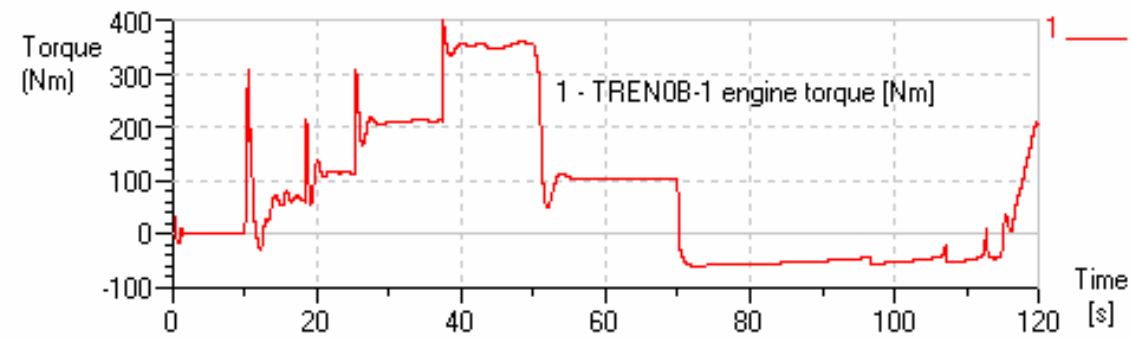

(b) Engine torque

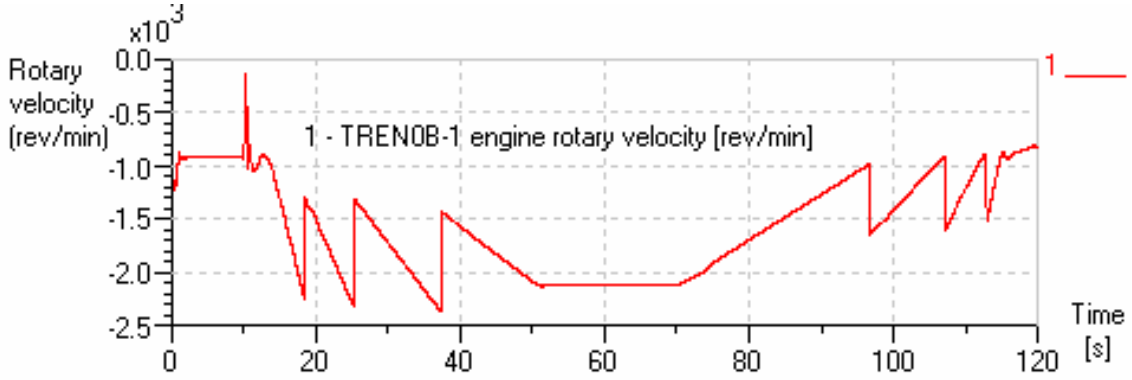

(c) Engine rotary speed

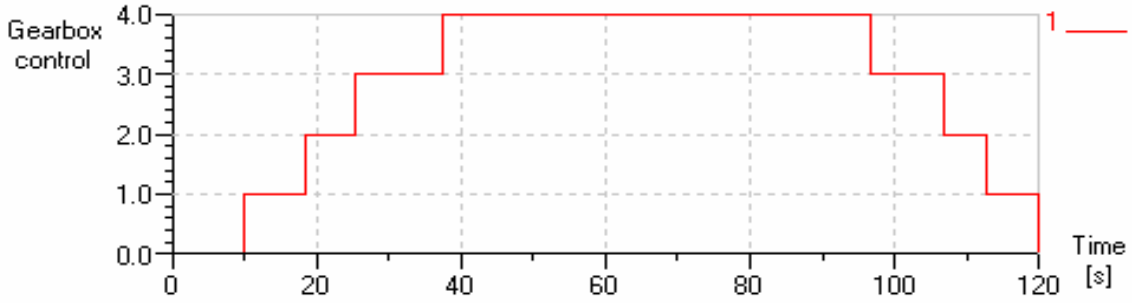

(d) Gearbox control

Figure 6-1 Simulation of the conventional truck - Basic duty cycle

Some assumptions have to be made for this simulation. Firstly, it is assumed that the engine has a function of idle stop. It is a practical assumption because this model has a second power source, the EM and battery. Secondly, the road slope is assumed to be zero, as there is no consideration on climbing data in drive cycles. Thirdly, the engine is at normal operating temperature. Finally, the initial battery SoC is 60%.

Based on the conditions mentioned above, the simulation on the basic drive cycle is carried out. Figure 6-2 represents the results. The HEV operates and follows the required velocity well. Figure 6-2 (b) indicates the operation modes determined by the mode selector. The number of modes was mentioned in Figure 5-22. Comparing this result with the velocity profile, it can be found that the mode changes from the motor only mode to the hybrid mode in the acceleration phase. In addition, usually the charge mode is selected in the cruise speed and the regeneration brake mode in the deceleration phase. The mechanical brake mode is chosen only during the gear shift in the deceleration phase.

The function of each operation mode can be explained in Figure 6-2 (c). In the figure, A is the motor only mode in which the engine is stopped and produces no torque. B means the engine only mode in which the ICE is the only power source without assistance from the EM. C represents the charge mode. The engine operates alone and charges the battery with spare torque. D indicates the regenerative brake mode. The output torque is negative and is used to recover the braking energy. Figure 6-2 (d) and (e) show the rotary speed and the selected gear step, respectively.

When the initial battery SoC is set to 60%, the change of SoC during the basic drive cycle, from 60% to 63.6%, is shown in Figure 6-2 (f). As estimated, the SoC decreases in the acceleration phase but increases in the cruise phase and deceleration phases. In addition, the energy recovery by the regenerative brake is bigger than that through the charge from the engine. This is dealt with in detail in the next section.

From the basic results, it is found that the integrated component model and controller works well. So this model can be used for the further tuning of the HEV controller.

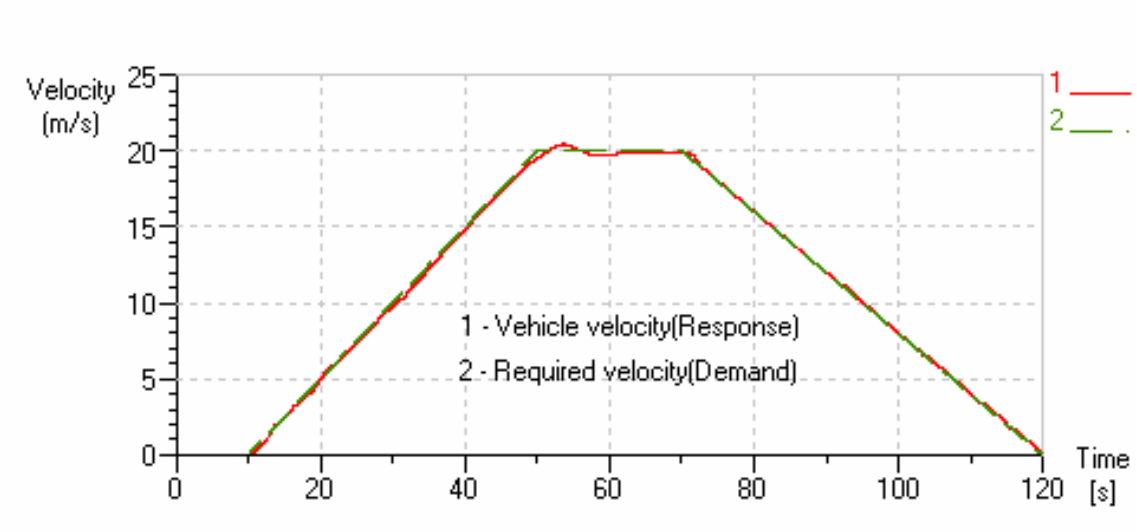

(a) Velocity profile

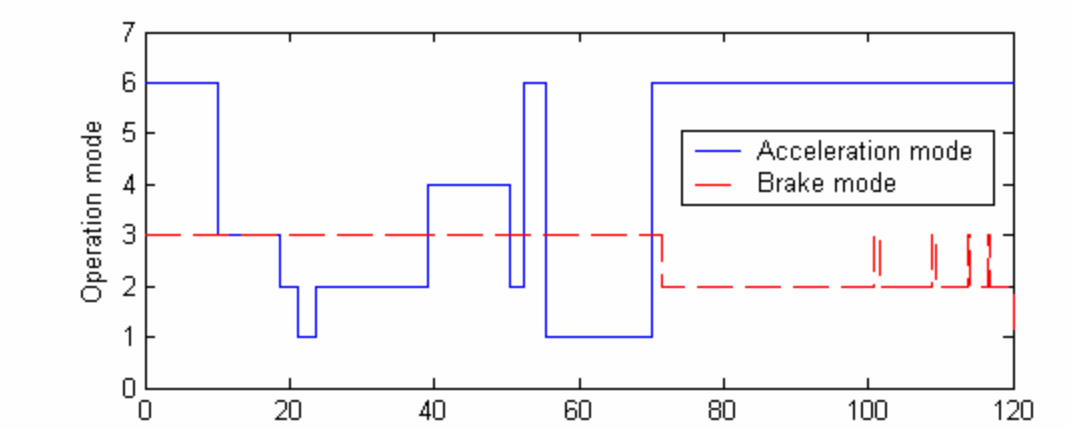

(b) Operation mode

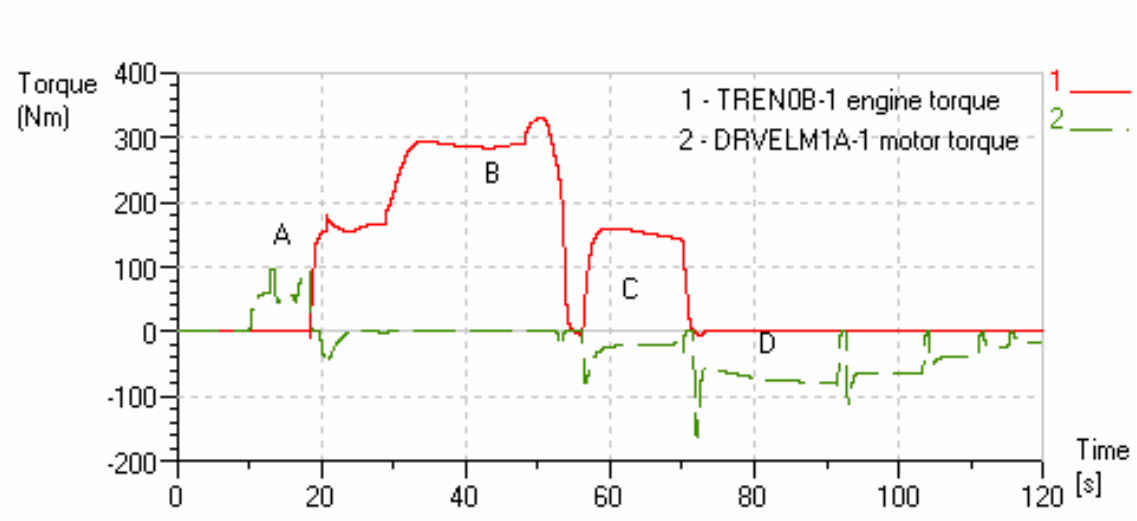

(c) ICE & EM torque

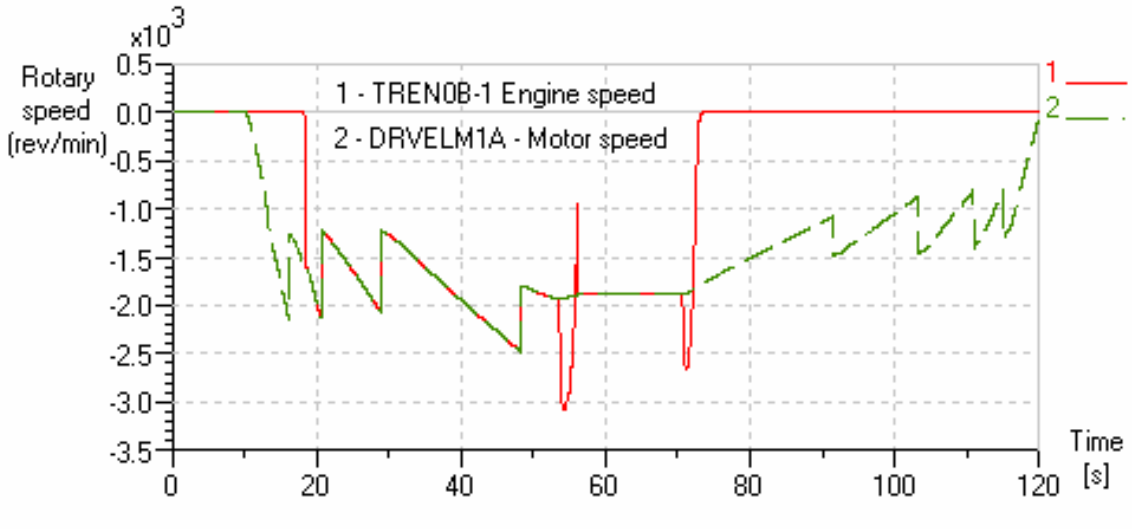

(d) ICE & EM rotary speed

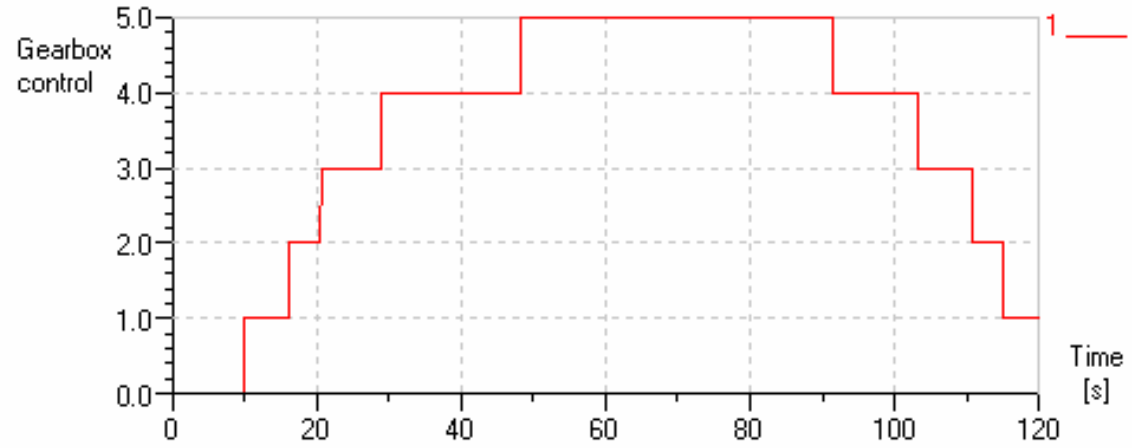

(e) Gearbox control

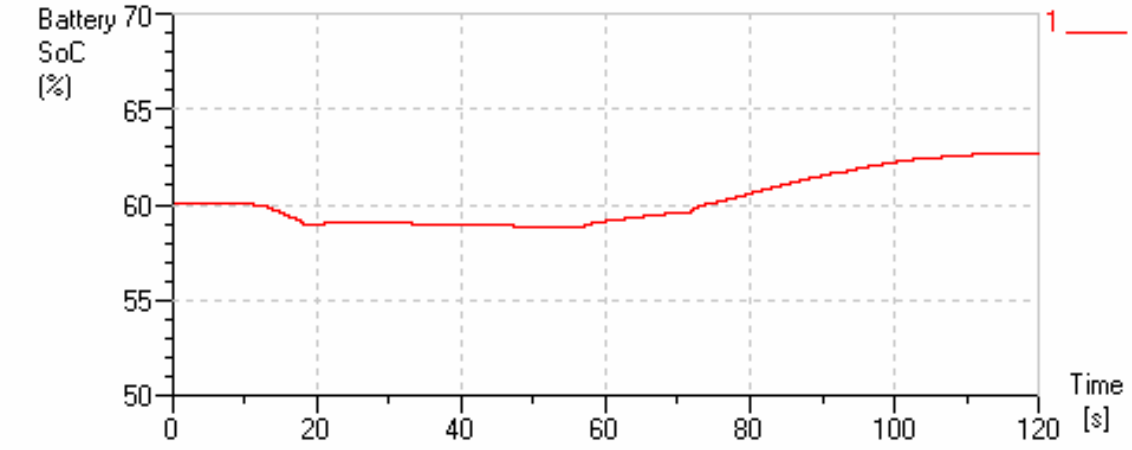

(f) ICE & EM torque

Figure 6-2 Simulation of the LD hybrid electric truck - Basic duty cycle

6.2 Effect of the engine operating zone

With the suggested concept to improve the HEV controller in section 5.2.6, several simulations are carried out for a number of drive cycles. This is for studying the effect on the engine operation zone. That is to say, according to the width of the operation zone, the change of the battery SoC is studied. The simulations are carried out along the change of the ICE operation threshold from 20% to 80%.

Figure 6-3 shows the simulation results performed on the CBDTRUCK cycle, JE05 cycle, and TRL LGV drive cycle, respectively. In this figure, the threshold means the engine operation threshold in terms of the normalised engine efficiency. As the threshold increases, the operation zone decreases near the OOL and the charging amount from the engine increases. The smaller threshold means that the ICE operation zone is increased to limit the charging from the engine. Therefore, the final battery SoC is affected by this threshold. As estimated, the final battery SoC increases with the threshold.

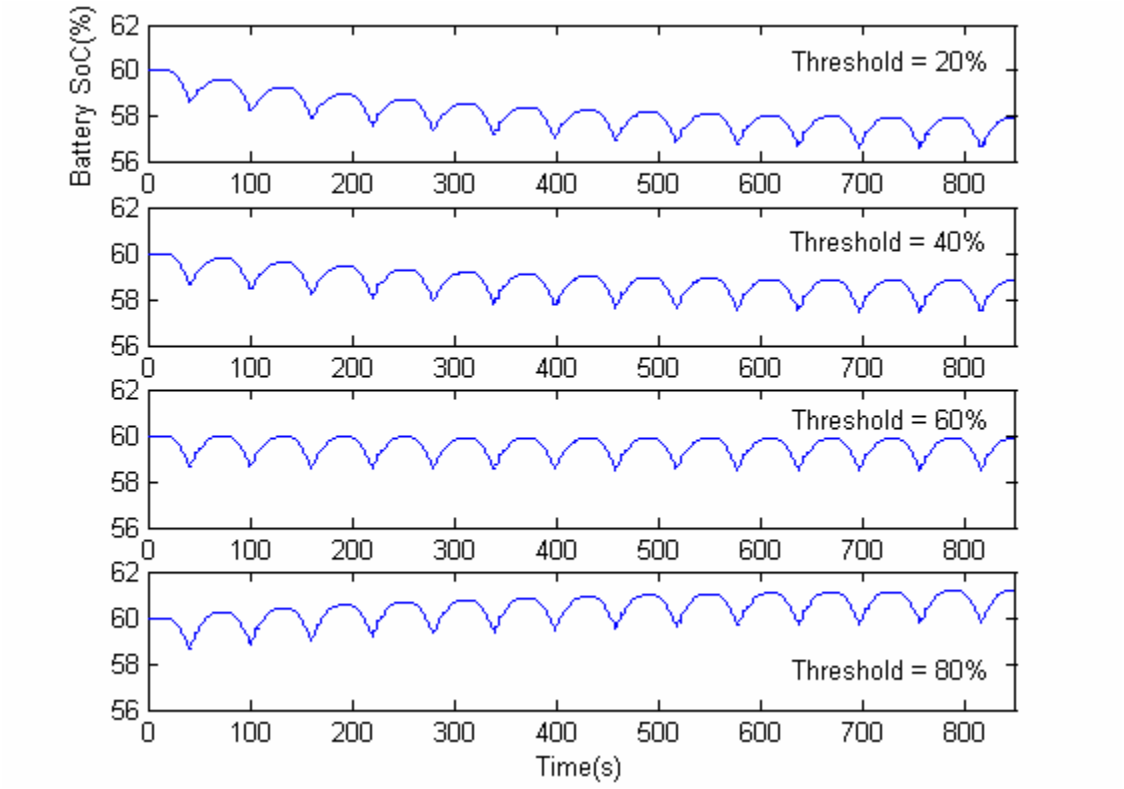

(a) CBDTRUCK cycle

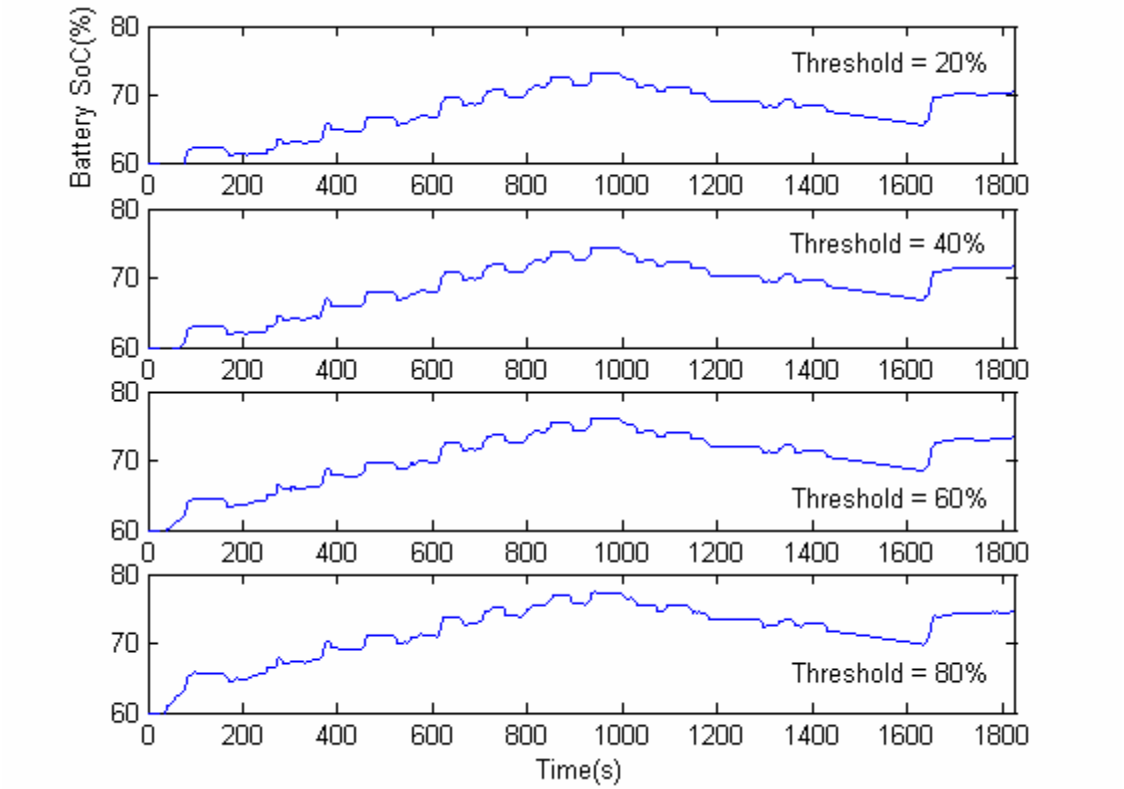

(b) JE05 cycle

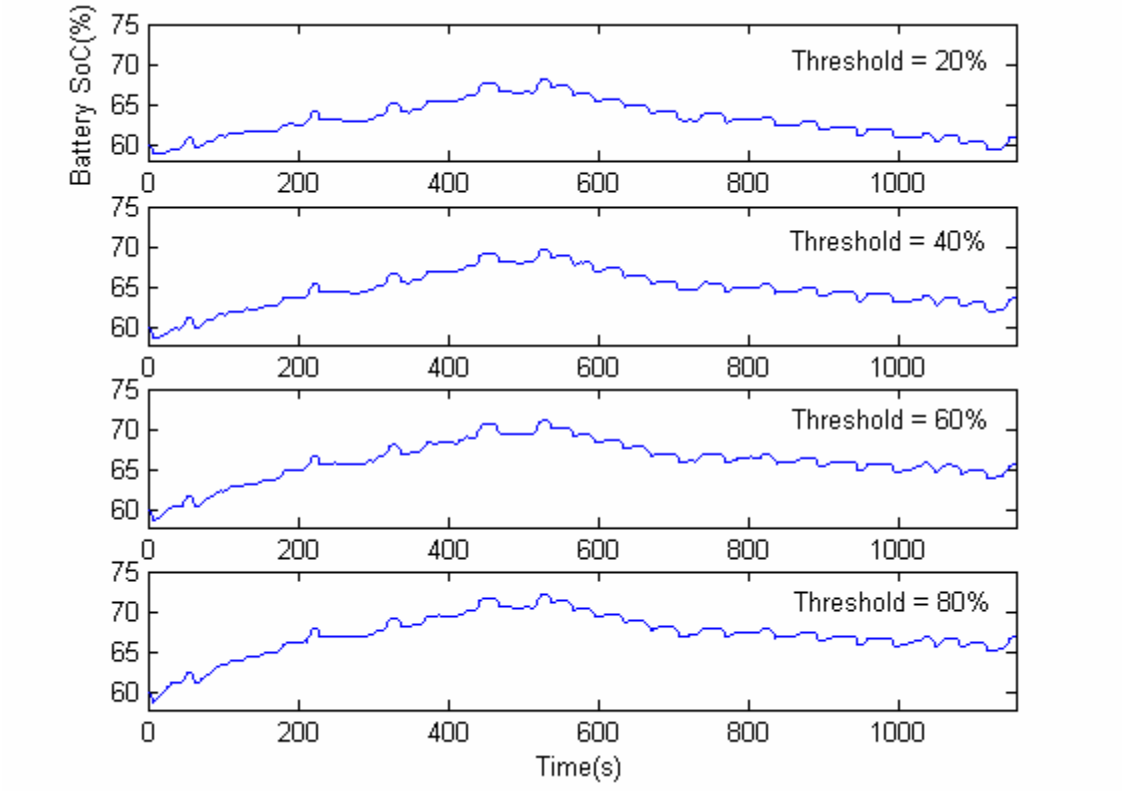

(c) TRL LGV drive cycle

Figure 6-3 Changes of the battery SoC according to the engine operation threshold

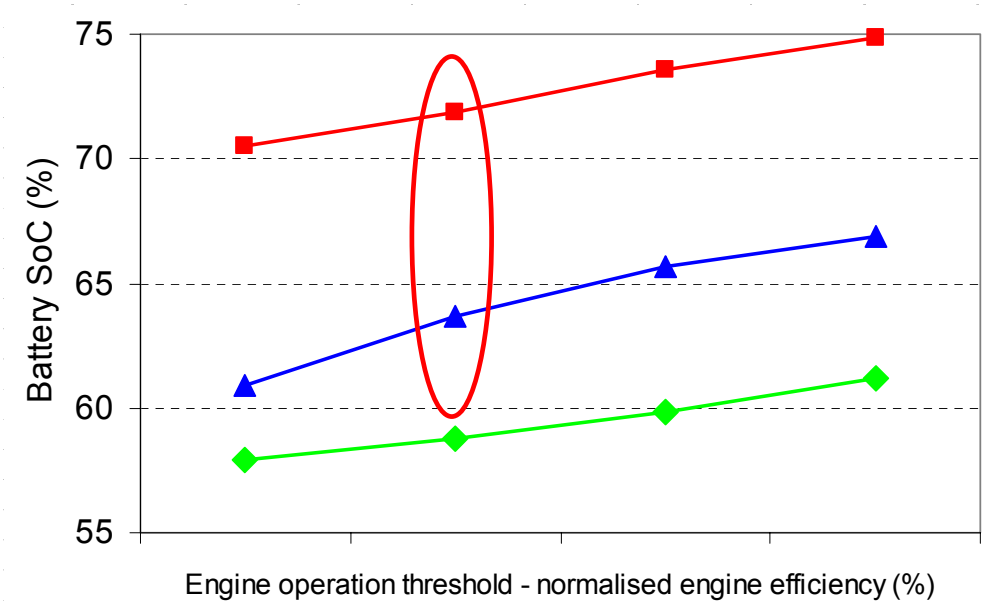

Figure 6-4 Changes of the final SoC according to the engine operation threshold

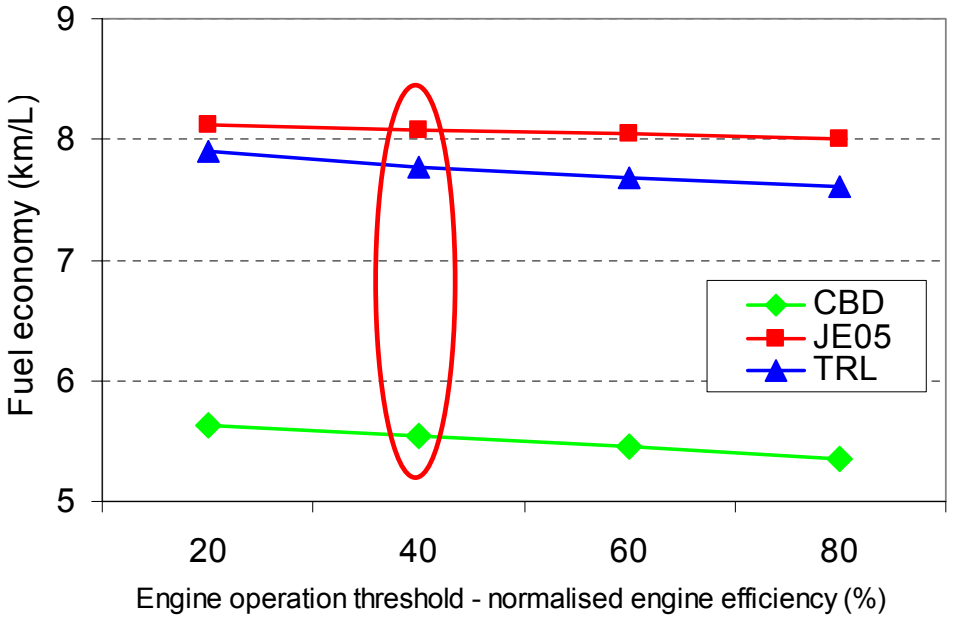

Figure 6-5 Fuel consumption according to the engine operation threshold

Although the target normal SoC limit is set to ±10%, the final SoC becomes over 70% in JE05 cycle as shown in Figure 6-3 (b). This is because there are severe deceleration zones in this cycle, compared to the other two cycles. In particular it can be seen that the big regeneration occurred after 1600s. So it can be presumed that the SoC change is more affected by the regenerative brake than by the engine operation zone in this mode.

On the other hand, the SoC in the JE05 and TRL drive cycles is relatively well maintained in the target operating limit.

Figures 6-4 and Figure 6-5 compare the final battery SoC and the fuel consumption according to the engine operation threshold, respectively. It is natural that the final SoC increases as the charge from the ICE increases, or the operating threshold increases. On the other hand, the fuel economy decreases slightly. This implies that the improvement of the ICE efficiency to increase the charge amount does not always secure the improvement of the total energy efficiency. In addition, this fuel consumption result is not considered to be exact, because the battery SoC increases.

If the JE05 cycle is not considered in which it is hard to maintain the SoC in the target operating range without the modification of the regenerative brake, the 40% of engine operation threshold is preferred. Although the 20% threshold is surely reasonable, 40% is selected for the further simulation, because 20% is too small to apply the charge mode designed in the controller.

6.3 Effect of the electric machine power capacity

In this section, the effect on the EM power capacity with the 40% of engine operation threshold is studied through simulations. The EM power capacity is concerned with fuel economy as well as vehicle performance, and is dependent on vehicle architecture, the control strategy, and the driving condition. If the architecture and the controller are designed, the power capacity has to be verified on the target drive cycle. Thus, the EM

power capacity which was determined based on the vehicle performance is simulated and verified on 3 drive cycles.

The simulations are performed for the EM with the power capacity of 10 kW, 20 kW, 30 kW, and 40 kW. Figures 6-6, 6-7 and 6-8 represent the simulation results. First of all, all the final battery SoCs are in the target limit on the condition of 10 kW capacity and represent the peak in the 20 kW capacity, except for the JE05 drive cycle, as shown in Figure 6-6. As the power capacity increases over 20 kW, the final SoC has a tendency to decrease. This is because the energy consumption from the EM increases with the increase of the power capacity.

Nevertheless, all the EMs meet the target SoC limit in the CBDTRUCK and TRL drive cycles. This implies that all the EM series within 10 kW to 40 kW are applicable from the point of energy recovery.

On the other hand, the fuel consumption is nearly similar in the range of over 20 kW of power capacity on JE05 and TRL cycles, whilst the fuel economy on CBDTRUCK cycle tends to decrease as the power capacity increases. It seems that the average velocity of the CBDTRUCK cycle is lower than the others, and the energy consumption increases through the motor only mode.

Finally, as the motor only mode is applied at low speed and used to start the vehicle in the designed controller, the startability by the EM has to be checked. The conventional vehicle has over 30% of startability which can be used the criteria to determine the EM power. As Figure 6-8 shows, the start performance is proportional to the power capacity. From the figure, it can be seen that the 30 kW EM can produce about 30% startability and can be applied. The 40 kW EM can also be equipped, but the battery capacity has to be increased.

All things considered, therefore, it is desirable to apply the EM with 30 kW or slightly over 30 kW power capacity.

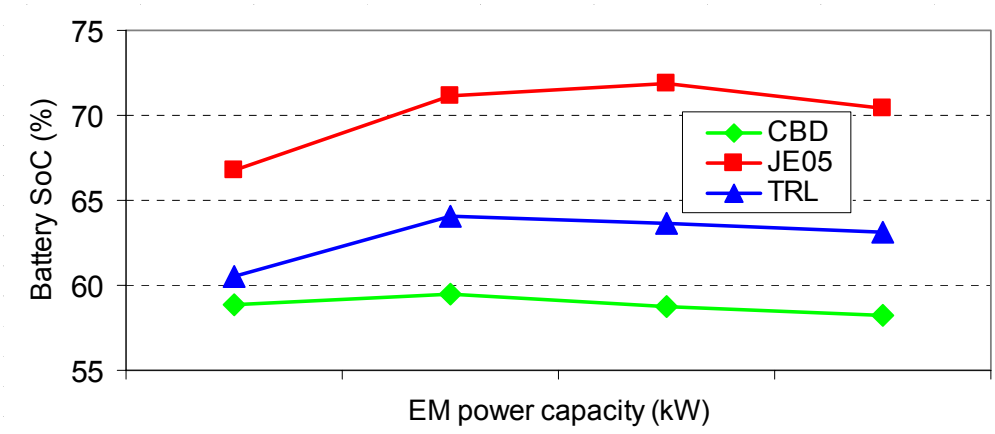

Figure 6-6 Final battery SoC vs. EM power capacity

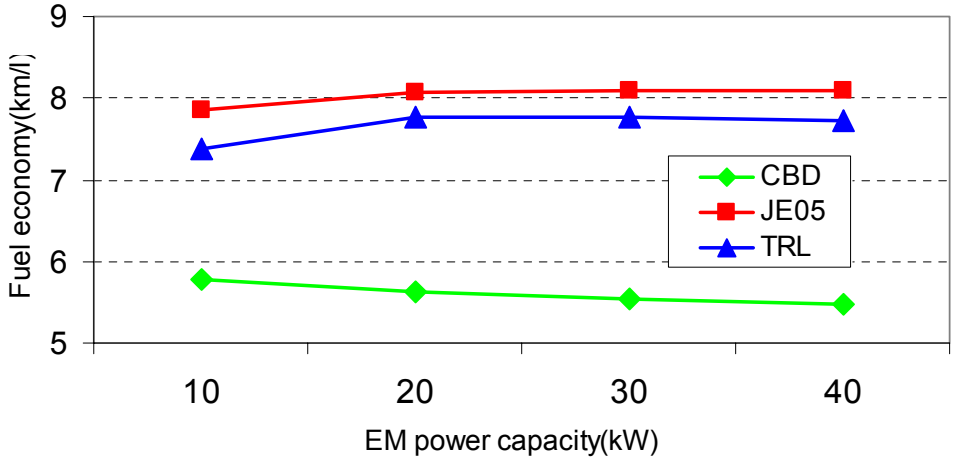

Figure 6-7 Fuel economy vs. EM power capacity

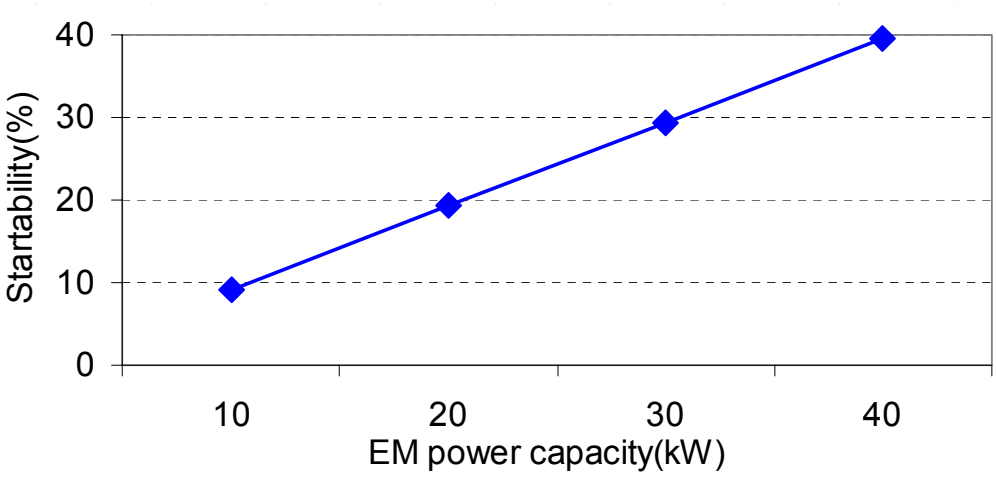

Figure 6-8 Startability vs. EM power capacity

6.4 Vehicle performance and fuel economy

With the engine operation threshold and the motor power capacity being determined, the comparative simulation between the conventional truck with diesel engine and the LD hybrid electric truck is carried out to study the improvement effect on fuel economy. Most of all, the basic performance of the HEV is verified compared to the conventional vehicle. After that, the fuel consumption is compared through the simulation on given drive cycles.

The basic performance, such as maximum velocity and maximum acceleration, can be confirmed by setting a simple vehicle control speed in AMESim. Figures 6-9 and 6-10 show the simulation results for the maximum velocity. The maximum speed of the HEV is 122km/h, whilst the conventional truck has a performance of 103km/h. Figures 6-11 and 6-12 are concerned with the maximum acceleration performance. As presented in Chapter 3, the required acceleration performance is 24 seconds to reach 80km/h from zero speed. The conventional truck manages to meet this requirement with 24.1 seconds, but the acceleration performance of the HEV is improved to 19.5 seconds. Therefore, it can be seen that this LD hybrid truck has enough performance to be applied and compete with conventional vehicles.

Next, the variation of the battery SoC, the total fuel consumption in g, and the torques of power sources are simulated on the given drive cycles. Figures 6-13 to 6-15 show the history of the vehicle behaviour. It is shown that the modelled HEV can follow all the required velocities adequately.

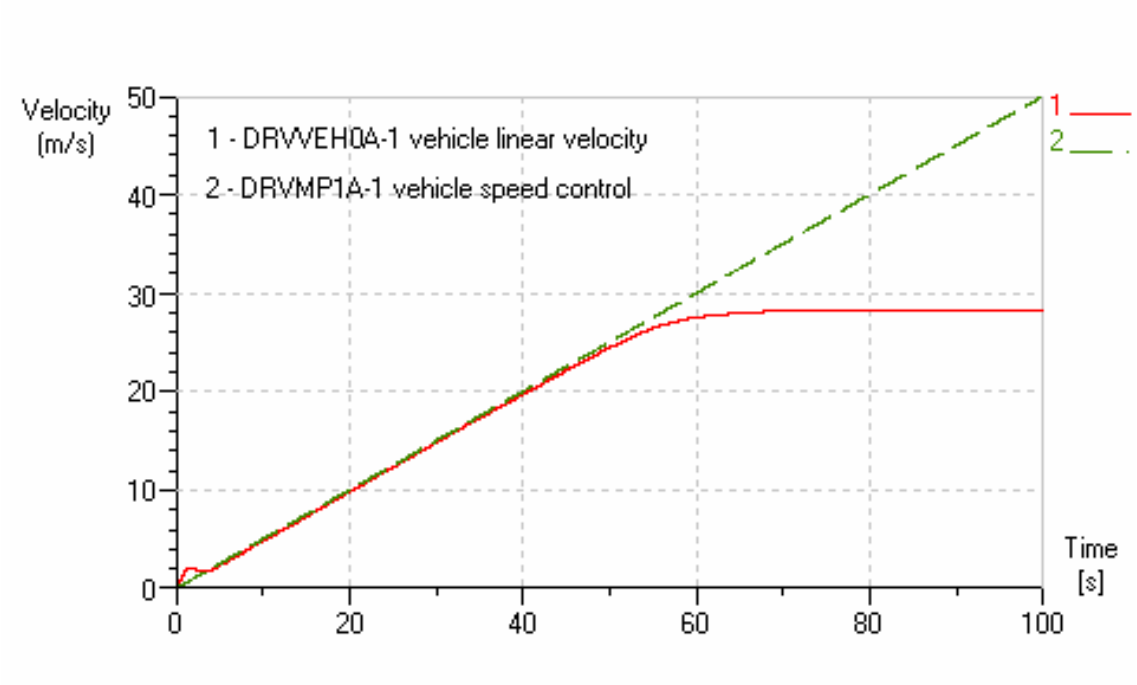

Figure 6-9 Maximum velocity of the conventional truck

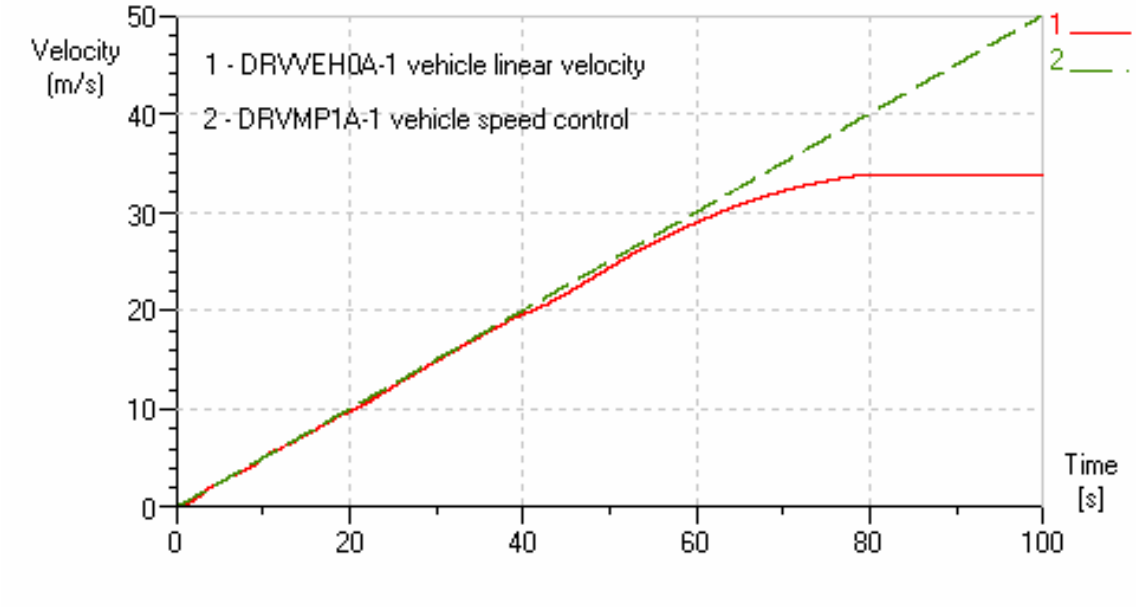

Figure 6-10 Maximum velocity of the LD hybrid electric truck

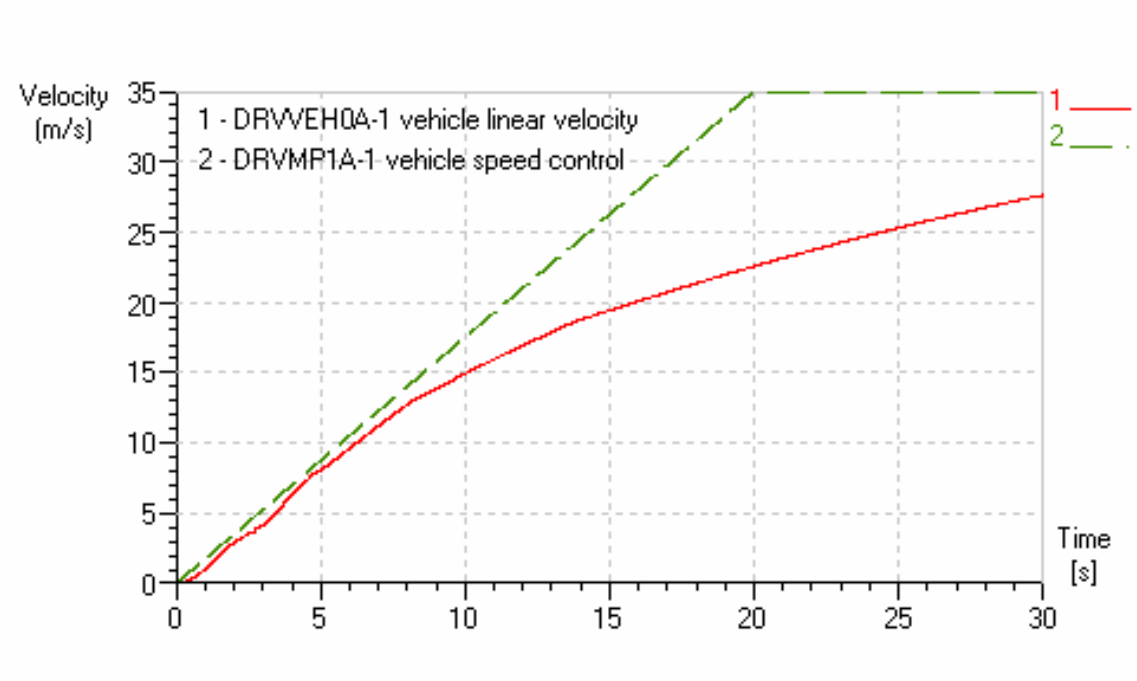

Figure 6-11 Maximum acceleration of the conventional truck

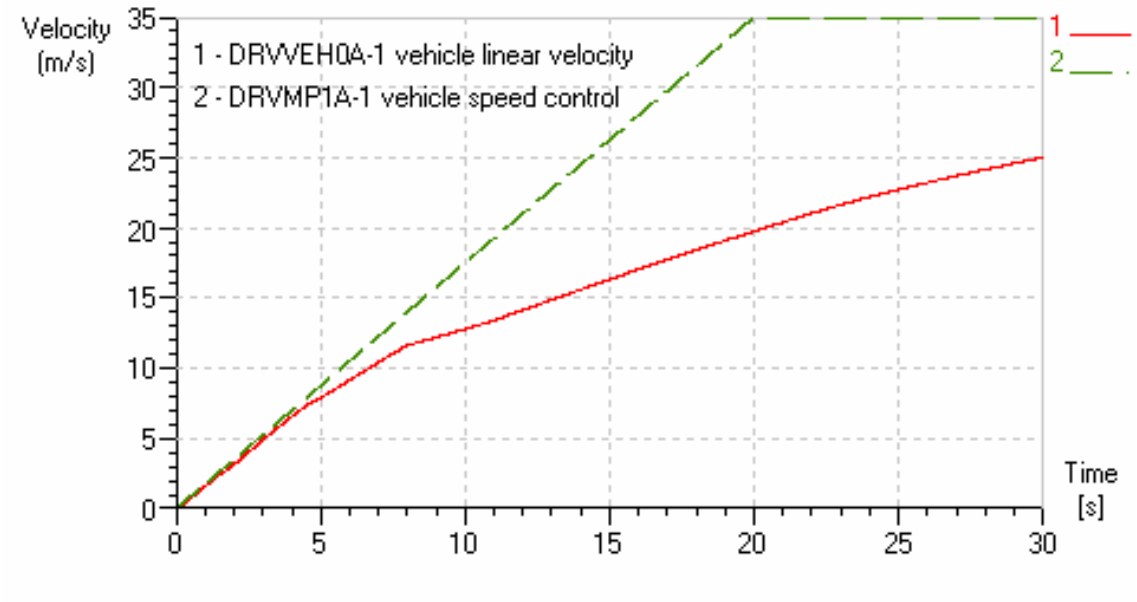

Figure 6-12 Maximum acceleration of the LD hybrid electric truck

As shown in Figure 6-13, the CBDTRUCK cycle is made up of the iteration of the same driving pattern. So it can be shown that the driving torques from the ICE and the EM are produced with the similar magnitude periodically. As there is no severe acceleration area, the magnitude of the EM torque is relatively small. However, the duration of the motor only mode increases because the vehicle is operated at low speed. The variation of the SoC is periodical by the charge and the discharge due to the iteration of acceleration and deceleration, and the final SoC is maintained in the target limit. In addition, the amount of fuel consumed tends to increase with the same pattern.

Figure 6-14 is the simulation results from the JE05 drive cycle. As can be estimated from the change of the battery SoC, this cycle includes the relative rapid deceleration from the high velocity. So the battery SoC control is limited by controlling only the engine operation zone. This suggests that more tuning of the HEV vehicle, the regeneration brake controller and mode selector in particular, will improve the charge-sustaining strategy. In other words, there is some more room to improve the fuel economy by using the surplus battery energy. In this thesis, as the maximum energy recovery strategy is set up and the excess SoC does not mean the deterioration of fuel economy, more improvement of the controller is not considered.

The simulation results on the TRL LGV drive cycle are plotted in Figure 6-15. As this cycle is based on the real drive cycle in an urban area, the velocity varies in the range between zero and 15m/s zone. So the required torque to drive the vehicle is larger than that of the CBDTRUCK cycle but smaller than that of the JE05 cycle in general. The battery SoC varies within the target limit and the tendency to increase the fuel consumption varies according to the velocity profile.

From the plotted data in Figures 6-13 to 6-15, the fuel economy can be obtained. After simulating the conventional LD truck on given drive cycles to calculate the base fuel economy, a comparative study is carried out. To sum up, the fuel economy on each drive cycle is compared in Figure 6-16. This shows that the fuel economy of the HEV is improved by 22% to 26% depending on the drive cycle.

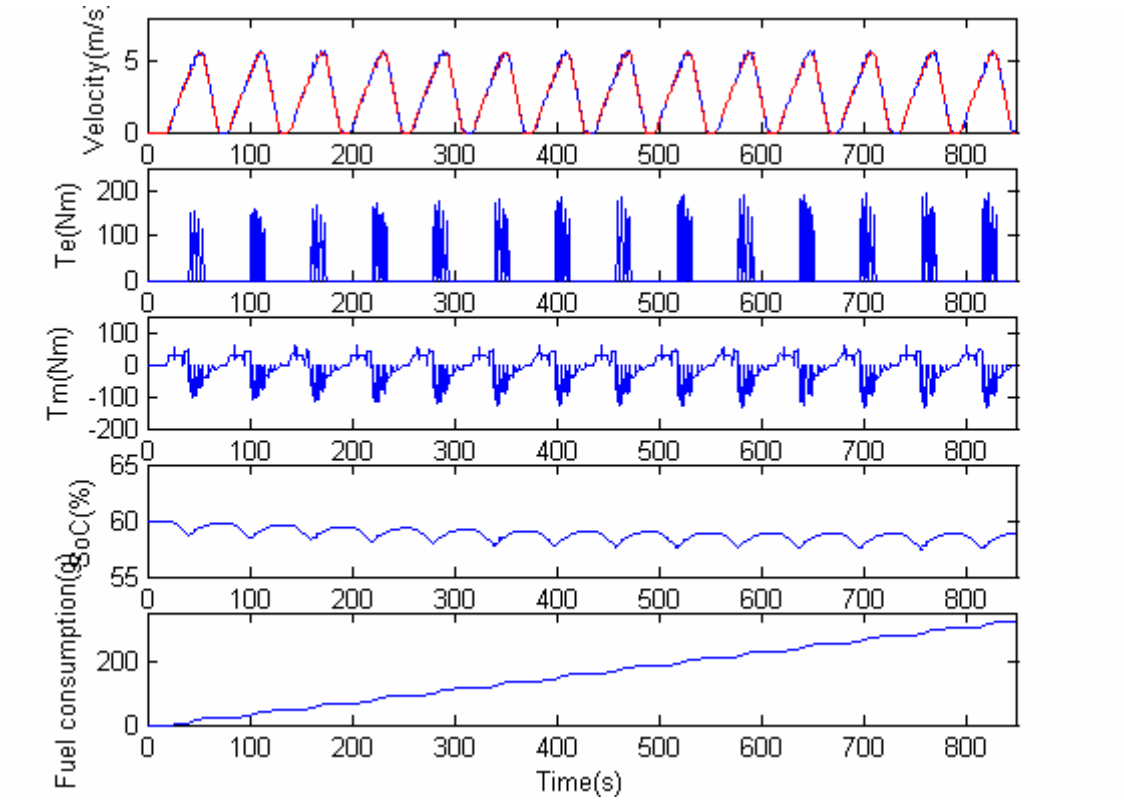

Figure 6-13 LD hybrid electric truck on CBDTRUCK drive cycle

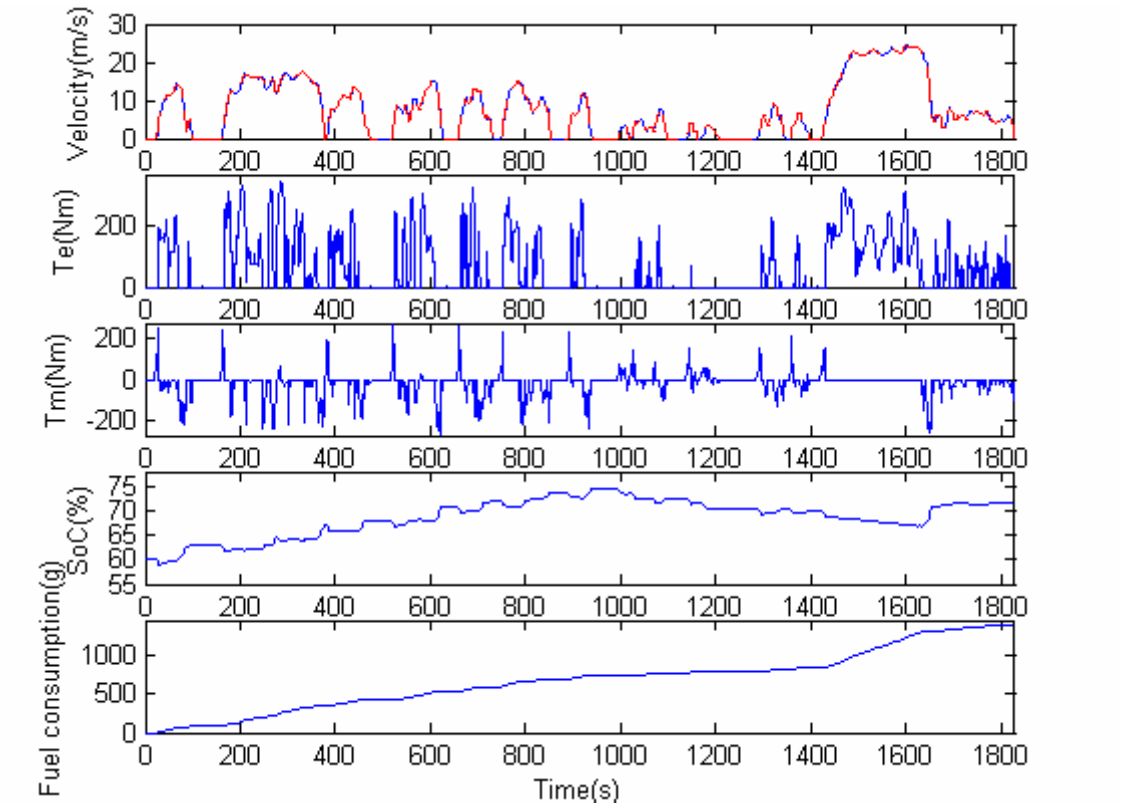

Figure 6-14 LD hybrid electric truck on JE05 drive cycle

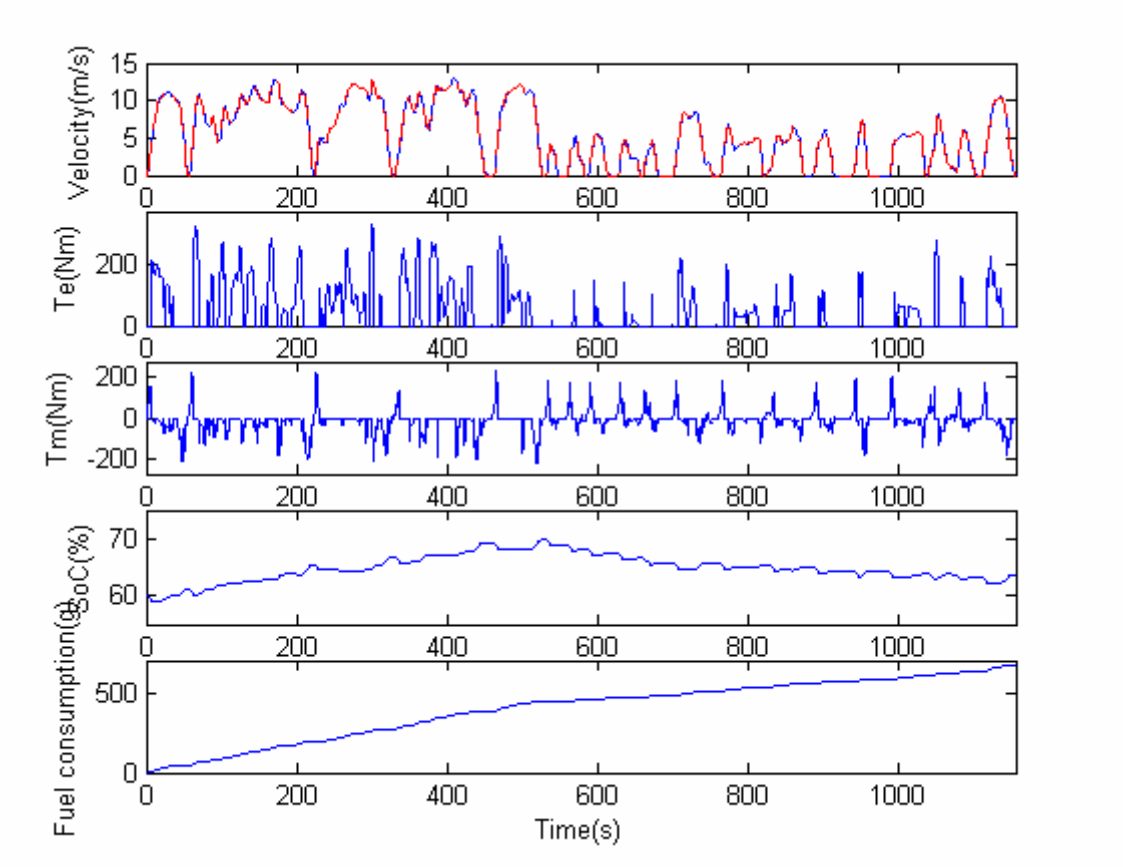

Figure 6-15 LD hybrid electric truck on TRL LGV drive cycle

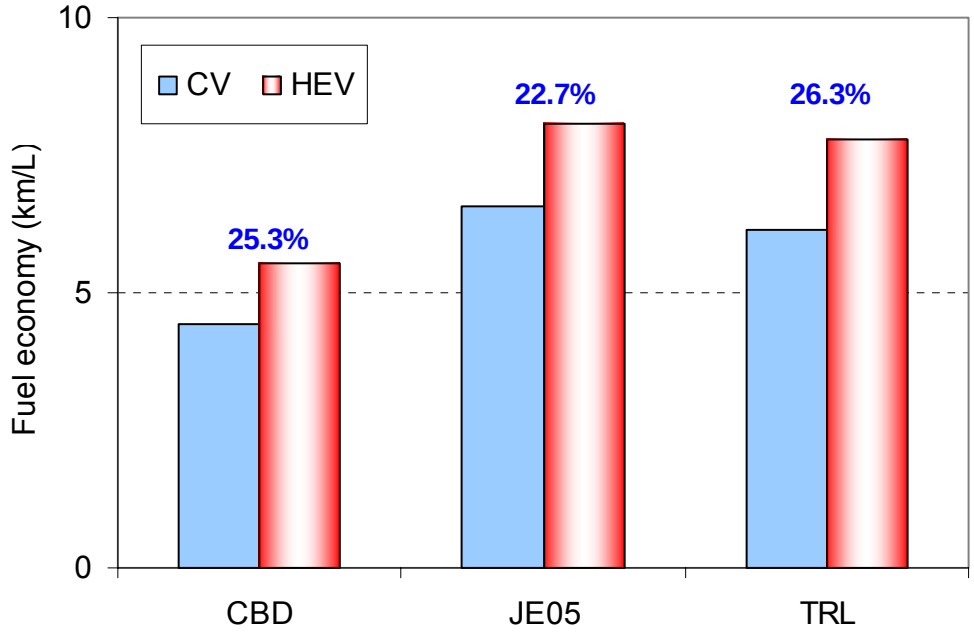

Figure 6-16 Comparison of the fuel economy

So far, it has been assumed that the hybrid electric truck has the same weight as the conventional vehicle. That is because the total axle capacity and the maximum gross vehicle weight is the same and the weight difference is not so big in the full load condition. However, in the unladen condition, the weight difference between the HEV and the conventional vehicle has to be considered. The weight can be estimated by using the data from reference [37] and the simple calculation [22]. The increase of the battery weight can be estimated as 120kg and the motor including the inverter is 47kg. It is, therefore, assumed that the weight of the HEV is heavier than the conventional truck by 170kg.

Some simulations were carried out to study the effect of the vehicle weight on the fuel economy. That is, the hybrid electric vehicle model with 170kg greater baseline weight than the conventional truck is tested with different payload conditions. Figures 6-17 and 6-18 show the simulation results. Compared to the results presented in Figure 6-16, the fuel economy is worse by about 2% in the fully-laden condition (Figure 6-17 c) due to the weight difference between the HEV and the conventional vehicle. So the fuel economy of the HEV is improved by 21% to 24% compared to the conventional vehicle, whilst Figure 6-16 shows 22% to 26% improvement. In addition, it is shown that the effect on the fuel economy improves, as the vehicle weight decreases. In the unladen condition, a maximum of 36% improvements are shown on the CBDTRUCK drive cycle. These results seem plausible, in that the improvement effect is similar to the test results presented in [13].

Figure 6-18 shows that, as expected, the fuel economy has a tendency to decrease with the increase of the vehicle weight. This implies that the weight of the hybrid electric system is another important key factor in designing the HEV.

If the vehicle operates within the GVW limit, then there would be a penalty on maximum payload of 170kg or 7%.

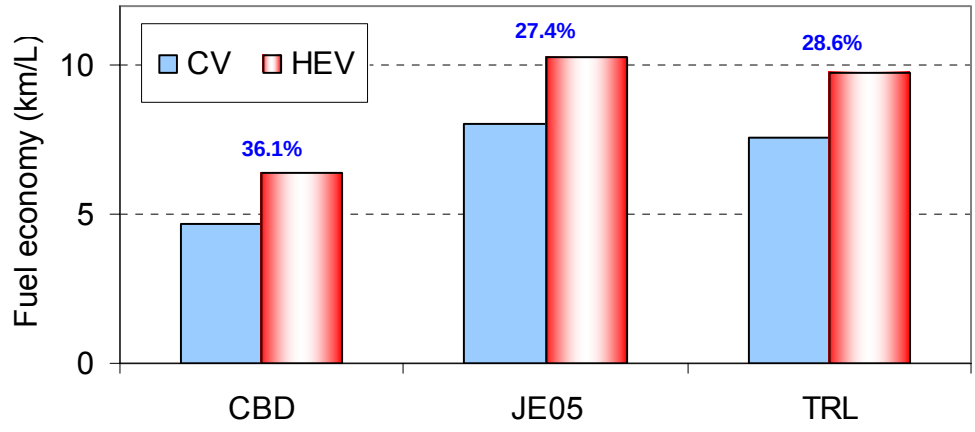

(a) Unladen condition

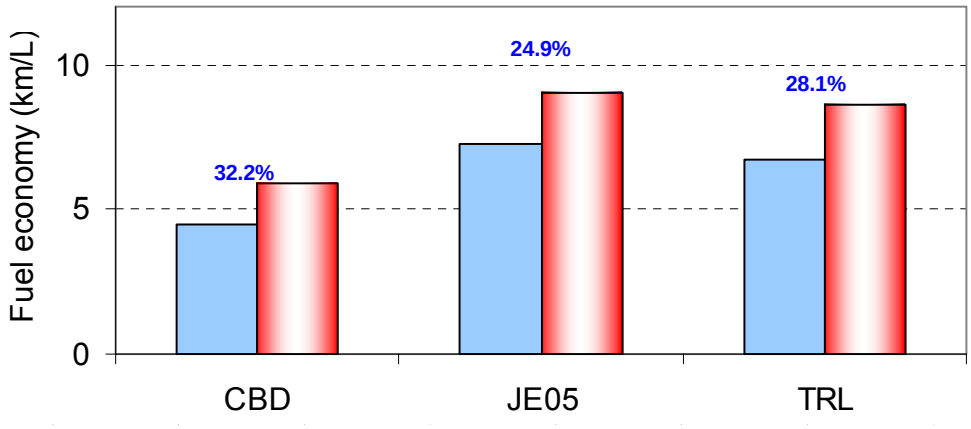

(b) Half-laden condition

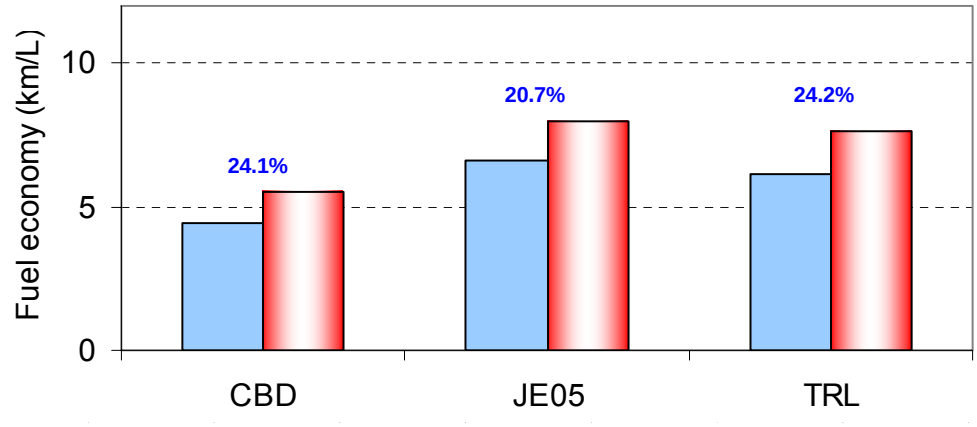

(c) Fully-laden condition

Figure 6-17 Comparison of the fuel economy by the vehicle weight condition (HEV heavier than CV by 170kg in all cases)

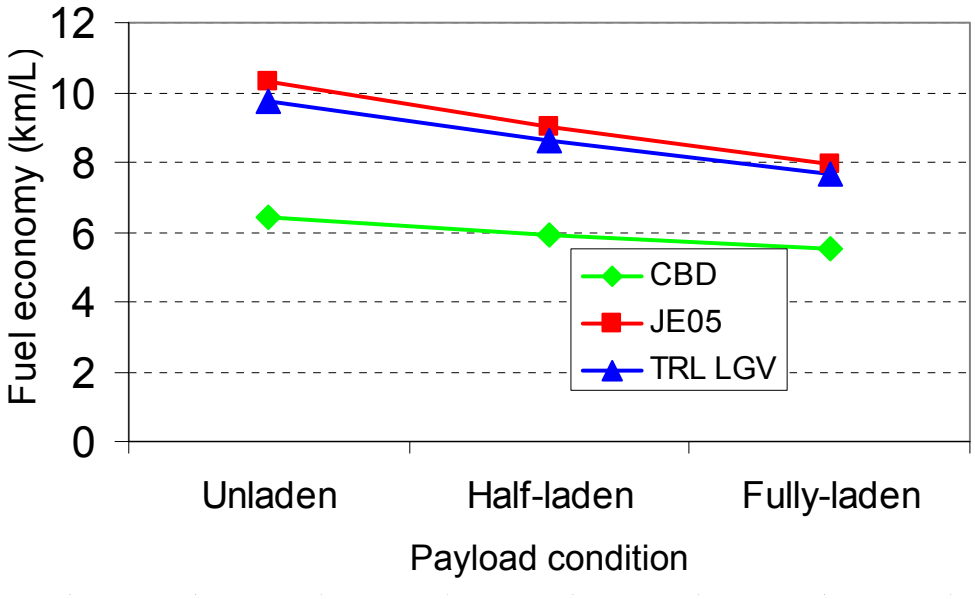

Figure 6-18 Effect of the vehicle weight on the fuel economy

7 Conclusion & Discussion

Through the initial study and the literature review, the current status and the research trends on the LD hybrid electric truck are well understood. Unfortunately, it is still in the initial stages of production and is not popular yet. So relatively few studies on the light duty hybrid electric truck have been carried out.

In general, the main stream of the research on the HEV is to optimise the hybrid architecture, the component efficiency, and the control strategy to improve total energy efficiency. For this purpose, various methodologies are suggested. Firstly, in order to define the component size, the methods based on the vehicle performance, the cost function, and the simulation are presented. These concepts are based on the same criteria from the technical point of view. Secondly, there have been three kinds of methodology to optimise the controller: rule-based concept, static optimisation, and dynamic optimisation through dynamic programming. Among them, the rule-based concept is adopted in this study by considering its application in a real condition with the available information.

In this study, the conventional truck and the LD hybrid electric truck were modelled to compare fuel economy and vehicle performance. The components have been developed by using AMESim and the controller was designed in Simulink. The pre-transmission hybrid architecture was determined as the most promising architecture through a comparative study on the advantages and disadvantages of each architecture. After that, the definition of the ICE or the EM power capacity was performed based on the required vehicle performance.

The control strategy was set up based on the information on the built components and the controller was constructed using this strategy. However, the charge-sustaining function of this controller was not satisfactory initially. So, a new control concept to determine the engine operating region according to the SoC was presented and the controller was improved.

In order to verify the functions and operations of the HEV, the basic simulation was carried out in advance. As a result of the simulation, it was found that the modelled vehicle followed the objective velocity profile adequately and the controller produced the appropriate functions according to the given condition. In addition, many simulations on a number of drive cycles were performed to study their effect of the engine operation zone and verify the motor power capacity. Through these simulations, the engine operation threshold, in terms of the normalised engine efficiency, was optimised to 40%, and the EM power capacity which was calculated by the required performance was verified.

Finally, the basic performance and the fuel economy were compared between the conventional truck and the LD hybrid electric truck through the simulation on the CBDTRUCK cycle for the USA, JE05 cycle for Asia, and TRL LGV drive cycle for Europe. It was shown that the vehicle performance and the fuel economy of the HEV were much better than that of the conventional vehicle. However, it was found that there was some room to improve the controller because the final battery SoC was beyond the target limit after simulation on the JE05 cycle.

To sum up, the modelling and design of the light-duty hybrid electric truck was carried out in this thesis and the improved control strategy to maintain the SoC in the target range was suggested. This complete HEV model which was integrated with the controller was simulated on various drive cycles, representing good performance and fuel economy when compared to the conventional vehicle.

From the simulation results and the problems during the research, some works are recommended as follows:

- Further improvement of the controller
  As pointed out in the study on the simulation on JE05 drive cycle, it is hard to meet the target SoC limit with a control of the engine operation zone alone. For the drive cycles which have much portion of rapid deceleration, further tuning of

the controller, the brake controller and the mode selector in particular, is recommended.

- Improvement of gearshift map

  In this thesis, only the efficiency of the architecture and the controller of the HEV are concentrated on. So the effect by the gearshift map is neglected. However, various gearshift strategies can be set and applied to improve the fuel economy as well as vehicle performance.

- Related test and reliable test results

  In order to fine-tune the controller, more information on the component built in the HEV is needed. As the LD hybrid electric truck is not yet common in the market, it is difficult to obtain exact data concerned with the designed component. So related tests have to be done and more reliable data have to be obtained. This will secure a refined controller.

- To establish the model under the integrated simulation tool environment

  To use the built-in component model is quite easy in the initial stages. However, the types of built-in component models are limited and they sometimes need to be modified. It is more difficult to modify the built-in model than what is modelled in general. Moreover, it takes too much time to simulate with the interface between two simulation tools. So an integrated, strong simulation tool is desirable in order to study the HEV.

8 References

1. *IPE Brent Crude Oil Price,* www.oilnergy.com.

2. *Emission Standards:European Union, Heavy-duty diesel truck and bus engines,* http://www.dieselnet.com/standards/eu/hd.html.

3. Kenji, M., *Automotive power source in 21st century.* JSAE Review, 2003. **24**(1): p. 3-7.

4. *Expansion of maket for hybrid electric vehicles (Japanese)*. News letter 2005, www.nri.co.jp.

5. *Central London congestion charging : Impact monitoring 2005,* www.tfl.gov.uk.

6. Jefferson, C. and R.H. Barnard, *Hybrid vehicle propulsion*. 2002, Southampton, UK ; Boston: WIT Press.

7. Chan, C.C., *The state of the art of electric and hybrid vehicles.* Proceedings of the IEEE, 2002. **90**(2): p. 247-275.

8. Ehsani, M., *Modern electric, hybrid electric, and fuel cell vehicles : fundamentals, theory, and design*. 2005, Boca Raton ; London: CRC Press.

9. Miller, J.M., *Propulsion systems for hybrid vehicles*. IEE power and energy series ; 45. 2004, London: Institution of Electrical Engineers.

10. Rahman, Z., K.L. Butler, and M. Ehsani, *A comparative study between two parallel hybrid control concepts*, SAE 2000-01-0994.

11. Van den Bossche, P., *Power sources for hybrid buses: comparative evaluation of the state of the art.* Journal of Power Sources, 1999. **80**(1-2): p. 213-216.

12. Kumagai, N., et al., *Super HEV system for Super low floor city-bus*, SAE 2001-01-0956.

13. Takada, Y., S. Ueki, and A. Saito, *Investigation into Fuel economy and NOx emissions of Light duty hybrid truck in Real traffic conditions*, SAE 2005-01-0265.

14. Nellums, R.A., J.H. Steffen, and S. Naito, *Class 4 Hybrid electric truck for pick up and delivery applications*, SAE 2003-01-3368.

15. Shougo, N., et al., *Development of capacitor hybrid truck.* JSAE Review, 2003. **24**(3): p. 249-254.

16. Dawood, V. and A. Emadi. *Performance and fuel economy comparative analysis of conventional, hybrid, and fuel cell heavy-duty transit buses*. in *Vehicular Technology Conference, 2003 IEEE 58th*. 2003: IEEE.

17. An, F., et al., *Scenario analysis of hybrid class 3-7 heavy vehicles*, SAE 2000-01-0989

18. Cho, S., et al. *A development of Shift Control Algorithm for Automated Manual Transmission in the Hybrid drivetrain*. in *FISITA World Automotive Congress*. 2000. Seoul, Korea.

19. Rahman, Z., K.L. Butler, and M. Ehsani, *A study of design issues on electrically peaking hybrid electric vehicle for diverse urban driving patterns*, SAE 1999-01-1151.

20. *Emission Test Cycles*, www.dieselnet.com.

21. Green, J.M. and T.J. Barlow, *Traffic management and air quality: realistic driving cycles for traffic management schemes*, in *TRL Report TRL596*. 2004, TRL: London.

22. Chu, L., Y. Li, and Q. Wang, *Study on the parametric optimization for a parallel hybrid electric vehicle powertrain*, SAE 2000-01-3109.

23. Chu, L. and Q. Wang, *Energy management strategy and parametric design for hybrid electric transit bus*, SAE 2001-01-2748.

24. Hellgren, J. and B. Jacobson, *A systematic way of choosing driveline configuration and sizing components in hybrid vehicles*, SAE 2000-01-3098.

25. Moularde, A., *Modelling of the Honda Insight Hybrid Vehicle using AMESim*. 2004, Cranfield University.

26. Lin, C.C., et al., *Modelling and control of a medium-duty hybrid electric truck.* International Journal of Heavy Vehicle Systems, 2004. **11**(3-4): p. 349-371.

27. Baumann, B.M., et al., *Mechatronic design and control of hybrid electric vehicles.* Mechatronics, IEEE/ASME Transactions on, 2000. **5**(1): p. 58-72.

28. Paganelli, G., et al., *General supervisory control policy for the energy optimization of charge-sustaining hybrid electric vehicles.* JSAE Review, 2001. **22**(4): p. 511-518.

29. Kim, C., et al., *Fuel economy optimization for parallel hybrid vehicles with CVT*, SAE 1999-01-1148.

30. Oh, K.C., et al., *Operating Algorithm of a Parallel HEV*, in *KSAE Autumn Conference*. 2001, KSAE.

31. Lin, C.-C., et al., *Control system development for an advanced-technology, medium-duty hybrid electric truck*, SAE 2003-01-3369.

32. Andersson, J., R. Axelsson, and B. Jacobson, *Route adaptation of control strategies for a hybrid city bus.* JSAE Review, 1999. **20**(4): p. 531-536.

33. Miller, T., G. Rizzoni, and Q. Li, *Simulation-based, hybrid-electric vehicle design search*, SAE 1999-01-1150.

34. *Power train application of AMESim*, www.amesim.com.

35. Gangadurai, M., *Methodology for optimal powertrain control*. 2003, Cranfield University.

36. *Low emission Fuso vehicles*. 2005, www.mitsubish-fuso.com/en.

37. *Introduction of Elf diesel hybrid,* www.isuzu,co.jp/world.

38. Kimura, Y., *Current status of EFVs in Japan*, in *The Development & Dissemination Of Environmentally Friendly Vehicles (EFVs)*. 2004.

39. Chu, L., et al., *Parametric design of hybrid power-train with ISG for transit bus*, SAE 2004-01-3065.

40. Husain, I., *Electric and hybrid vehicles : design fundamentals*. 2003, Boca Raton, Fla. ; London: CRC Press. 270 p.

41. *AMESim manual*.

42. Gillespie, T.D., *Fundamentals of vehicle dynamics*. 1992, Warrendale, PA: Society of Automotive Engineers.

43. Kim, H.S. and K.S. Park, *Vehicle dynamics*. 1999: Iljin company.

9 APPENDICES

1. Matlab program to calculate the engine spare power

```
% These statements calculate the spare power of the engine
% to the total resistance

vel=44:2:80;   % velocity(km/h)
r_tot=5500*0.01*9.81+0.5*1.205*0.6*3.73*(vel.^2)/(3.6^2) %total
resistance(N), vel=km/h
vel_c=[43.2 51.8 60.4 69.1 77.7 86.3]; % current velocity
eng_for=[2044 2815 2923 2923 2923 2931]; % Engine traction force
eng_for_inter=interp1(vel_c,eng_for,vel) % ETforce interpolation

spare_for=(eng_for_inter-r_tot) % Spare traction force
spare_power=mean(spare_for.*vel./3.6)/1000 % average spare
power(kW)
```

2. Matlab program to calculate the engine friction data

```
% These statements calculate the engine friction loss at zero
torque demand
% of the conventional engine and the downsized engine for HEV
% based on the existing loss data, 1 litre and 4.8 litre engine,
respectively.

displacement = [1 4.8]; % 1 litre & 4.8 litre
eng_rpm = [800 1000 1200 1400 1600 1800 2000 2200 2500 2900
3200];

[disp,rpm] = meshgrid(displacement,eng_rpm);
eng_loss= [-7 -40; -8 -45; -9 -50; -10 -54; -10 -56; -11 -58;...
          -12 -60; -12.5 -65; -13.3 -70; -13.6 -80; -15.2 -85];

eng_loss_39 = interp2(disp,rpm,eng_loss,3.9,eng_rpm) % friction
loss for 3.9 litre engine
eng_loss_43 = interp2(disp,rpm,eng_loss,4.3,eng_rpm) % friction
loss for 4.3 litre engine
```

3. Matlab program to calculate the power loss of the EM

```
% Data source: Isuzu report for ELF hybrid electric truck

%%%%%%%%%%%%%%%%%%%%%%%%%%%%%%%%%%%%%%%%%%%%
% SPEED & TORQUE RANGES over which data is defined
%%%%%%%%%%%%%%%%%%%%%%%%%%%%%%%%%%%%%%%%%%%%
% (N*m), torque range of the motor
mc_map_trq_int=[-235 -200 -150 -100 -50 -25 -10 ...
   0 10 25 50 100 150 200 235];
trq_scale=30000/(125*2*pi*2000/60);  % 30000:30 kW , that is the
required power for scaling
mc_map_trq=trq_scale*mc_map_trq_int;

% (rad/s), speed range of the motor
mc_map_rpm=[0 500 1000 1100 1500 2000 2500 3000 3500 4000];
mc_map_spd=mc_map_rpm*(2*pi)/60;


%%%%%%%%%%%%%%%%%%%%%%%%%%%%%%%%%%%%%%%%%%%%
% LOSSES AND EFFICIENCIES
%%%%%%%%%%%%%%%%%%%%%%%%%%%%%%%%%%%%%%%%%%%%
mc_eff_map = 0.01*[...
60  62  65  64  64  64  65  60  65  67  70  72  70  65  65
70  72  75  80  80  75  70  65  70  75  80  82  80  76  74
82  83  85  86  84  80  70  65  70  80  85  87  87  85  84
84  86  86.5    86.5    85  80  70  65  70  80  86  88  88  87
85
86  87  89  88  86  80  70  65  70  80  86  89  89  89  89
91  91  91  91  86.5    80  70  65  70  80  87  91  91  91  91
91  91  91  91  86.5    80  70  65  70  80  87  90  90  90  90
90  90  90  90  86.5    80  70  65  68  80  87  90  90  90  90
88  88  88  88  85  78  68  63  65  80  88  88  88  88  88
83  83  83  83  82  75  65  62  65  75  85  85  85  85  86
];

% CONVERT EFFICIENCY MAP TO INPUT POWER MAP
[temp_T,temp_w]=meshgrid(mc_map_trq,mc_map_spd);
temp_mc_outpwr_map=temp_T.*temp_w;
temp_mc_losspwr_map=(1./mc_eff_map-
1).*temp_mc_outpwr_map.*(temp_T>0)+...
   (mc_eff_map-1).*temp_mc_outpwr_map.*(temp_T<0);

%% to compute losses in entire operating range
%% ASSUME that losses at zero torque are the same as those at
the lowest
%% negative torque, and
%% ASSUME that losses at zero speed are the same as those at the
lowest positive
%% speed
temp_zti=find(mc_map_trq==0);
temp_zsi=find(mc_map_spd==0);
```

```
if ~isempty(temp_zti)

temp_mc_losspwr_map(:,temp_zti)=temp_mc_losspwr_map(:,temp_zti-
1);
end
if ~isempty(temp_zsi)

temp_mc_losspwr_map(temp_zsi,:)=temp_mc_losspwr_map(temp_zsi+1,:
);
end

% CONVERT EFFICIENCY MAP TO INPUT POWER MAP
%% find indices of well-defined efficiencies (where speed and
torque > 0)
%pos_trqs=find(mc_map_trq>0);
%pos_spds=find(mc_map_spd>0);

%% compute losses in well-defined efficiency area
%[T1,w1]=meshgrid(mc_map_trq(pos_trqs),mc_map_spd(pos_spds));
%mc_outpwr1_map=T1.*w1;
%mc_losspwr_map=(1./mc_eff_map(pos_spds,pos_trqs)-
1).*mc_outpwr1_map;

%% to compute losses in entire operating range
%% ASSUME that losses are symmetric about zero-torque axis, and
%% ASSUME that losses at zero torque are the same as those at
the lowest
%% positive torque, and
%% ASSUME that losses at zero speed are the same as those at the
lowest positive
%% speed
%mc_losspwr_map=[fliplr(mc_losspwr_map) mc_losspwr_map(:,1)
mc_losspwr_map];
%mc_losspwr_map=[mc_losspwr_map(1,:);mc_losspwr_map];


% LIMITS

% maximum continuous torque corresponding to speeds in
mc_map_spd
mc_max_trq=[235 235 235 235 170 125 85 65 50 42]*trq_scale; %
(N*m)

mc_max_gen_trq=[-235 -235 -235 -235 -210 -140 -105 -80 -65 -
50]*trq_scale; % (N*m)

% OTHER DATA
mc_inertia=0.0226; % (kg*m^2), rotor's rotational inertia

% CLEAN UP
clear T w mc_outpwr_map mc_outpwr1_map T1 w1
```

4. Matlab program to generate the regenerative brake map

```
% These statements generate the regenerative brake map
% for the FR type of light-duty hybrid electric truck.

brk_com=0:0.1:1; % brake command 0~1

t_brk_max=13729; % the maximum braking torque (Nm)
t_brk_com = t_brk_max.*brk_com; % the toral braking torque by
the brake command

% Data for ideal braking torque line : the total braking torque
vs. the braking torque at rear wheels
t_brk=[0.0 1980.1 3960.3 5940.4 7920.6 9900.7 11880.9 13861.0];
t_brk_rear=[0.0 1124.1 2141.3 3051.4 3854.6 4550.7 5139.9
5622.0];

% the braking torque at rear wheels by the brake torque command
t_brk_com_rear = interp1(t_brk, t_brk_rear, t_brk_com);

% Max torque of generator
gen_rpm=[0 500 1000 1100 1500 2000 2500 3000 3500 4000];
t_gen_max=[-269.3     -269.3     -269.3     -269.3     -240.6
      -160.4     -120.3     -91.7 -74.5 -57.3];

% Data for gearbox
gear_ratio = [5.38 3.028 1.7 1 0.722];
fg_ratio=4.625;

for i=1:5; % loop by the gear number
    t_gen=t_brk_com_rear./(gear_ratio(i)*fg_ratio)*-1;

    for k=1:10
        for j=1:11
                if (abs(t_gen(j)) <= abs(t_gen_max(k)))
                    t_reg(j,k,i)=t_gen(j);
                else
                    t_reg(j,k,i)=t_gen_max(k);
                end
         end
    end
end
```